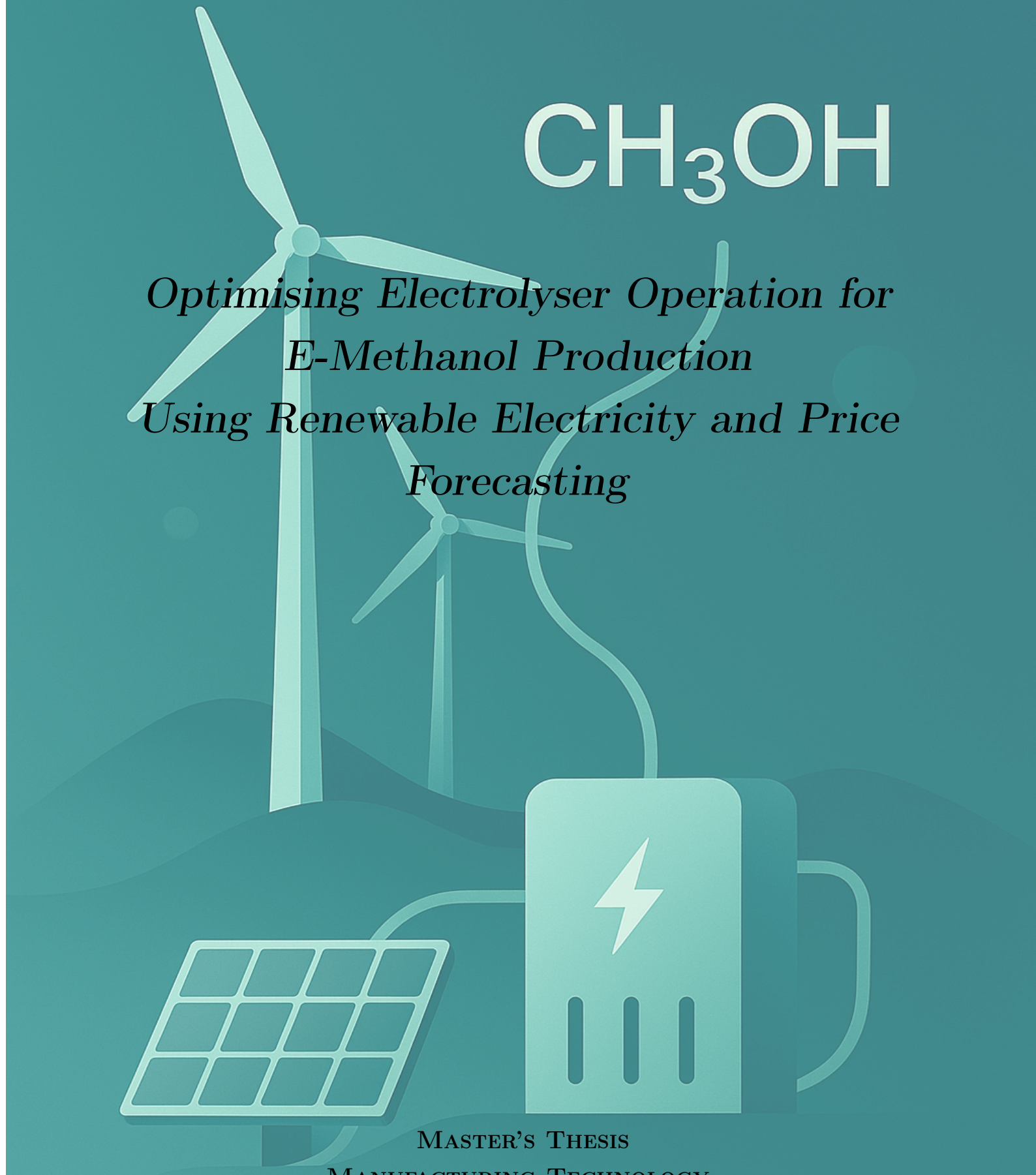

Optimising Electrolyser Operation for E-Methanol Production Using Renewable Electricity and Price Forecasting

Master's Thesis
Manufacturing Technology
Aalborg University
May 30th 2025

AALBORG UNIVERSITY
STUDENT REPORT

Studienævn for Mekanik og Fysik /
Studienævn for Produktion
Fibigerstræde 16
DK - 9220 Aalborg Øst
Tlf. 99 40 99 40
snmp@mp.aau.dk / snp@mp.aau.dk
www.mp.aau.dk

Dansk titel:	Optimering af elektrolyserdrift til E-Methanol produktion ved hjælp af vedvarende El- og prisprognose
English title:	Optimising Electrolyser Operation for E-Methanol Production Using Renewable Electricity and Price Forecasting
Semester:	4. semester
Semester theme:	Master's Thesis
Projekt period:	February 2025 - May 2025
ECTS:	30 ECTS
Supervisor:	Poul Kyvsgaard Hansen

Participants:

Filip Džigurski

Edition:	1
No. of pages:	96 pages
Appendix:	6 pcs.

Abstract:

This thesis explores the development of a modelling framework for optimising electrolyser operation in e-methanol production, using wind and solar electricity under fluctuating market conditions. A key focus lies in forecasting electricity prices with machine learning methods, including XGBoost and LSTM, to enable predictive control of electrolyser operation. By integrating these forecasts into a MILP-based scheduling model, the electrolyser is dynamically managed across three operational states(running, standby, and shutdown) to minimise total production cost while ensuring a fixed methanol output. The model incorporates transition constraints, variable electricity pricing, and CO_2 sourcing costs to reflect realistic system behaviour. Scenario analysis demonstrates that electricity prices and electrolyser efficiency are the most critical cost drivers, while CO_2 cost variations have a limited effect. The results highlight the importance of combining accurate short-term forecasting with flexible operation to enhance economic viability. Future work should prioritise advancements in electrolyser technology, electricity cost reduction strategies, and real-time model integration.

By signing this document, each group member confirms that everyone has participated equally in the project work, and thus, all collectively assume responsibility for the content of the report.
The content of the report is confidential.

Summary

This thesis develops an integrated modelling framework for optimising the operation of an electrolyser in e-methanol production, using variable electricity prices primarily driven by renewable energy sources. The objective is to minimise total operational cost while meeting a fixed annual methanol production target. The model focuses on Danish electricity market conditions and renewable generation trends expected in future Power-to-X scenarios.

A hybrid electricity price forecasting model was developed using machine learning. Forecasts for solar, offshore wind, and onshore wind generation, as well as electricity demand, were generated using LSTM networks. These outputs were then used as features in an XGBoost model to predict hourly electricity prices. The combined model achieved an MAE (Mean Absolute Error) of 268.5 DKK/MWh and an RMSE of 334.8 DKK/MWh on the test dataset, with the LSTM components showing strong performance in capturing daily and seasonal cycles.

The forecasted prices were fed into a Mixed Integer Linear Programming optimisation model for electrolyser scheduling. The model considered three primary operation states (running, standby, shutdown), transition dynamics (cold and hot starts, ramping times) and electricity costs. Over a 168 hour rolling window for whole year, the model made binary decisions for each hour and operational state, solving roughly 2000 binary variables per weekly optimisation.

Results from the full-year simulation showed that flexible operation reduced electricity costs by approximately 15% compared to fixed full-load operation. Specifically, the total cost of electricity consumption decreased from 254,140,507.17 DKK to 212,702,443.56, while still meeting the fixed methanol production requirement of 25,000 tons per year.

Future improvements should focus on enhancing model complexity (e.g., continuous load levels), enabling sub-hourly operation and including dynamic CO_2 sourcing options. R&D priorities include lowering electricity prices through system integration and advancing electrolyser efficiency, responsiveness and lifetime performance.

Preface

This master's thesis was written at the Department of Materials and Production at Aalborg University as the final project for my Master of Science in Manufacturing Engineering program. The project was supervised by Associate Professor Poul Kyvsgaard Hansen.

The thesis was carried out in collaboration with two fellow students from the Department of Energy at Aalborg University, Matej Vinko Primorac and Marin Veršić. While their work focused on the process development of the electrolyser system and methanol synthesis and distillation processes, this thesis centres on the development of a machine learning model for forecasting electricity prices, integrating those forecasts into operational planning and optimising methanol production accordingly. Although the projects were developed independently, they are integrated in a joint case study toward the end of the work.

I would like to express my sincere gratitude to my supervisor, Associate Professor Poul Kyvsgaard Hansen, for his valuable guidance, insightful discussions, and continuous support throughout the project.

Contents

Nomenclature

Abbreviations

ALK	Alkaline Electrolysis
AR	Autoregressive Model
ASU	Air Separation Unit
CAPEX	Capital Expenditure
CCS	Carbon Capture and Storage
DME	Dimethyl-ether
EAR	Error-to-Average Ration
eMeOH	electricity-based Methanol
ENTSO-e	European Network of Transmission System Operators for Electricity
EPF	Electricity Price Forecasting
fMeOH	fuel-based Methanol
HAWT	Horizontal-Axis Wind Turbine
IEA	International Energy Agency
LSTM	Long-Short Term Memory
MAE	Mean Absolute Error
MAPE	Mean Absolute Percentage Error
MILP	Mixed Integer Linear Programming
MSD	Methanol Synthesis and Distillation
MSE	Mean Squared Error
MSR	Methanol Synthesis Reactor
NAO	North Atlantic Oscillation
PEM	Polymer Electrolyte Membrane
PPA	Power Purchase Agreement
PtA	Power-to-Ammonia
PtH2	Power-to-Hydrogen
PtMeOH	Power-to-Methanol
PtX	Power-to-X
RF	Random Forests
RMSE	Root Mean Squared Error
RNN	Recurrent Neural Network
SMR	Steam Methane Reforming
SNG	Synthetic Natural Gas
SOEC	Solid Oxide Electrolyser Cell
SVM	Support Vector Machines
VAWT	Vertical-Axis Wind Turbines
WECS	Wind Energy Conversion System

Chemical Symbols

Al_2O_3	Aluminium oxide
CH_3OH	Methanol
CH_4	Methane
CO_2	Carbon dioxide
Cu	Copper
H_2	Hydrogen
H_2O	Water
N_2	Nitrogen
NH_3	Ammonia
O_2	Oxygen
Zn	Zinc

Symbols

$\dot{M}_{\mathrm{MeOH}}$	Methanol production rate (kg/h)
λ	Indicates different load levels (40% - 100%), it is a part of i
ν	Set of transition and idle states
C_{cold}	Fixed cold start cost (DKK)
C_{hot}	Fixed hot start cost (DKK)
C_{run}	Total cost for running mode (DKK)
$C_{shutdown}$	Total cost for shutdown mode (DKK)
$C_{standby}$	Total cost for standby mode (DKK)
$C_{startup}$	Total cost for both cold and hot starts (DKK)
$C_{transition}$	Total cost for both standby and shutdown transitions (DKK)
E_{CS}	Total electricity used during cold start (MWh)
$E_{el,i}$	Electrolyser power at i state (MWh)
$E^i_{EL,t}$	Electricity consumption at hour t in operating state i (MWh)
E_{HS}	Total electricity used during hot start (MWh)
$E_{msd,i}$	MSD power at i state (MWh)
f_{el}	Objective function minimising operational costs (DKK)
M_i	Methanol target for week i (t)
M_t^{base}	Methanol production while in one of λ modes (kg)
M_t^{CS}	Methanol production during cold start (kg)
M_t^{HS}	Methanol production during hot start (kg)
$M_t^{SB\_SD}$	Methanol production during shutdown transition (kg)
$M_t^{SB\_TR}$	Methanol production during standby transition (kg)
M_{target}	Yearly methanol target (t)
P_t	Predicted electricity price at time t (DKK/MWh)
T	Time horizon (h)
t_{cold}	Time it takes electrolyser for cold start (h)
t_{hot}	Time it takes electrolyser for hot start (h)
t_{msd_up}	Time it takes MSD to enter running mode (h)

t_{prod}	Remaining time for full operation (h)
t_{SB}	Time it takes electrolyser to go to standby or shutdown (h)
t_{tank}	Time it takes to fill the buffer tank (h)
w_i	Weight dedicated to week i
$x_{t,i}$	Binary decision variable indicating whether the system is in the state i during hour t

Introduction 1

As the global energy sector transitions towards renewable energy, integrating fluctuating renewable sources such as wind or solar power presents significant operational challenges. While renewable sources offer substantial environmental benefits and resource availability, their variable nature leads to discrepancies between power generation and consumption. To mitigate these fluctuations, technologies categorised under Power-to-X(PtX) have been introduced. PtX includes methods that convert renewable electricity, whether surplus or intentionally generated, into alternative energy carriers or chemical products such as hydrogen, ammonia, methane, and methanol. This supports energy sector coupling and enhances system flexibility. [16] [15]

Methanol has gained significant attention as a PtX product due to its high energy density, liquid form at ambient conditions, and compatibility with existing transport, storage and distribution infrastructure. Compared to hydrogen, methanol is easier and more cost-effective to store and transport, making it a practical renewable fuel and chemical feedstock.[18] Methanol production can follow two principal pathways, conventional fossil-based methanol (fMeOH), which relies on natural gas or coal and results in high carbon emissions, and renewable electricity-based methanol (eMeOH), which combines green hydrogen, produced by electrolysis powered by wind or solar, with captured CO_2, substantially lowering lifecycle emissions and supporting climate goals.[51]

This thesis focuses on a critical component in eMeOH production that is the electrolyser, which converts water into hydrogen and oxygen using renewable electricity. Its operational efficiency and economic viability are strongly influenced by fluctuating electricity prices. Therefore, optimising the operational strategy, not only deciding when to run, enter standby, or shut down, but also at what capacity, is essential to minimise electricity costs and ensure stable hydrogen supply. Moreover, as methanol synthesis efficiency depends on the hydrogen flow, this coupling must be considered to maximise overall system performance. [32] [61]

This thesis is carried out in a collaboration with another student group from the Energy Department at Aalborg University, who are developing an e-methanol production setup. While their focus includes broader process integration and system design, this thesis specifically targets optimising the operational strategy of the electrolyser in response to fluctuating electricity prices from wind-generated electricity.

Consequently, this leads to the initial problem statement that is formulated as following:

How can the operational strategy of an electrolyser in an e-methanol production system be optimised to minimise electricity costs while ensuring an efficient and stable hydrogen supply for methanol synthesis?

Problem analysis 2

This chapter establishes the foundation for the project and works toward refining the initial problem statement into a clearer and more focused version. It begins with an overview of Power-to-X and the possible energy carriers represented by "X". The three most commonly used energy carriers are introduced and described, each with their own strengths and limitations. Special attention is given to Power-to-Methanol, which is explained more detailed. Secondly, the chapter covers renewable electricity from wind turbines and how its pricing is determined. Finally, the developed methanol production plant is analysed through its production stages, with a focus on the key input parameters that will be used in the later optimisation of the electrolyser.

2.1 Power-to-X

Traditional energy sources are considered as a main cause to climate change due to their significant greenhouse gas emissions. Report by the International Energy Agency(IEA) indicates that carbon dioxide (CO_2) emissions from fossil fuel-based energy sources have surpassed 13 gigatons of CO_2, accounting for about 40% of global emissions [17]. As a result, there is a pressing need to transition toward highly promising renewable energy sources. However, renewable energy faces significant challenges due to its unpredictable and irregular nature, with the quantity of electricity supplied fluctuating considerably. Therefore, it becomes crucial to store electricity during peak production periods. The latest advancements suggest storing electricity in the form of chemicals, an approach summarised by the concept known as Power-to-X (PtX). [40]

PtX (also referred to as P2X) involves the transformation of renewable electricity sourced from wind, water or solar into a versatile energy carrier, denoted as "X" [10]. It outlines methods that utilise surplus or allocated renewable electrical power in various sectors through storage, conversion into alternative fuels, and subsequent reconversion techniques. This process is referred to as sector coupling, where the power sector is linked to the transportation sector through power-to-mobility. Furthermore, it is connected to the heating sector via power-to-heat, either through direct electrical heating or heat pumps, and finally to the industrial sector, including the chemical industry and agriculture, where synthetic fuels and gases serve as chemical feedstock, where this concept is depicted in **Fig. 2.1**.[8]

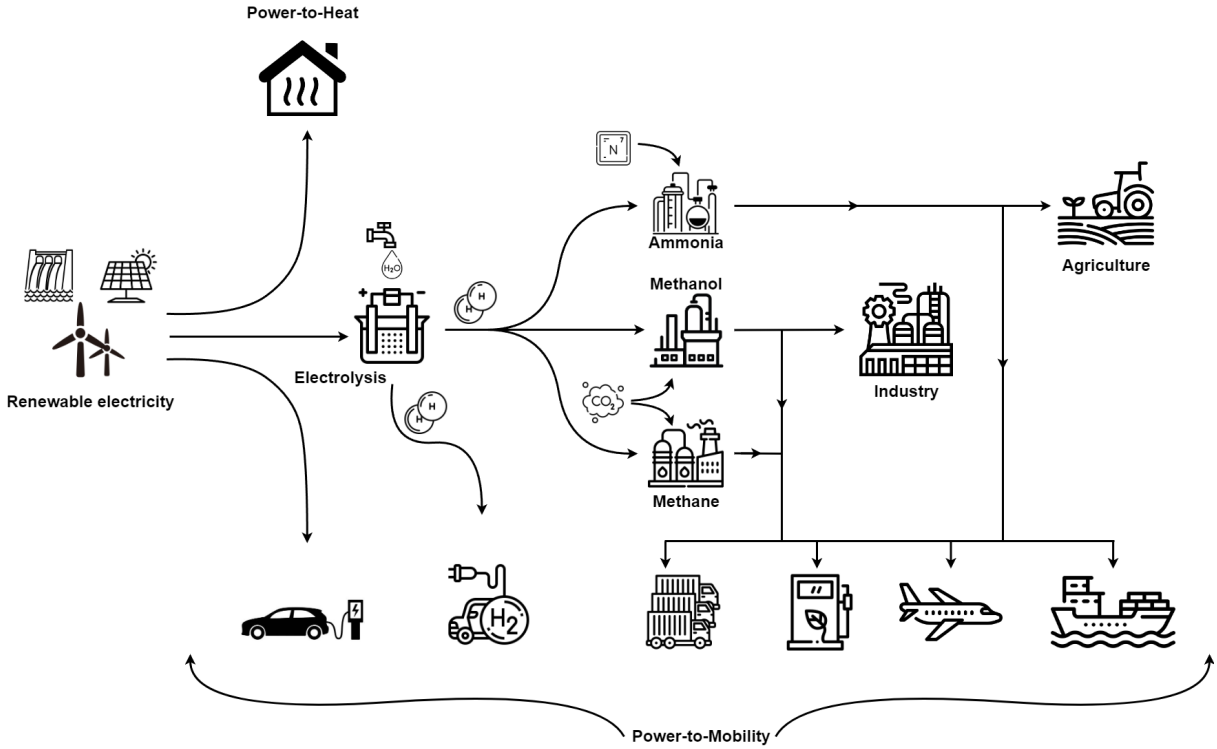

Figure 2.1
Graphical visualisation of PtX concept.

As shown in **Fig. 2.1**, at the core of PtX concept is the utilisation of renewable electricity to produce hydrogen (H_2) through the electrolysis of water. Hydrogen can be employed directly as the final energy carrier or further transformed into other forms such as methane, methanol or ammonia. Besides water for electrolysis, PtX processes typically need additional substances to create synthetic fuels and chemicals. For example, as noted in **Fig. 2.1**, producing methanol and methane requires a source of CO_2, and ammonia production requires N_2. CO_2 can be obtained from local renewable methods, such as capturing CO_2 from the atmosphere or biomass sources like biofuel and biogas plants, which currently release their CO_2 by-products into the atmosphere.[8] [12]

Furthermore, as previously mentioned, energy carrier "X" can be divided into the following four main chemicals:

- Hydrogen - H_2
- Ammonia - NH_3
- Methane - CH_4
- Methanol - CH_3OH

In the following sections, each energy carrier is described in terms of how it is obtained, and the advantages and disadvantages it presents.

Power-to-Hydrogen - PtH2

Generally, based on the production process and the source of hydrogen, four different types of hydrogen can be identified: black, grey, blue, and green, listed in order of decreasing environmental impact, depicted in **Fig. 2.2**. Currently, the majority of hydrogen is produced from natural gas through a process called Steam Methane Reforming(SMR). This method is fossil fuel-based and releases almost as much CO_2 as burning the natural gas itself, resulting in what is known as grey hydrogen. When the CO_2 emitted during this process is captured and stored using Carbon Capture and Storage (CCS), the resulting hydrogen is referred to as blue hydrogen. Additionally, hydrogen can be produced from coal via pyrolysis, leading to the production of black hydrogen, which, similar to SMR, results in CO_2 emissions comparable to those from coal combustion. Finally, when hydrogen is produced through the electrolysis of water using renewable electricity, it is termed green hydrogen and does not produce direct CO_2 emissions during its production.[3]

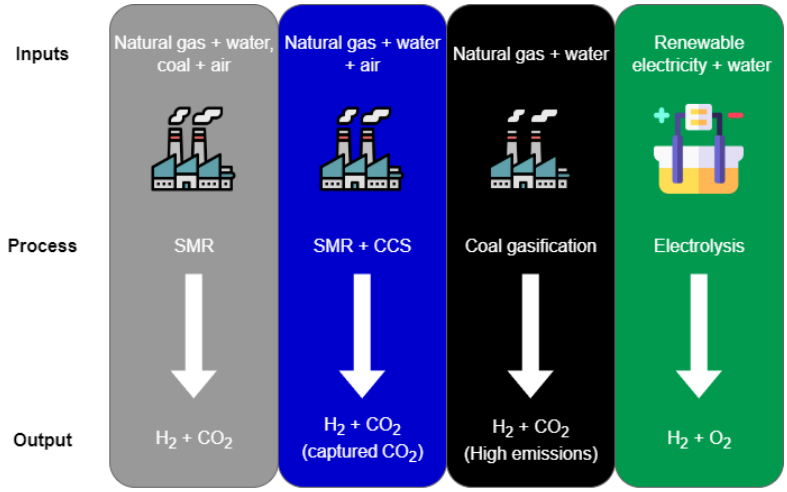

Figure 2.2

Graphical visualisation of different types of hydrogen, based on the inputs, process on how it is made and final products.

Electrolysis is a chemical process where H_2O is split, with the use of electricity, into H_2 and O_2. There are three major electrolysis technologies:

- **Alkaline electrolysis - ALK**
  ALK is the most mature technology, been used since 1920, with a market share of about 70% [28]. This technology benefits from low costs and a long operational lifespan. However, a disadvantage is that the ALK process needs to operate continuously to avoid damage, meaning that variable renewable energy sources should not be the sole power supply. [3]
- **Polymer Electrolyte Membrane - PEM**
  PEM electrolysis uses membrane as ionic conductor. The electrolyte, consisting of a thin, solid polysulfonated membranes, is used to transfer proton from the anode to the cathode side and separates hydrogen and oxygen gases. PEM technology has higher efficiency and faster response time, suitable for renewable energy sources. On the other hand, expensive materials have to be used, such as platinum and iridium.[8]
- **Solid Oxide Electrolyser Cell - SOEC**
  A technology that presents significant expectations due to its low expected capital cost and

high efficiency is the SOEC, which has recently entered the market with approximately 150 kW of capacity installed to date [60]. The operating temperatures for high-temperature steam electrolysis in SOEC's range from 700 to 1000 ℃. These higher temperatures enhance the thermodynamic conditions of the reaction, potentially reducing electricity usage as heat can be integrated into the process. However, some drawbacks of this technology include instability and delamination of electrodes, along with safety concerns.

Lastly, strengths and limitations of the PtH2 are presented in **Tab. 2.1**.

Table 2.1
Advantages and Disadvantages of Power-to-Hydrogen.[3] [8] [61]

Power-to-Hydrogen	
✓ **Storage** - Allows for large-scale storage of surplus renewable electricity	X **Production Costs** - Higher compared to traditional (grey) hydrogen
✓ **Versatile Application** - Usable for power generation, transportation, and industrial feedstock	X **Storage & Transport** - Requires compression or liquefaction due to low energy density
✓ **Zero Emissions** - Supports decarbonization efforts	X **Energy Losses** - Involves efficiency losses in electrolysis and conversion
✓ **Sector Coupling** - Integrates different sectors, enhancing system flexibility and efficiency	

Power-to-Ammonia - PtA

Ammonia is colourless gas with a strong smell that can easily dissolve in liquid water and water vapour. Above 75% of global ammonia production is used as fertiliser, but it is also widely used as a refrigeration fluid and in household cleaning solutions [22]. The production of PtA consists of three following key steps, depicted in **Fig. 2.3**:

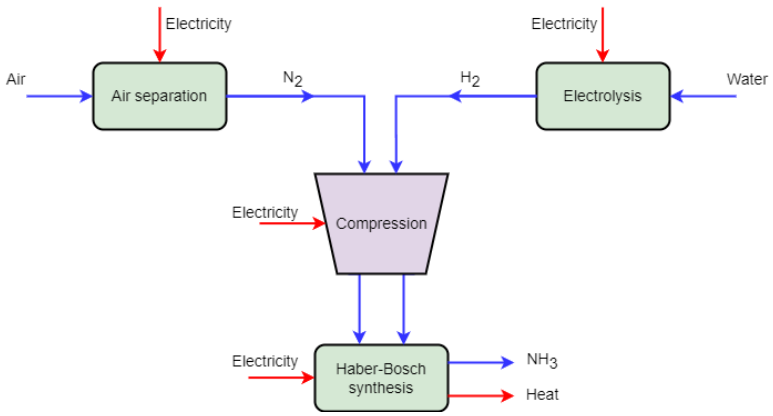

Figure 2.3
Graphical visualisation of ammonia production process.

- Hydrogen Production - As mentioned in **Sec. 2.1**, hydrogen is produced in electrolyser, where renewable electricity is used to split water into H_2 and O_2
- Air Separation - Nitrogen(N_2) is extracted from the air using an Air Separation Unit(ASU)
- Haber-Bosch Synthesis - H_2 and N_2 react at high temperatures and pressures in the H-B process to form NH_3, with an overall efficiency of 50-55% [23]

In the production of ammonia via water electrolysis, approximately 95% of the electricity is utilized for hydrogen production, while the remaining portion is allocated for air separation and the Haber-Bosch synthesis unit [34]. Strengths and limitations of PtA are presented in **Tab. 2.2**.

Table 2.2
Advantages and Disadvantages of Power-to-Ammonia.[35] [34] [33]

Power-to-Ammonia	
✓**Energy Storage** - NH_3 offers higher volumetric energy density than hydrogen and can be stored as a liquid at -33°C under moderate pressure	X **Energy Intensity** - Haber-Bosch process requires high temperatures ($\sim 450°C$) and pressures ($\sim 200bar$), leading to significant energy losses
✓**Carbon-Free** - NH_3 used as a clean fuel for power plants, shipping, and industrial heating	X **Safety Risks** - Ammonia is corrosive and toxic, necessitating strict handling and transport regulations
✓ **Infrastructure** - Existing ammonia production, transport, and storage infrastructure can scale up green ammonia applications	X **Combustion Issues** - NH_3 combustion may produce high NH_x emissions, requiring advanced emission control technologies
✓ **Grid Flexibility** - PtA can stabilize electricity grids by absorbing excess renewable power	X **Production Costs** - Higher than for fossil-based ammonia production

Power-to-Methane - PtM

Methane (CH_4) is colourless and combustible gas, and the main component of natural gas. A PtM plant mainly includes water electrolyser, a CO_2 separation unit(if CO_2 is not already available as pure gas or in a suitable mixture), and methanation unit. Inside of the methanation unit, H_2 reacts with captured CO_2 to form a gas mixture that mainly consists CH_4 and H_2O. Furthermore, the gas is processed into Synthetic Natural Gas(SNG). The final SNG can be used as fuel for transport, in homes, for power generation when electricity demand is higher than supply or as feedstock in industry.[25] **Fig. 2.4** depicts described process of methane production.

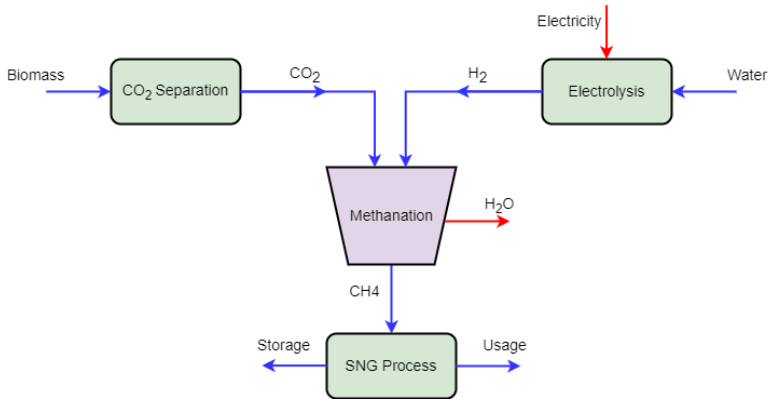

Figure 2.4
Graphical visualisation of methane production process.

As previously mentioned ammonia, methane as well has its strengths and limitations, which are presented in **Tab. 2.3**.

Table 2.3
Advantages and Disadvantages of Power-to-Methane.

Power-to-Methane	
✓ **Infrastructure** – SNG can be injected directly into existing natural gas pipelines, storage and distribution systems	X **Conversion Losses** – Two-step process (electrolysis and methanation) leads to low efficiency (35–40%)
✓ **Energy Storage** – Enables long-term and large-scale storage of renewable energy	X **High Costs** – PtM systems involve high capital and operational expenses
✓ **Carbon Reduction** – Utilises captured CO_2, supporting carbon cycles and emission reduction	X **Environmental Risk** – Methane leakage in the supply chain can cause significant harm if not managed properly

In addition to PtH2, which serves as the base for three commonly used energy carriers in PtX, PtA and PtM are also presented to give a broader view of current technologies. These pathways highlight the versatility of hydrogen as a starting point in different conversion routes. Finally, since PtMeOH is the main focus of this thesis, it is introduced in the following section for a more detailed discussion.

2.2 Power-to-Methanol

Methanol is one of the most widely produced chemical substances globally [14]. It can be used as a transportation fuel, hydrogen carrier for fuel cell or for electricity generation.Methanol production is generally divided into two categories: conventional fossil-based methanol (fMeOH) and electricity-based methanol (eMeOH). Fossil-based MeOH is typically produced through a two-step process. First, steam methane reforming (SMR) converts CH_4 into syngas, that is a mixture of H_2, CO and CO_2. Then, this syngas is synthesized into methanol at elevated temperature ($\sim 523.15K$) and pressure ($50 - 100$bar).[2] This process can be observed in **Fig. 2.5**. Close to 90% of produced methanol is produced as fMeOH [53]. However, its reliance on fossil-based SMR process and associated net-positive CO_2 emissions present a major challenge for sustainable development [43]. Consequently, focus should be on the development of eMeOH, that's produced with electricity from renewable sources.

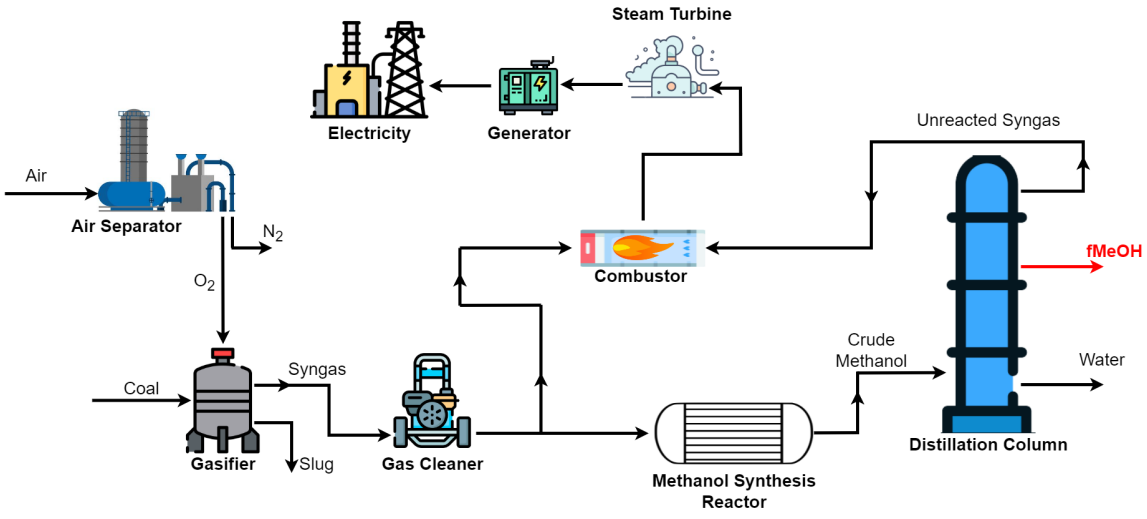

Figure 2.5
Graphical visualisation of fossil-based methanol production

As mentioned in **Sec. 2.1**, methanol can serve as an energy carrier for seasonally generated electricity. One of its key advantages over hydrogen and methane is that methanol remains liquid at ambient conditions, which makes it easier to store and transport. Additionally, studies show that methanol can be produced with higher overall efficiency compared to other chemical energy carriers.[45] Methanol is also a highly versatile product, it can be converted back into electricity, used directly in gasoline engines or upgraded to diesel substitute dimethyl-ether (DME). Furthermore, when produced from captured CO_2 and renewable electricity, methanol provides an excellent renewable carbon source for the chemical industry.[42]

A PtMeOH system typically incorporates an electricity source, an electrolysis unit, a carbon source, a methanol synthesis plant and a distillation plant. Layout of a eMeOH production plant can be observed in **Fig. 2.6**

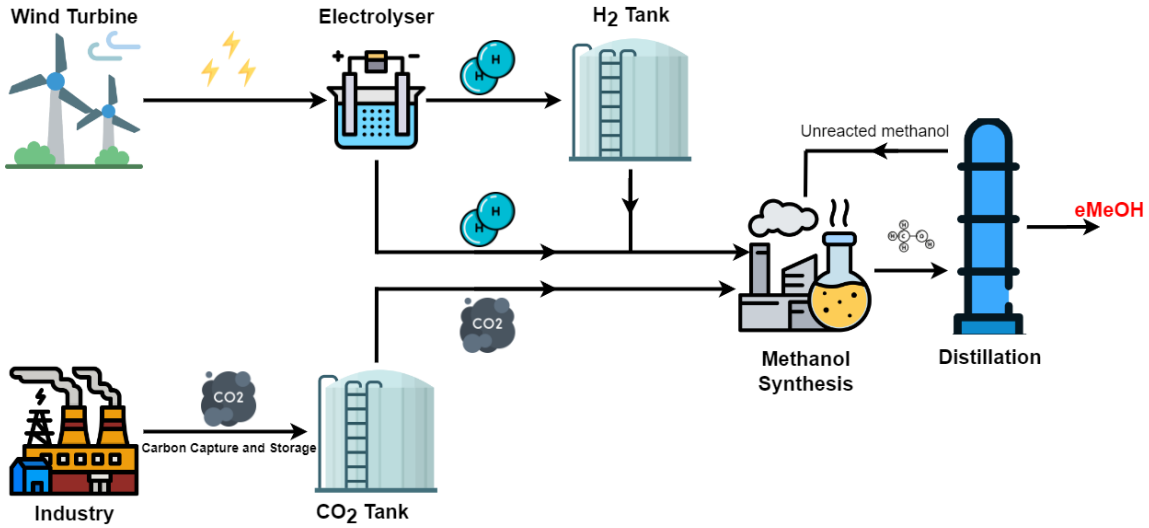

Figure 2.6
Graphical visualisation of electricity-based methanol production

Wind Turbine

Electricity generated from wind turbines is used to power water electrolysis, making the process fully renewable. The drop in electricity prices from wind power, alongside increasing capacity installations, significantly improves the economic feasibility of PtMeOH pathways. According to Adnan and Kibria [2], PtMeOH routes become cost-competitive when electricity prices fall below 3 cents per kWh. Additionally, electricity with a low carbon intensity ($<$130 gCO_2/kWh) is necessary to ensure climate benefits over fossil-based methanol.

Water Electrolysis and H_2 Storage

Renewable electricity power electrolysers, either PEM, ALK or SOEC types, which split water into H_2 and O_2, as explained in detail in **Sec. 2.1**. The produced hydrogen, which serves as the main feedstock for methanol synthesis, can either be used immediately or stored temporarily to buffer fluctuations in electricity supply and ensure stable reactor operation. Incorporating hydrogen storage increases plant reliability and helps align hydrogen production with the availability of renewable electricity.[43]

Carbon Capture and Storage

CO_2 is sourced from industrial point sources such as cement or power plant via carbon capture technologies, including chemical absorption and membrane separation. It is then compressed and stored in dedicated tanks. CO_2 supply is a critical component in the PtMeOH system, enabling the conversion of waste carbon into a valuable product. Recent advancements have made post-combustion capture economically viable, especially when integrated with CO_2 utilisation technologies.[47]

Methanol Synthesis Reactor

The methanol reactor receives a stoichiometric blend of H_2 and CO_2. Inside the reactor, these gases undergo catalytic conversion at 200-300 ℃ and 50-100 bar, primarily following the reactions:

$$CO_2 + 3H_2 \rightarrow CH_3OH + H_2O \tag{2.1}$$

$$CO + 2H_2 \rightarrow CH_3OH \tag{2.2}$$

$$CO_2 + H_2 \rightarrow CO + H_2O \quad \text{(Reverse Water–Gas Shift)} \tag{2.3}$$

The process uses a $Cu/Zn/Al_2O_3$ catalyst and benefits from syngas loop recycling, which maximises conversion and energy efficiency.[43]

Distillation and Product Purification

The reactor output, a mixture of methanol and water, is purified through distillation. The distillation column separates pure eMeOH($\geq$99%) from water and unreacted components. The unreacted gases are typically recycled back into the reactor, improving overall efficiency. Purification can account for up to 15% of the system's energy consumption.[14]

Produced eMeOH has both its own strengths and limitations, which are presented in **Tab. 2.4**.

Table 2.4

Advantages and Disadvantages of Power-to-Methanol.[14][42][43][53][2]

Power-to-Methanol	
✓ **Range of Application** – Used not only as a fuel but also as a feedstock in the chemical industry	X **Production Costs** – Current cost of green hydrogen and CO_2 capture makes eMeOH more expensive than fMeOH
✓ **Liquid** – Unlike hydrogen, methanol is a stable liquid at room temperature, easier to transport and store	X **Overall Efficiency** – Conversion from electricity to hydrogen and then methanol involves energy losses
✓ **Infrastructure Compatibility** – Can be blended with gasoline, used in combustion engines, or converted into other fuels	X **Source Dependency** – Production relies on sustainable CO_2 and purified water for electrolysis
✓ **Carbon-Neutral** – eMeOH is produced from green hydrogen and captured CO_2	

PtMeOH presents a highly promising pathway for transforming renewable electricity and captured carbon into a storable, transportable and carbon-neutral fuel. Its compatibility with existing infrastructure and broad applicability in both the energy and chemical sectors make eMeOH

a standout option among PtX options. However, its practical implementation relies heavily on the availability of affordable green hydrogen, captured CO_2 and a stable supply of renewable electricity. Since electricity pricing and generation pattern directly impact the efficiency and cost of eMeOH production, it is crucial to understand how renewable energy, especially wind power which serves as the primary electricity source in this project, is generated and priced. Therefore, the next section focuses on the operation of wind turbines and the mechanisms behind electricity price formation and fluctuations.

2.3 Wind Industry

The wind energy sector has emerged as one of the foundations of the global transition toward renewable energy. As a clean, abundant and cost-effective electricity source, wind power plays a vital role in decarbonising the global energy system. Technological improvements and supportive policies have significantly boosted wind power capacity in both developed and developing regions.[27] According to the latest statistics from the International Renewable Energy Agency (IRENA), wind energy accounted for approximately 9.0% of global electricity generation in 2022, which is significant increase from just 3.5% a decade earlier. Within the European Union, installed wind power capacity grew from 202 GW in 2020 to over 225 GW by 2023, showing the region's strong commitment to climate neutrality and energy security through domestic renewable sources.[46] **Fig. 2.7** shows how global wind share and installed power capacity in EU have changes in this century.

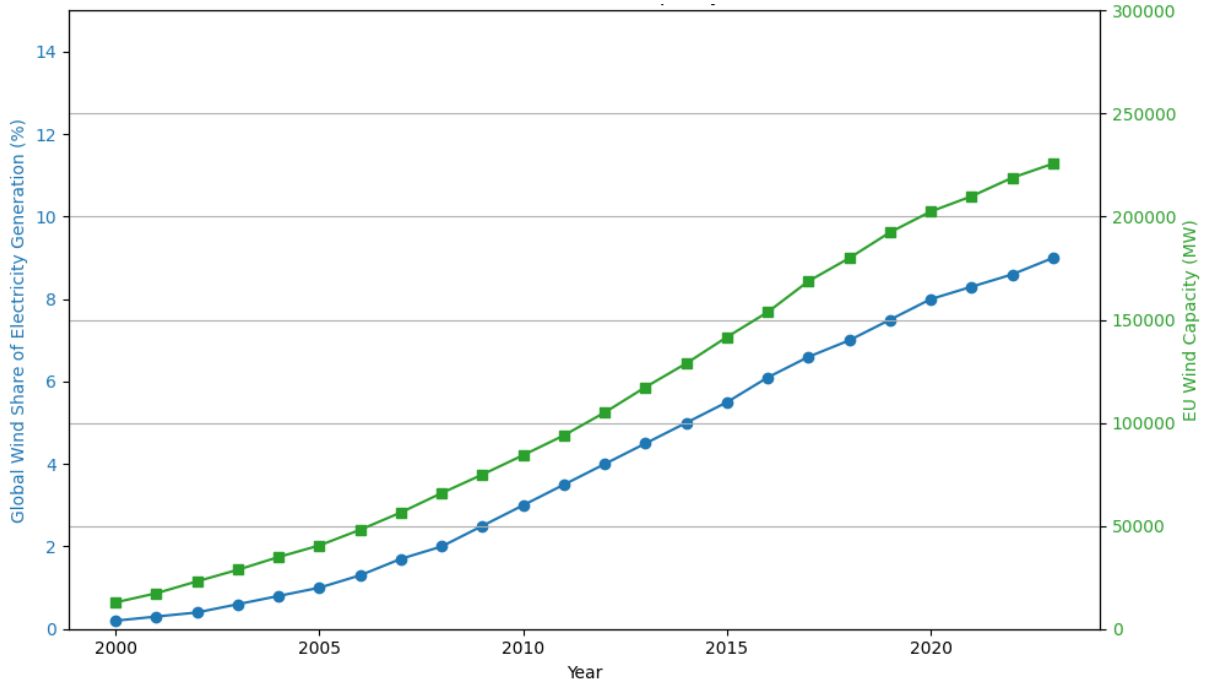

Figure 2.7

Graph showing global wind share(green) and installed wind capacity in European Union(blue).[20] [27] [46]

The rise of wind energy is not entirely a result of environmental objectives. Economically, wind power has become one of the most affordable sources of new electricity generation, outcompeting many fossil-based alternatives. With levelised costs (LCOE) for onshore projects that in average

are $30-75/MWh, it undercuts coal and gas in most markets [27]. This cost decline, driven by economies of scale and turbine efficiencies, position wind as central to national energy strategies [5].

This increasing share of wind power in electricity grids necessitates a comprehensive understanding of wind turbine operation. To evaluate the technical and economic viability of downstream applications such as PtX systems, it is essential to analyse how wind turbines generate electricity, which parameters govern their performance and how this electricity output changes in fluctuating wind conditions.

2.3.1 Wind Turbines - Mechanical

Wind turbines are electromechanical devices that convert the kinetic energy of moving air into electrical energy. This process forms the basis of modern wind energy systems and is critical for integrating renewable electricity into PtX technologies. The wind energy conversion system (WECS) consists of several integrated subsystems designed to optimise power capture, adapt to varying wind conditions and efficiently deliver electricity to the grid or local consumers.[56]

The most commonly deployed configuration is the horizontal-axis wind turbine (HAWT), see **Fig. 2.8**, in which rotor blades spin around a horizontal axis and face the wind via a yaw control system. These systems dominate both onshore and offshore markets due to their superior aerodynamic efficiency and scalability. Vertical-axis wind turbines (VAWT), while easier to maintain, are less efficient and generally limited to small-scale or urban applications.[1]

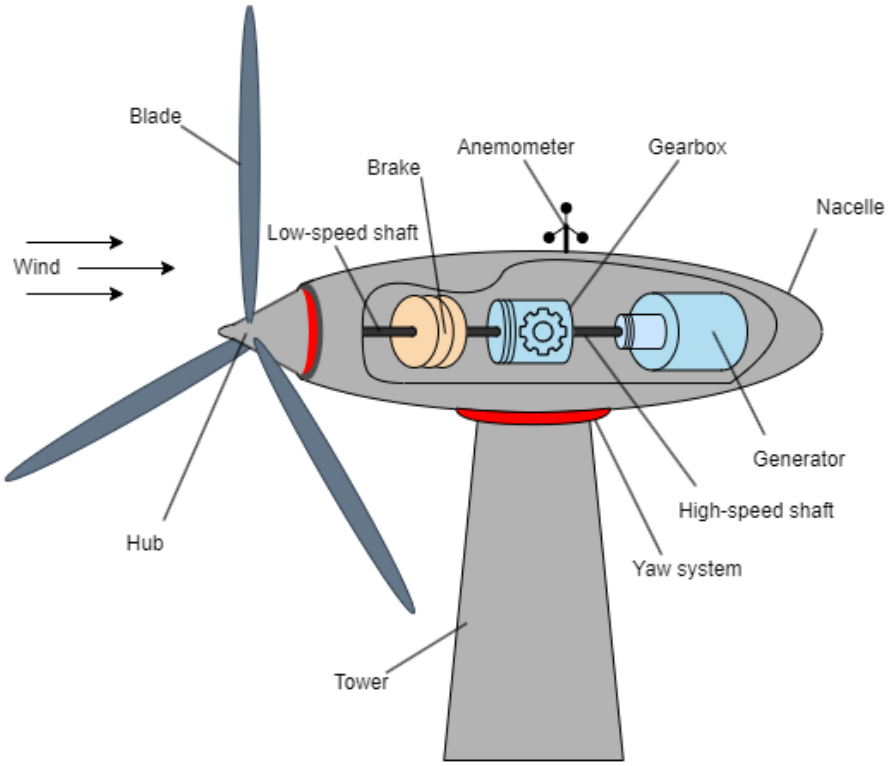

Figure 2.8
Graphical visualisation of HAWT, with key components being named.

Tower

The tower supports the nacelle and rotor, elevating them to heights where wind speeds are stronger and more consistent. Tower height typically ranges from 80 to 160 meters, depending on turbine size and site conditions. Taller towers increase energy yield but also impose higher structural and transportation demands.[2]

Rotor Blades and Hub

The rotor consists of two or three aerodynamic blades attached to a central hub. These blades are designed to extract kinetic energy from the wind using lift, like airplane wings. The blades are made from composite material (fibreglass or carbon fibre-reinforced polymers) to achieve a balance between strength and lightness. Blade length significantly affect energy capture, with longer blades increasing the swept area and potential power output.[1]

Nacelle

The nacelle carries key component including the gearbox, generator, brake system and control electronics. The gearbox converts the low-speed rotation of the rotor(10-20 rpm) into high-speed rotation, up to 1500 rpm, suitable for the generator. Some of the turbines use direct-drive systems that eliminate the gearbox, reducing maintenance and improving reliability, especially in offshore applications.[20] The generator converts mechanical energy from the rotating shaft into electrical energy. Most modern turbines use synchronous or asynchronous generators depending on the grid connection setup. Power electronics, such as inverters and transformers, ensure that the output is compatible with the grid in terms of frequency and voltage.[1]

Sub-Systems

The Yaw system rotates the nacelle to face the wind direction, maximising energy capture. Sensors continuously monitor wind direction and motors adjust the nacelle position accordingly. Yaw control is essential in HAWT to maintain alignment with the wind flow. Furthermore, each blade is connected to a pitch mechanics system that allows it to rotate along its longitudinal axis. This control adjust the angle of attack to optimise lift under different wind speeds. Modern turbines have active pitch control system for better load management and energy efficiency [43]. Lastly, wind turbines are equipped with embedded control systems that manage performance, monitor loads and ensure safe operations. Supervisory Control and Data Acquisition (SCADA) system is used for remote monitoring and diagnostics.

2.3.2 Wind Turbine - Operations

The electrical power produced by a wind turbine is primarily determined by the kinetic energy available in the wind and the turbine's ability to convert that energy into electricity. Since wind speed is highly variable, understanding how it influences power output is crucial for modelling and optimising wind-powered systems.

Available Wind Power

The theoretical power available from wind is given by:

$$P_{\text{wind}} = \frac{1}{2} \cdot \rho \cdot A \cdot v^3 \tag{2.4}$$

Where:

- P_{wind} - Power in watts (W),
- ρ - Air density (kg/m^3), typically 1.225 kg/m^3 at sea level,
- A - Swept area of the rotor ($A = \pi L^2$, in m^2),
- L - Blade length,
- v - Wind speed in meters per second (m/s).

This equation shows that the power increases with the cube of wind speed, meaning that small changes in wind can have a large impact on energy output.[57]

Betz Limit and Efficiency Factors

Due to physical constraints, it is not possible to capture all the kinetic energy from the wind. The Betz limit states that the maximum fraction of energy that can be extracted is 59.3% [44], defined by:

$$P_{\text{max}} = \frac{16}{27} \cdot P_{\text{wind}} \tag{2.5}$$

This theoretical maximum power is in real-world conditions reduced even further, where wind power is multiplied with efficiency factor that equals to:

$$\mu = (1 - k_m) \cdot (1 - k_e) \cdot (1 - k_{e,t}) \cdot (1 - k_t) \cdot (1 - k_w) \cdot C_p \tag{2.6}$$

where:

- C_p – Turbine efficiency (it must be lower than the **Betz limit (59.3%)** and is typically between 30–40%) [57];
- k_w – Wake losses due to neighbouring turbines and terrain topography, typically 3–10%;
- k_m – Mechanical losses of the blades and gearbox, typically 0–0.3%;
- k_e – Electrical losses of the turbine, typically 1–1.5%;
- $k_{e,t}$ – Electrical losses from transmission to the grid, typically 3–10%;
- k_t – Percentage of time out of order due to failure or maintenance, typically 2–3%;
- μ – Real efficiency.

Finally, the actual electrical power output is then equal to:

$$P_{\text{output}} = \mu \cdot P_{\text{wind}} \tag{2.7}$$

Due to structural limitations, wind turbines operates within defined limits of wind speed, which are:

- Cut-in speed $\sim 3\ m/s$; the minimum required for generation
- Rated speed $\sim 12 - 15\ m/s$; where turbine reaches peak capacity
- Cut-out speed $\sim 25\ m/s$; turbine shuts down for safety

Because wind is inconsistent, turbines rarely operate at rated capacity. Instead, the capacity factor, defined as the ratio of a turbine's actual energy output over a period to its theoretical maximum output if it operated at full capacity continuously:

$$CF = \frac{Actual\ energy\ Output(kWh)}{Rated\ Power(kW) \cdot time(h)} \tag{2.8}$$

Where CF equals to: [38]

- Onshore turbines - Typically 25-40% depending the site conditions
- Offshore turbines - Often exceed 50% due to steadier and stronger wind flows

High capacity factors indicate more efficient use of installed capacity and are essential for reducing the LCOE [20].

With a detailed understanding of wind turbine operation and its influence on electricity generation, the next step is to explore how this variable and weather dependent power supply interacts with electricity market mechanisms. In particular, it is essential to investigate how fluctuations in wind energy production impact electricity price dynamics and how these patterns shape the cost environment for energy processes like electrolysis.

2.4 Electricity Price Forecasting

Electricity generated from renewable sources such as wind and solar has become a central component of energy systems, especially in countries like Denmark with high levels of renewable penetration. While these sources are environmentally sustainable and cost-effective in the long term, they are also variable due to their dependence on weather and daylight conditions. This variability introduces significant challenges in electricity market stability and price formulation, as the supply of renewable electricity does not always align with real-time demand.

2.4.1 Nature of Renewable Power Variability

Renewable energy generation, particularly from wind and solar sources, is subject to fluctuations across multiple timescales and geographic locations. These variations comes from the dynamic nature of atmospheric and environmental conditions and they directly influence the stability of electricity supply. **Fig. 2.9** presents different types of nature changes and how they influence electricity output.

Short-Term Variability

Wind speed varies rapidly over seconds to minutes due to turbulence, gusts and micro-scale meteorological phenomena. Similarly, solar generation may experience short-term drops in output due to cloud cover or shading. These fast changes introduce operational uncertainty for grid operators, often requiring balancing mechanisms to maintain system stability. While such fast fluctuations do not impact day-ahead electricity prices, they contribute to operational uncertainty and influence the behaviour of market participants.[52]

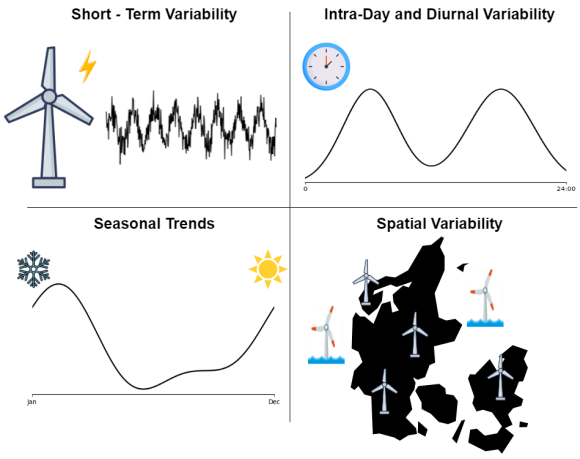

Figure 2.9
Graphical visualisation of different types of nature changes in wind power.

Intra-Day and Diurnal Variability

Both wind and solar energy demonstrate characteristic intra-day patterns. In Northern Europe, wind speeds often peak during the early morning and late evening, while slowing during midday when atmospheric stratification is strongest [29]. On the other hand, solar output follows a more predictable diurnal curve, peaking around noon and dropping to zero during the night. These temporal mismatches between renewable supply and electricity demand create price imbalances. For example, lower prices during nighttime wind surpluses or midday solar peaks, and higher prices during evening demand peaks with reduced generation.

Seasonal Trends

Yearly differences in wind energy production are primarily driven by large-scale climate patterns such as the North Atlantic Oscillation (NAO). These patterns can significantly affect wind speeds over the North Sea and surrounding areas, altering the expected generation and economic performance of wind projects from one year to the next.[26] Similarly, solar output is influenced by seasonal changes in sunlight hours and sun angle. While these long-term trends are more relevant for investment analysis, they also influence the baseline expectations in price modelling.

Spatial Variability

Wind and solar resources are not distributed evenly across regions. Factors such as terrain, altitude and proximity to coastlines influence wind conditions, while solar output is affected by latitude, cloud cover and local weather patterns. In Denmark notable differences exist between the western (DK1) and eastern (DK2) zones due to regional wind resources and transmission capacity. These spatial differences can lead to zonal price separations, especially when grid constraints prevent efficient energy transfer between regions.[19]

Understanding these sources of variability is essential for accurately capturing the behaviour of electricity markets dominated by renewable energy. Recognising the distinct temporal and spatial patterns of wind and solar generation enables better modelling of electricity prices and supports more effective optimisation strategies for flexible systems like electrolysers.

2.4.2 Price Formulation

Electricity prices in modern power markets are determined by the dynamic interaction of supply and demand, with renewable power playing an increasingly influential role due to its low marginal cost and variable output. This section outlines the key mechanisms and parameters that drive price formation in wind integrated electricity markets.

Each region in world has its own zonal electricity market where prices are forming, which for Denmark is Nord Pool day-ahead market. At zonal electricity market producers and consumers submit bids for each hour of the next day. Prices are determined by the intersection of the aggregated supply and demand curves, with the price set by the marginal unit, which is the last accepted offer needed to balance the system for a given hour.[49]

This process is based on marginal cost bidding, where each producer offers electricity at its short-run production cost. Renewable generators like wind and solar typically bid at or near zero marginal cost because they do not require fuel. As a result, renewable power displaces more expensive fossil-based generation in the merit order, driving down the market clearing prices. This phenomenon is widely known as the Merit Order Effect, shown in **Fig. 2.10**.[36]

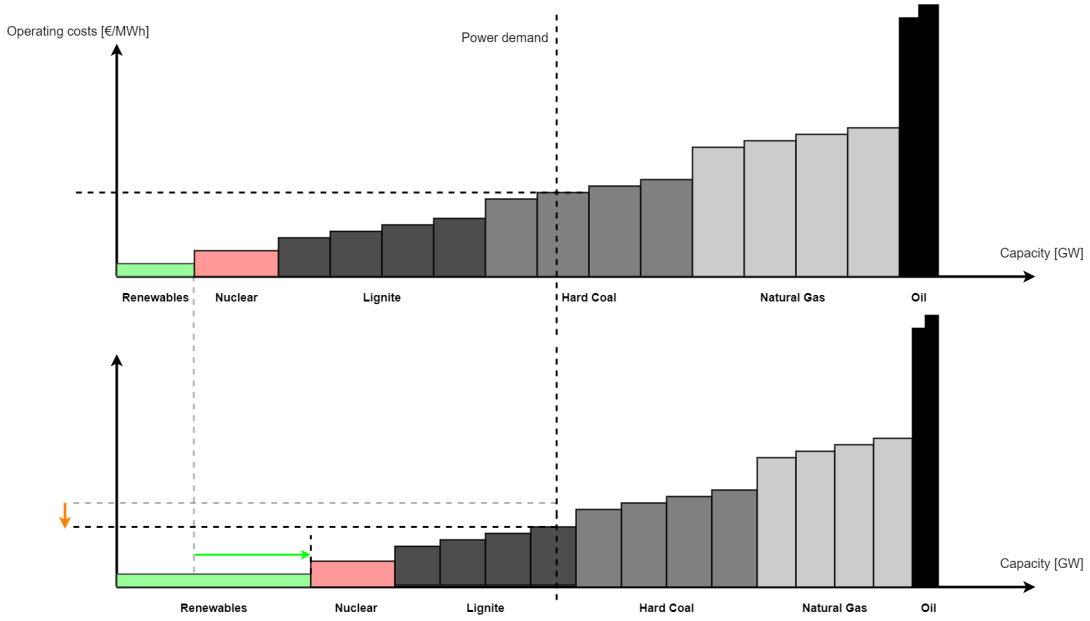

Figure 2.10

Graphical visualisation of Merit Order Effect, where increasing capacity of wind power reduces market prices.

Under conditions of high renewable generation and low demand, such as during night time, supply can exceed local demand. This situation often leads to negative electricity prices, where producers are effectively paying to stay online rather than shutting down, which may be costly or technically constrained.[36]

The main drivers of hourly electricity prices in renewable integrated systems can be grouped into several categories, which is shown in **Fig. 2.11**

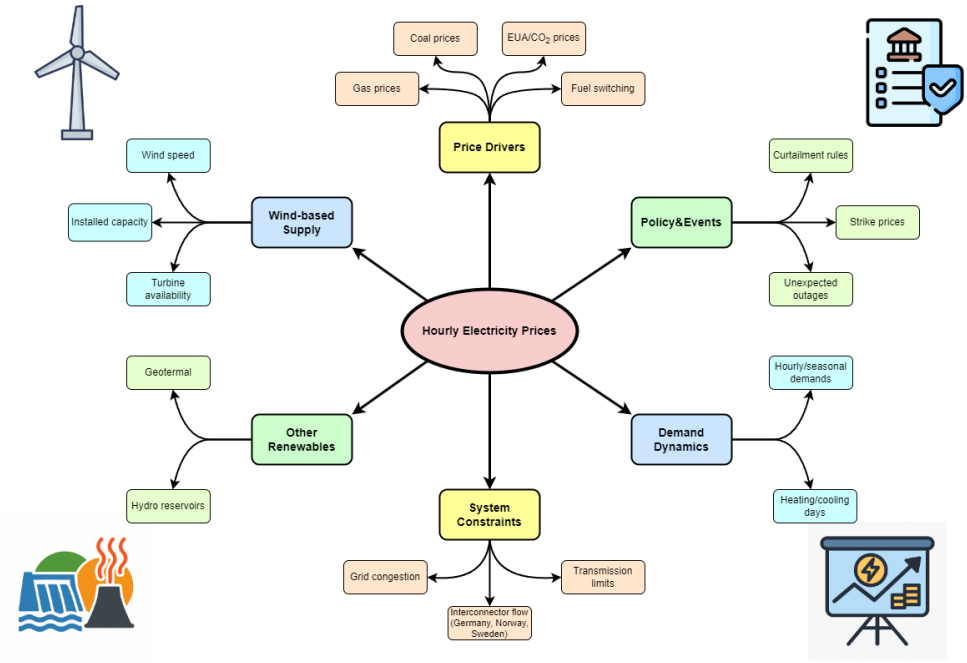

Figure 2.11
Mental map presenting drivers for hourly electricity pricing.

2.4.3 Input Parameters for Price Forecasting Models

Accurate short-term price predictions are essential for market participants, including flexible consumers such as energy storage systems, demand response unit and industrial processes powered by electricity. While forecasting techniques vary widely in complexity, they all depend on the selection of relevant input variables, commonly referred to as exogenous variables or features in predictive modelling.[41]

The forecast target in most electricity price modelling frameworks is the hourly zonal clearing price from the day-ahead market. Forecast horizons typically span 24 to 72 hours, depending on the decision-making context. In high-resolution models, price prediction can be extended to 15 minute intervals, especially in intra day markets or for real-time dispatch.[58]

Electricity price formation is both temporal and spatially dependent, requiring the inclusion of:

- Lagged variables - Historical values of electricity prices or generation
- Rolling averages - Moving averages of demand or generation
- Zone-specific data - Renewable forecasts and inter-connector flows for specific part of world

Multivariate modelling approaches often include hour-of-day, day-of-week and seasonality flags to capture recurring demand and supply structures [41].

Electricity prices in renewable-integrated markets are influenced by a wide set of technical, environmental, and market-related variables. As outlined in this section, accurate price forecasting might depend on selecting relevant exogenous inputs such as weather conditions, demand profiles, fuel markets, grid constraints and operational disruptions. These inputs provide the structural

foundation for time series or machine learning models to anticipate short-term price movements. While the specific modelling approach can vary, the richness and resolution of these features critically determine the model's performance and applicability for operational decision-making in modern electricity systems.

On the other hand, electricity forecasting model can be autoregressive, where most of the discussed external variables are not directly included in the modelling process. Nevertheless, a conceptual understanding of these drivers remains essential to interpret the forecasted prices and their implication for electrolyser optimisation.

2.5 Methanol Production

The methanol production process analysed in this section is developed in a collaboration with a parallel student group focused on designing the complete e-methanol synthesis system. Their design integrates green hydrogen produced via electrolysis, together with captured CO_2 stream, to generate synthetic methanol through catalytic synthesis. While the detailed engineering and process flow of the methanol plant fall outside the scope of this thesis, the layout and operational structure of their system provide the necessary boundary conditions for the electrolyser operation model developed in this thesis.

The electrolyser is the most electricity intensive unit in the system and presents the greatest opportunity for cost optimisation in response to fluctuating electricity prices. Importantly, the system is designed to achieve a predefined annual methanol production target, which imposes a hydrogen demand that the electrolyser must satisfy over the year. Therefore, the optimisation problem addressed in this thesis is not to maximise profit or track electricity prices blindly, but rather to determine how and at what capacity the electrolyser should operate, across three operational states, to meet this hydrogen demand at the lowest possible operational cost. Additionally, the model considers that the methanol synthesis reactor adjusts its hydrogen consumption efficiency based on the electrolyser's output, introducing a dynamic coupling that affects overall system performance.

Consequently, this section introduces the physical system layout, describes key assumptions and outlines specific input parameters that define the optimisation framework used throughout this thesis.

2.5.1 System Layout

The methanol production system evaluated in this work consists of two primary systems, an upstream electrolyser and a downstream methanol synthesis and distillation system. All hydrogen produced by the electrolyser is consumed by the MSR, creating a tightly coupled system. Methanol output is assumed to be nonlinear and influenced by both the quantity and continuity of hydrogen flow. The system, shown in **Fig. 2.12**, is used to meet a predefined annual methanol production target, which is translated into a cumulative hydrogen demand.

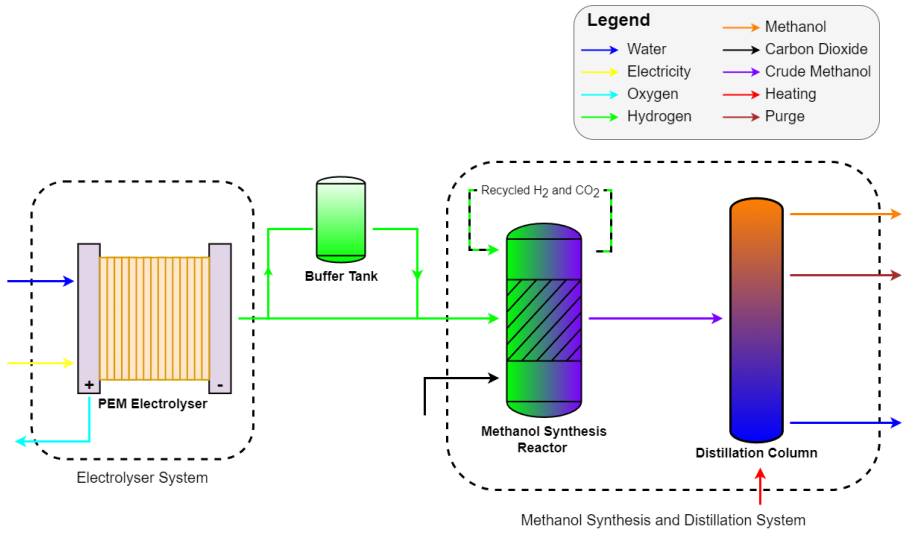

Figure 2.12
Simplified process flow diagram of the Power-to-Methanol (PtMeOH) system.

To ensure methanol synthesis continuity during transitions from running to standby or shutdown, a small hydrogen buffer tank is introduced, as shown in **Fig. 2.12**. This tank supplies the MSR with 17 $kmol\ H_2$ during a transition period of one hour. When the electrolyser resumes operation, the first 17 $kmol\ H_2$ produced is allocated to refilling the tank. Any remaining hydrogen is used by the MSR. This buffering logic governs temporary decoupling of production and demand.

The system is analysed over a total of 8760 hours, representing one year of operation. All system behaviour is modelled at an hourly resolution. For each hour, electrolyser is considered to be in one of three operational modes:

- **Running** - Hydrogen production
- **Standby** - Minimal electricity use to keep the unit warm and pressurised, but no hydrogen output
- **Shutdown** - Completely off, with no electricity consumption or hydrogen output

Transition between these modes are only allowed at the beginning of an hour. Once a mode is set for a given hour, it remains fixed for that entire interval. These operating rules reflect technical constraints such as thermal cycling limits and ramping behaviour.

The methanol reactor is assumed to operate continuously, and its conversion ration is tied to the hydrogen supplied from the electrolyser. The relationship between hydrogen and methanol production, along with other system specific parameters, is described in the following sections.

2.5.2 Electrolyser System

The electrolyser unit used in this thesis is based on Siemens Silyzer 300, a state-of-the-art PEM electrolyser designed for industrial scale hydrogen production[50]. In this layout, three Silyzer 300 modules are installed and operated in parallel, providing the necessary hydrogen supply for the methanol synthesis process. The system is modular, highly dynamic and capable of fast load

changes, making it well suited for integration with fluctuating renewable electricity. **Fig. 2.13** captures simplified schematic of the electrolyser system layout.

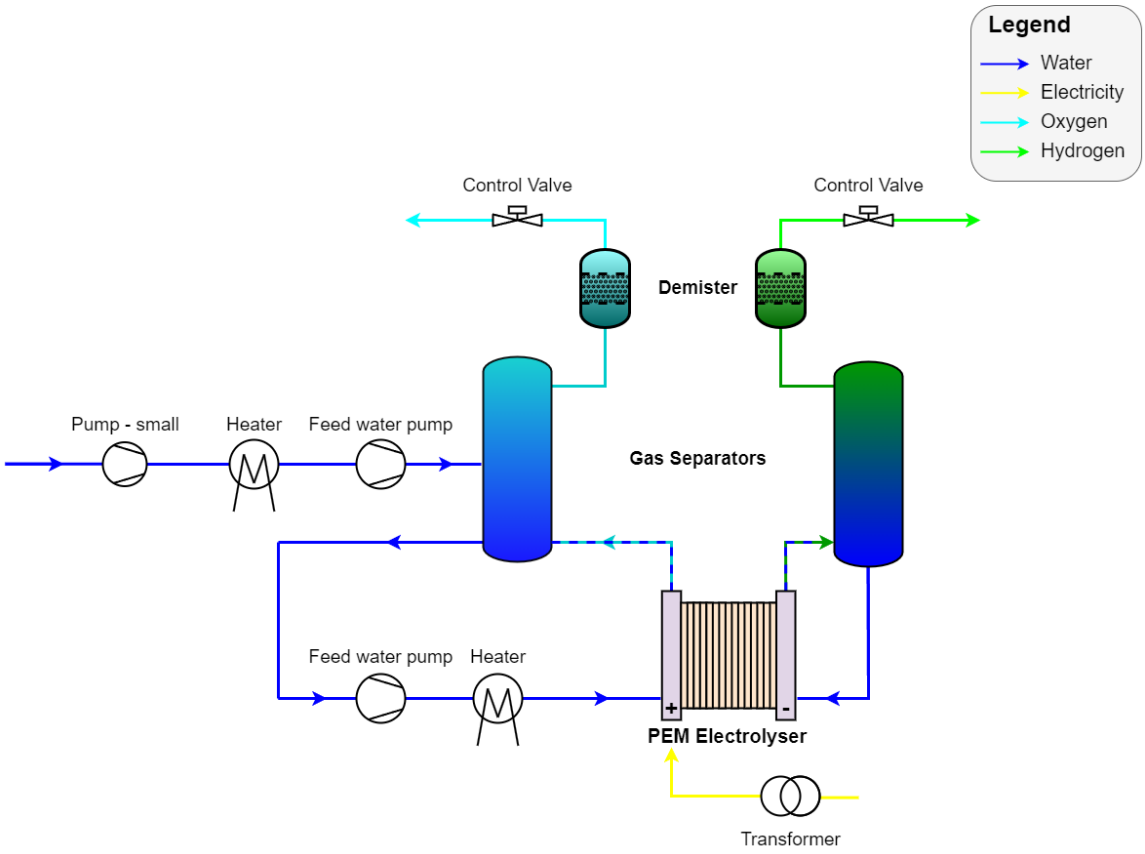

Figure 2.13
Detailed process flow of the PEM electrolyser system, illustrating water circulation, gas separation, and demisting.

As shown in **Fig. 2.13**, water is supplied through a series of pumps and heaters, ensuring the feed water is pressurised and preheated to optimal conditions before entering the electrolyser stack. Inside the PEM electrolyser, water is split into H_2 and O_2 using electrical energy supplied through a dedicated transformer, which transforms AC to DC electricity. The produced gases are subsequently separated in dedicated gas separator units. To improve product purity and system safety, demisters are used to remove residual water droplets from both the hydrogen and oxygen streams before final control valves regulate their output. The hydrogen flow continues towards the MSR.

Operational Modes

The electrolyser can operate, as mentioned previously, in three distinct states, each representing a different energy and hydrogen production behaviour:

- **Running:** The electrolyser is actively producing hydrogen and consuming electricity. In this state, it can run at different percentage levels of nominal load. Each level corresponds to different electricity consumptions and hydrogen production values, shown in **Tab. 2.5**
- **Standby:** The electrolyser is not producing hydrogen but remains warm and pressurised,

allowing for faster restart, for which small portion of electricity has to be used.

- **Shutdown:** The electrolyser is completely off, with zero electricity consumption or hydrogen output. Restart from this state takes slightly longer compared to standby.

Values for used electricity and produced hydrogen, across different states, are presented in **Tab. 2.5**

Table 2.5

Electrolyser power consumption, hydrogen production rate, and efficiency at different load levels.

Load Level	Power Consumption [kW]	H_2 Production [kmol/h]	Efficiency [%]
Shutdown	0	0	-
Standby	165	0	-
40 %	17064.08	172.468	77.5
50 %	21961.85	215.585	75.8
60 %	27098.38	258.700	74.1
70 %	32471.63	301.820	72.3
80 %	38080.09	344.940	70.7
90 %	43922.57	388.050	69.1
100 %	49998.09	431.170	67.5

Transition Logic

As mentioned in **Sec. 2.5.1**, the electrolyser can only switch states at the beginning of each hour. Once a mode is set, it is maintained for the full hour. However, transitions between operational states are not instantaneous steps, they require transition periods, which introduce both time delays and energy costs. These transitions are critical to capture in the optimisation model, as they impact both hydrogen availability and electricity consumption. The allowed transitions are visualised in **Fig. 2.14**.

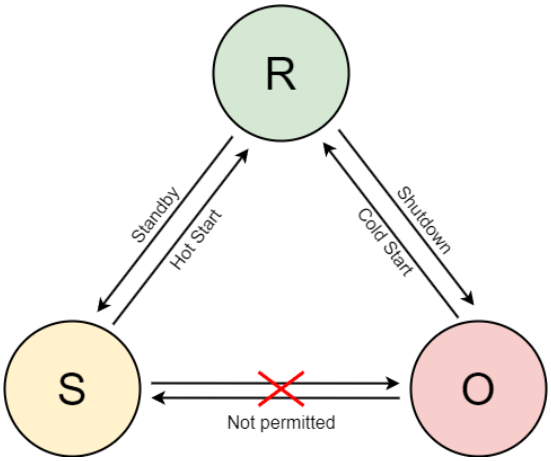

Figure 2.14

Electrolyser operational state transitions.

Following transitions are captured:

- ***R* → *S* – Standby**:
  This transition involves a controlled ramp down of the electrolyser over a defined transition period, during which hydrogen output decreases while the system continues to consume a reduced amount of electricity to maintain thermal and pressure conditions. At the same time, the MSR begins its own one hour transition to standby mode. To keep the MSR active during this ramp down, 17 $kmol\ H_2$ is taken from a buffer tank. This transition is technically smoother and less costly than a full shutdown but still incurs operational energy costs.

- ***S* → *R* – Hot Start**:

Hot start transition benefits from the electrolyser being already warm and pressurised, allowing for a faster return to hydrogen production. Although quicker than a cold start, it still incurs a defined energy cost. Upon resuming operation, the electrolyser first refill the 100 $kmol\ H_2$ used from the buffer tank before supplying any hydrogen to the MSR. In the following hour, the MSR resumes full production, aligned with the electrolyser's output

- $\boldsymbol{R \rightarrow O}$ – **Shutdown**:
  Complete ramp down of the electrolyser is involved in this transition, resulting in zero hydrogen production and electricity consumption. The process takes same time as the standby transition. During this transition, the MSR again requires 100 $kmol\ H_2$ from the buffer tank to complete its own standby transition.
- $\boldsymbol{O \rightarrow R}$ – **Cold Start**:
  This cold start transition represent the most energy intensive and time consuming change of state. The electrolyser must be reheated and re-pressurised from ambient conditions, leading to increased electricity consumption during startup. As with the hot start, the first 100 $kmol\ H_2$ produced is still used to refill the buffer tank before the MSR can resume full scale operation.
- $\boldsymbol{S \not\rightleftharpoons O}$:
  Transitions between standby and shutdown are not allowed in the model. These are considered technically feasible but economically inefficient, as they incur additional cycling stress and low system utilisation. Preventing these transitions simplifies the model and reflects strategies aimed at reducing wear and minimising unproductive switching.[61]

Tab. 2.6 captures values for costs and durations of previously mentioned transitions.

Table 2.6

Transition durations and associated costs between electrolyser load levels. Transitions between Standby (S) and Shutdown (O) are not permitted.

Load Level	**Duration [min]**	**Cost [DKK]**
R → S	6	-
S → R	2	82.50
R → O	6	-
O → R	42	1200
S ⇌ O	Not Allowed	

The operation of the electrolyser is not only influenced by electricity price dynamics and transition costs, but also by the requirements of the downstream methanol synthesis reactor. As all produced hydrogen is directly consumed by the MSR, any changes in electrolyser state have immediate implications for methanol production. To ensure stable and continuous methanol output, the interaction between the electrolyser and MSR, including transition timing, buffer usage and production levels, must be carefully coordinated. The following section introduces the methanol synthesis system, its hydrogen dependency and the key modelling assumptions governing its integration with the electrolyser.

2.5.3 Methanol Synthesis and Distillation System

The downstream methanol production system consist of two major subsystems, the methanol synthesis reactor (MSR), see **Fig. 2.15** and the distillation column, see **Fig. 2.16**. These units operate in sequence and are directly dependent on the hydrogen flow rate from the upstream electrolyser. Consequently, any fluctuations in electrolyser capacity immediately impacts the performance and energy consumption of the MSD system. The following subsections describe each unit individually, along with their modelling assumptions, operating constraints and key parameters used in the optimisation model.

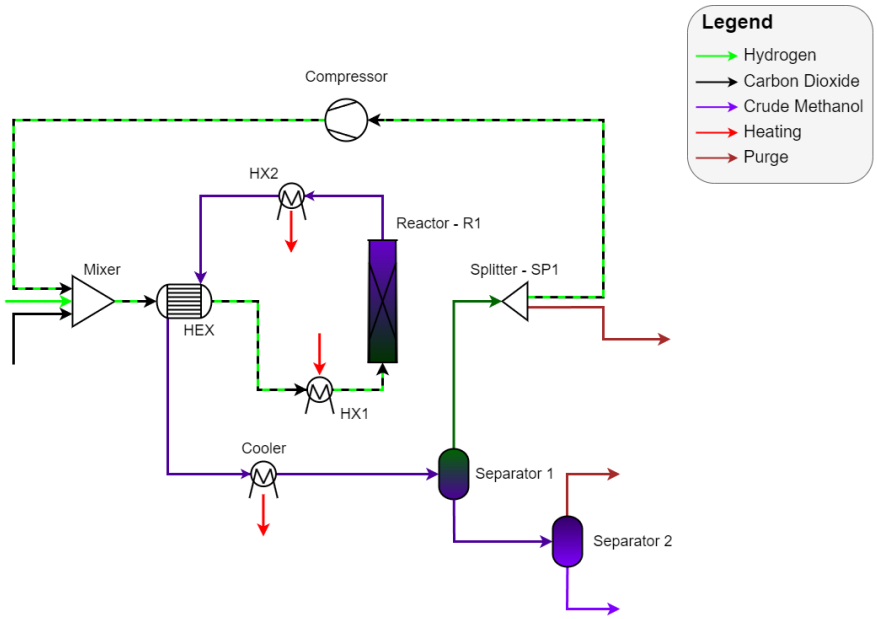

Figure 2.15
Process flow diagram of the methanol synthesis reactor system.

Methanol Synthesis Reactor - MSR

The MSR receives a hydrogen flow of 450 $kmol/h$ from the electrolyser under nominal load. This is combined with a CO_2 input of 150 $kmol/h$, following the stoichiometric requirement of a $3:1$ $H_2:CO_2$ ratio. The CO_2 stream is assumed to be continuously available from upstream carbon capture units, and its supply and variability are considered outside the scope of this project. The gas mixture is compressed and preheated in HEX(for initial start of production, mixture is heated with HX1) before entering the catalytic reactor R1, where methanol and water are formed.

After the reactor, the hot stream is cooled in heat exchanger HX2, recovering approximately 1.59 MW of thermal energy. This heat is transferred to the reboiler in the distillation section, reducing external heating demand. As the crude methanol-water mixture continues downstream, it undergoes further cooling before reaching the separator (SEP 1). The associated low-grade heat from this second cooling step is considered surplus and is assumed to be sold to a district heating network, providing additional value from excess thermal energy.

Following separation, approximately 4.12 $kmol/h$ of hydrogen is purged to stabilise the recycle

loop after splitting with SP1, while the remaining unreacted gases are compressed and returned upstream. Crude methanol from SEP 1 is depressurised is passed down to SEP 2. This pressure drop causes dissolved unreacted gases to be released. The separated gases are removed from the system through valve outlet, while the degassed crude methanol with water is directed to the distillation section for further purification.

The reactor is designed to operate within a minimum load threshold of 40% of nominal hydrogen input. Below this point, temperature control and reaction kinetics become unstable and methanol production is not feasible.

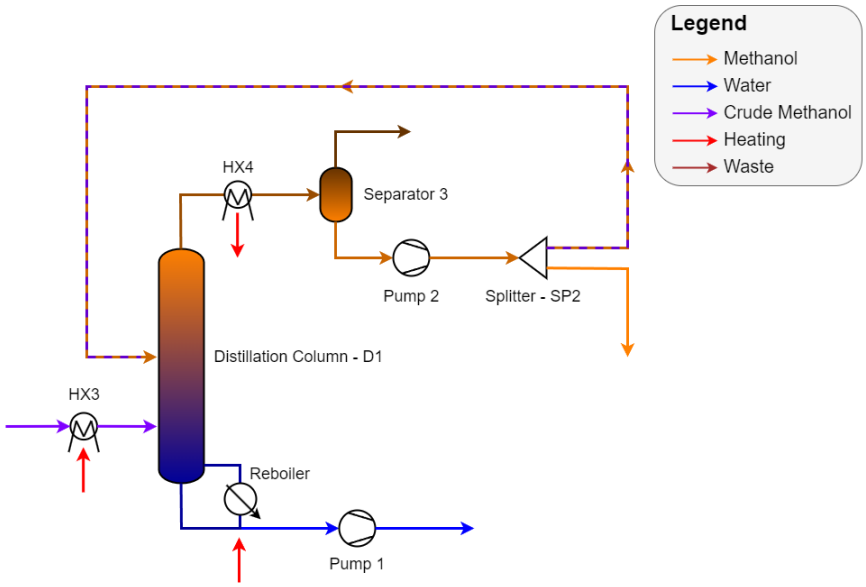

Figure 2.16
Process flow diagram of the methanol distillation system.

Distillation Column

As shown in **Fig. 2.16**, the distillation system D1 receives the crude methanol-water mixture feed, that was previously depressurised and preheated. The column is powered by a reboiler with a nominal energy demand of 2.93 MW, partially offset by the heat recovered from HX2.

Reboiler heats column to $\sim 60°$, where methanol evaporates while water stays at the bottom of the column. Overhead vapours are condensed at HX4 and separated at SEP3 into gaseous and liquid fractions. The purified methanol stream passes through pumps and valves to SP2, where unreacted methanol is transferred back to distillation column. Produced methanol under nominal production has a final flow rate of 146.8 $kmol/h$, which is approximately 4700 kg/h. Remaining water is with the help of pumps removed from the system.

The MSD system is highly sensitive to variations in electrolyser output, as hydrogen flow directly governs both the reaction rate in the MSR and the availability of feedstock for the distillation column. The thermal integration between HX2 and reboiler further links the performance of these two units, making coordinated operation essential for system efficiency. By modelling the MSD section with these dependencies and process constraints, the optimisation framework can realistically evaluate how electrolyser operation strategies impact final methanol production,

energy consumption and overall production feasibility.

Optimisation Parameters Summary

To enable the development of a realistic and constraint optimisation model, the most relevant technical and operational parameters from electrolyser, MSR and distillation column are summarised in **Tab. 2.7**. These values define the system's physical boundaries, energy requirements and coupling logic between subsystems. All values are based on nominal operating conditions, unless stated otherwise.

Table 2.7

Key technical and operational parameters of the main components in the Power-to-Methanol (PtMeOH) system.

Component	Parameter	Value [Unit]	Description
Electrolyser	Operational load levels	40 - 100 [%]	Discrete states
	Electricity consumption	49 998 [kW]	At 100% load
	Standby consumption	166 [kW]	No H_2 output
	H_2 Production rate	431.17 [kmol/h]	At 100% load
	Transition duration, on	2 / 42 [min]	S → R / O → R
	Transition cost	82.50 / 1200 [DKK]	S → R / O → R
Buffer tank	Capacity	17 [kmol]	MSR standby transition
	Recharge/Discharge	1 [h]	Supplies MSR for 1 hour
MSR	Stable operating range	≥40 [% H_2 load]	Reactor threshold
	CO_2 input flow	150 [kmol/h]	Fixed 3:1 H_2:CO_2 ratio
	Heat Surplus – HX2	–1590 [kW]	Reused in reboiler
	Surplus heat to district heating	111 [kW]	From post-reactor cooling before SEP
Distillation	Reboiler energy demand	2930 [kW]	Heating distillation column
	Compressor consumption	334 [kW]	For MSD process
	Heat exchanger – HX3	349 [kW]	Heating distillation column
	Final methanol output	146.8 [kmol/h]	At full electrolyser load

The values presented in **Tab. 2.7** form the quantitative foundation for the optimisation framework developed in the **Sec. 4.2**. By combining fixed operating states, transition costs, heat recovery potentials and subsystem dependencies, the model can accurately reflect the dynamic and interconnected nature of PtMeOH process. This enables the formulation of an optimisation strategy that balances electricity costs, equipment constraints and methanol production targets.

2.6 Summary

This chapter provided the contextual and technical foundation for the thesis. It introduced Power-to-X technologies with a focus on Power-to-Methanol, examined the generation and pricing of renewable energy, and explored the implications of electricity price variability. **Sec. 2.5** outlined the methanol production setup developed in collaboration with the partnering group, identifying the main input parameters relevant for optimisation. While wind energy remains the primary focus, solar generation is also included in the forecasting model to improve accuracy. However, due to its predictable diurnal and seasonal patterns, solar power is not technically analysed in this chapter.

Problem statement 3

E-methanol production systems that rely on electrolyser, shown in **Sec. 2.5**, face challenges in minimising operational costs due to the volatility of electricity price in wind industry. Since electricity is the dominant cost driver, it is essential to align hydrogen production with hours of lower electricity prices. However, the objective is not to maximise profit by exploiting price fluctuations, but to ensure that the system meets a fixed methanol production target over a year in the most cost-effective way. Electricity price forecasting serves as a support tool to identify when the electrolyser should operate, and at what capacity, while navigating between three operational states. The optimisation framework developed in this thesis focuses on how to minimise total operational costs while satisfying downstream hydrogen requirements, rather than increasing output based on market opportunities.

This leads to the final problem statement:

How can the operation of an electrolyser in an e-methanol production system be optimised to minimise total operational costs over a one-year horizon, while ensuring a fixed e-methanol production target is met, using renewable electricity price forecasts in Denmark as guidance for scheduling decisions?

3.1 Design Requirements

The goal of this thesis is to develop an optimisation approach for the operation of an electrolyser, supported by short-term electricity price forecasting. To guide the development process, the following design requirements have been defined:

- **Electricity Price Forecasting** - A forecasting model must be developed to estimate hourly electricity prices over a one-year period using historical data and relevant time-based patterns.
- **Developed Forecast Model** – The forecasting model has to base its predictions solely on renewable electricity generation (onshore wind, offshore wind, solar) and electricity demand, to align with the focus on PtX applications.
- **Forecast Integration** - The electricity price forecasts must serve as inputs for the optimisation model, enabling hour-by-hour decision making.
- **Operational Modes** - The optimisation model must include at least three discrete operational states for the electrolyser: running, standby, and shutdown, each with its own energy and transition behaviour.

- **Hourly Decision-Making** - The optimisation model must determine the electrolyser's operational mode on an hourly basis, aligned with the resolution of the forecast input.
- **Economic Response** - The model must prioritise cost-efficient operation, clearly demonstrating lower total operational costs compared to non-optimised or fixed scheduling approaches, while ensuring the annual e-methanol production target is met.

3.2 Delimitation

This section highlights the areas that were intentionally excluded to maintain a focused and manageable project scope. The following delimitations have been identified:

- **Electricity Market Modelling** - This thesis does not aim to replicate or model the full complexity of the Nord Pool electricity market. The price forecasting components serve only as a supportive tool for the optimisation task and is not intended to predict extreme market behaviour or capture detailed market bidding structures.
- **Economic Policy Uncertainty** - The model does not account for long-term price uncertainty, fuel market fluctuations, policy changes or carbon taxation scenarios. Price inputs are assumed to be known, either through historic data or short-term forecasting.
- **Real-Time System Integration** - Implementation into a live control system or production environment is outside the scope. The optimisation is developed as a decision-support tool for offline or day-ahead scheduling scenarios.

Methodology 4

This chapter presents the methodological approach used to address the problem defined in **Chap. 3**. Chapter outlines the methods applied to develop the forecasting and optimisation models, therefore, it is structured in two parts. **Sec. 4.1** describes the approach to forecasting electricity prices, presenting two modelling strategies and explaining how they are combined into a hybrid method. **Sec. 4.2** introduces the optimisation framework, which determines the hourly operational schedule of the system. While the electrolyser is the primary control point in the optimisation process, the downstream methanol synthesis and distillation system is fully coupled to its operation. As such, changes in electrolyser scheduling directly affect methanol output and overall system performance. The electricity prices predicted by the forecasting model serve as input to the optimisation model, ensuring decision-making across the full production chain. Together, these components form the core methodology for evaluating cost-efficient and demand-driven e-methanol production.

4.1 Electricity Forecasting Framework

Accurate short-term electricity price forecasting is essential for cost-efficient operation in processes such as electrolysis. This section presents the methodology used to forecast hourly electricity prices over a 24-hour horizon. Two modelling approaches are evaluated, one using exogenous input features and one based on autoregressive principles, followed by a detailed description of the selected forecasting framework.

4.1.1 Method Selection

Two main approaches were considered for short-term electricity price forecasting. The first is an exogenous model that incorporates external predictors. The second is an autoregressive model that relies solely on historical price patterns and time-based variables. The selection between these methods is based on subjective evaluation of factors such as accuracy, simplicity, data requirements and suitability for integration with the optimisation framework.

Exogenous Forecasting Model

Exogenous models aim to predict electricity prices by incorporating external variables that are known to drive price formation. Models rely on multiple predictors that drive electricity prices, such as:

- Wind and solar generation forecasts

- Load demand
- CO_2 prices
- Fuel prices
- Time and location effects

Such models are often implemented using machine learning techniques capable of capturing complex, non-linear relationships. Their strength lies in representing real-time market dynamics when high-quality and timely data is available.[37] Model's strengths and limitations are presented in **Tab. 4.1**.

Table 4.1
Advantages and Disadvantages of Exogenous Models.[37][41]

Exogenous Models	
✓ **High Accuracy** – Performs well when external forecast inputs are reliable	X **Data Dependency** – Strong reliance on availability and quality of external data
✓ **Realistic Dynamics** – Captures market and system behaviour more effectively	X **Complexity** – More difficult to implement, maintain, and troubleshoot
✓ **Multivariable Interaction** – Capable of modelling relationships between multiple influencing factors	X **Poor Suitability for Lightweight Use** – Less ideal for rapid or minimal-resource deployment
	X **Forecast Sensitivity** – Prone to error propagation from inaccurate upstream inputs

Autoregressive Forecasting Model

Autoregressive models take a data-driven approach based solely on the historical behaviour of electricity prices and time-related features such as the hour of the day and day of the week. They are rooted in classical time series forecasting methods but can also be enhanced with machine learning algorithms such as XGBoost to improve non-linear pattern recognition [62]. These models are well established in the literature and are particularly favoured for their simplicity, speed and independence from external data [58]. Autoregressive model has both its own advantages and disadvantages, which are presented in **Tab. 4.2**

Table 4.2
Advantages and Disadvantages of Autoregressive Models.[58][62][39]

Autoregressive Models	
✓ **Lightweight and Self-Contained** – Simple structure that does not rely on external inputs	X **Limited Responsiveness** – Cannot capture unexpected price spikes such as wind drops or market shocks
✓ **Data Robustness** – Performs well even when external data is missing or delayed	X **Volatility Sensitivity** – Accuracy may decline under highly volatile conditions
✓ **Interpretability** – Easy to understand and maintain	X **Market Blindness** – Does not reflect trends in fuel or emissions markets
✓ **Quick Deployment** – Fast to train and deploy, suitable for time-sensitive applications	

Method Selection

Tab. 4.3 summarises presented methods by subjective criteria parameters, based on knowledge provided from literature.

Table 4.3

Table showing different aspects of two presented models within subjectively selected criteria parameters.

Criteria	Exogenous Model	Autoregressive Model
Inputs	Wind, demand, CO_2, time features	History data, time features
Accuracy	High(with reliable inputs)	Moderate
Complexity	High	Low
External dependency	Required	None
Implementation time	Long	Short
Integration suitability	Moderate High	High

As shown in **Tab. 4.3**, and mentioned in previous subsections, it is clear that both methods have their own strengths and limitations. To address the limitations of both models, a hybrid approach is adopted in this thesis. In this method, external price-driving variables such as renewable generation and electricity demand are first forecasted using separate data-driven models. These forecasts are then used as input features in an XGBoost AR model for electricity price forecasting.

This hybrid approach allows the forecasting system to maintain the structural simplicity and interpretability of AR models while also accounting for real-time external system dynamics. Such approaches have shown strong performance in academic literature, particularly in volatile electricity markets where both internal and external patterns influence prices [39].

4.1.2 Hybrid Method

The hybrid forecasted method used for forecasting electricity prices integrates two powerful modelling strategies to improve both the realism and robustness of prediction. In the first stage the Recurrent Neural Network (RNN) is used to estimate future system conditions. Second stage uses a structured machine learning model to estimate electricity prices based on those conditions. The reason for this design is to capture both long-term temporal dynamics and complex multivariable relationship, which are typical for electricity market behaviour. Structure of hybrid model is presented in **Fig. 4.1**.

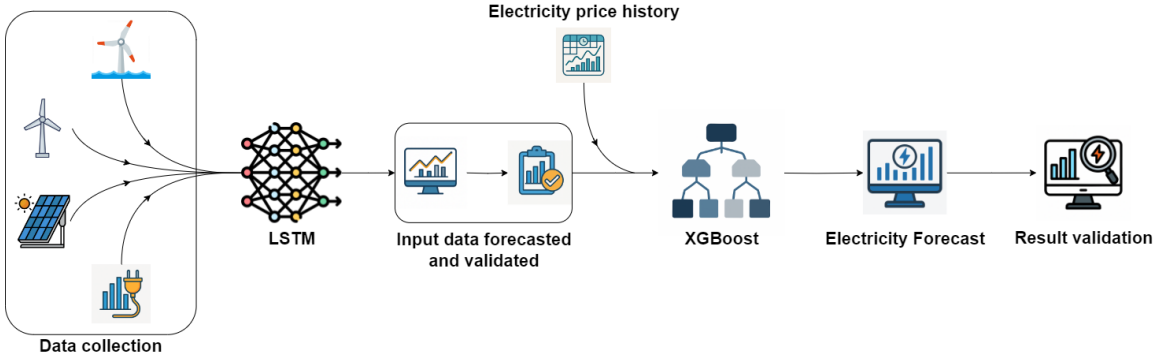

Figure 4.1

Graphical visualisation of hybrid model used to forecast electricity.

First Stage - Input Parameters Forecasting

Long Short-Term Memory (LSTM) networks are a class of RNN specifically designed to overcome the limitations of standard RNNs when dealing with long sequences. They are capable of learning patterns with long-range dependencies and are especially well-suited for forecasting in time series data where both seasonality and sudden shifts may exist.[30] LSTM architecture is built from a series of interconnected components called memory blocks. These blocks are designed to retain information over time and control the flow of data using non-linear gating mechanisms. As shown in **Fig. 4.2**, LSTM block includes input signals x^t, outputs y^t, activation functions, various gates and peephole connections, which allows the gates to access the internal cell state directly, improving the network's ability to learn precise timing-based patterns.

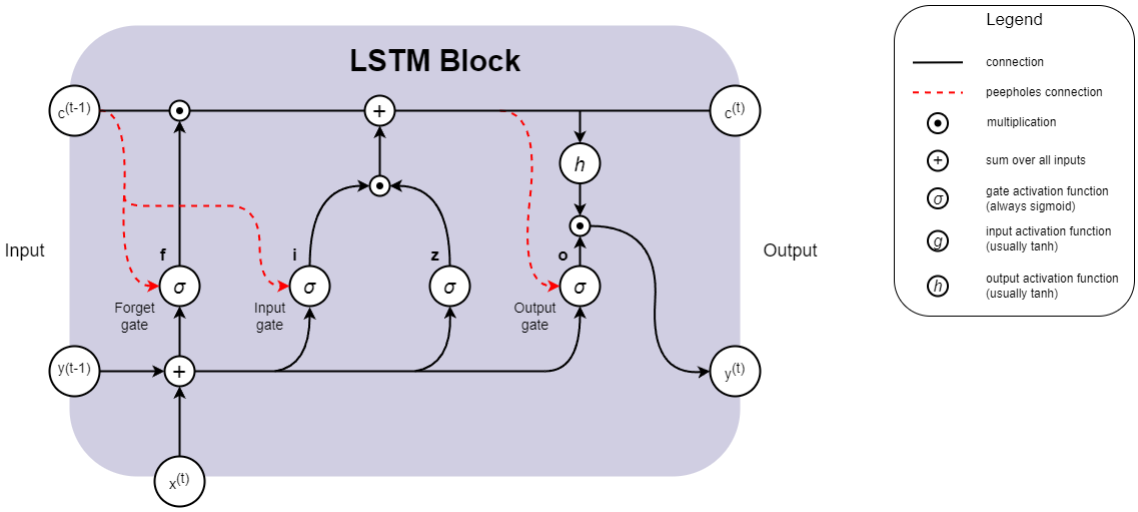

Figure 4.2
Graphical visualisation of LSTM Block and logic it uses.

Model starts its iteration at **Block input**, in bottom left corner, which combines the current input $x^{(t)}$ and the output of previous iteration $y^{(t-1)}$. This can be shown with following equation:

$$z^{(t)} = g\left(W_z x^{(t)} + R_z y^{(t-1)} + b_z\right) \tag{4.1}$$

Where W_z and R_z are the weights associated with $x^{(t)}$ and $y^{(t-1)}$ while b_z stands for the bias weight vector.

Next step is update at the **Input gate**, which is performed with the combination of current input $x^{(t)}$, the output of previous iteration $y^{(t-1)}$ and the cell value $c^{(t-1)}$ from previous iteration, which could be defined as in **Eq. 4.2**. The cell state is the internal memory of an LSTM unit, designed to carry information across time steps.

$$i^{(t)} = \sigma\left(W_i x^{(t)} + R_i y^{(t-1)} + p_i \odot c^{(t-1)} + b_i\right) \tag{4.2}$$

Where $\odot$ denotes point-wise multiplication of two vectors. W_i, R_i and p_i are the weights for mentioned parameters while b_i is bias vector.

At **Forget gate** the LSTM layer decides which information from the previous cell state $c^{(t-1)}$ should be discarded. To achieve this, the forget gate activation values $f^{(t)}$ are computed at time step t, using the current input $x^{(t)}$, the previous output $y^{(t-1)}$, the prior cell state $c^{(t-1)}$, peephole connections and the forget gate bias term b_f. The calculation is performed as follows:

$$f^{(t)} = \sigma\left(W_f x^{(t)} + R_f y^{(t-1)} + p_f \odot c^{(t-1)} + b_f\right) \tag{4.3}$$

Here, W_f, R_f, and p_f represent the weight matrices linked to the current input $x^{(t)}$, the previous output $y^{(t-1)}$, and the prior cell state $c^{(t-1)}$, respectively.

Cell state values are updated by combining the block input $z^{(t)}$ with the input gate $i^{(t)}$ and the forget gate $f^{(t)}$, along with the previous cell state. This process can be expressed as:

$$c^{(t)} = z^{(t)} \odot i^{(t)} + c^{(t-1)} \odot f^{(t)}. \tag{4.4}$$

At **Output gate**, current input $x^{(t)}$, previous output $y^{(t-1)}$ and prior cell state $c^{(t-1)}$ are combined in following way:

$$o^{(t)} = \sigma\left(W_o x^{(t)} + R_o y^{(t-1)} + p_o \odot c^{(t)} + b_o\right) \tag{4.5}$$

In this equation, W_o, R_o, and p_o are the weight parameters corresponding to the current input $x^{(t)}$, the previous output $y^{(t-1)}$, and the current cell state $c^{(t)}$, respectively. The term b_o represents the bias vector used in the output gate.

Lastly, the **Block output** is defined as combination of the current cell value $c^{(t)}$ and output gate value as follows:

$$y^{(t)} = g\left(c^{(t)}\right) \odot o^{(t)}. \tag{4.6}$$

In the equations above, σ, g, and h represent point-wise non-linear activation functions. The logistic sigmoid function, defined as $\sigma(x) = \frac{1}{1+e^{-x}}$, is typically used for gate activations. Meanwhile, the hyperbolic tangent function, expressed as $g(x) = h(x) = \tanh(x)$, is commonly applied as the activation function for both the block input and the output.

This gated architecture allows for LSTM to remember patterns over long time horizon without suffering from vanishing gradients, which is common problem for standard RNNs.

In this hybrid model, LSTM models are trained to forecast following variables:

- Offshore wind generation
- Onshore wind generation

- Solar generation
- Electricity demand

Each LSTM model takes as input a multivariate time sequence that includes both the target variable and cyclical time feature (hour-of-day, day-of-year). These time features help the model learn seasonal variations and daily usage cycles. The outputs from the LSTM models represent the systems future state. These variables are then provided into next stage, which is forecasting the electricity using AR model.

Second Stage - Electricity Price Forecasting

The second stage of the hybrid model involves forecasting electricity prices using AR model. While linear AR models are effective at modelling persistent patterns, they often fall short in capturing the non-linear and dynamic behaviour typical for electricity markets. To address this, the linear regression component is replaced by a non-linear mapping function learning through XGBoost.

XGBoost (Extreme Gradient Boosting) is a tree-based machine learning algorithm that builds an ensemble of weak learners, typically decision trees, in a stage-wise manner. This allows the model to capture complex, non-linear relationships between input features and the forecasted value.[59] In the context of Electricity Price Forecasting (EPF), XGBoost has demonstrated competitive performance and has been shown to outperform traditional models such as Support Vector Machines (SVM) and Random Forests (RF) in both accuracy and computational efficiency [4].

Function which XGBoost is using to evaluate predicted electricity price is defined as:

$$P_t = f(P_{t-1}, \ldots, P_{t-n}, \overline{P}_{t-24}, \widehat{R}_t, \widehat{L}_t, T_t, \text{ResidualLoad}_t, \ldots) \tag{4.7}$$

Where:

- P_t is the predicted electricity price at time t
- $P_{t-1} \ldots P_{t-24}$ are lagged prices
- $\overline{P}_{t-24}$ is the rolling average
- $\widehat{W}_t$ is the forecasted renewable generation (from LSTM)
- $\widehat{L}_t$ is the forecasted demand (from LSTM)
- T_t represents temporal features (hour, day of week, month)
- Residual Load and volatility features are engineered from LSTM outputs

Temporal and rolling features are commonly used in AR-based forecasting and are theoretically justified by their ability to represent diurnal and weekly seasonality, which are dominant in electricity price formulation [58].

The model is trained to generate 24-hours ahead forecasts using a recursive strategy. Firstly, the model predicts the price for $t + 1$ using known historical values. Furthermore, it uses the

predicted P_{t+1} as an input for forecast P_{t+2} and so on until P_{t+24}. This rolling prediction method aligns with common practices in short-term EPF and reflects real-world operational use cases [39]. Although recursive forecasting introduces the risk of compounding errors, this is mitigated by frequent retraining and daily updates of the model. Presented framework for forecasting electricity prices is showcased as a process flow in **Fig. 4.3**

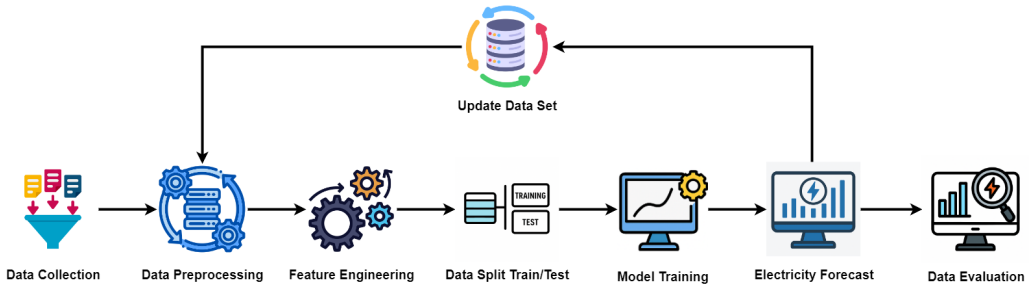

Figure 4.3
Graphical visualisation of flow for forecasting electricity price.

By separating the forecasting process into tasks of driver estimation and EPF, the hybrid method enables a more realistic and modular representation of electricity market behaviour. The use of LSTM models provides temporal foresight into supply and demand conditions, while the XGBoost model integrates these signals with historical pricing dynamics and engineered variables to produce reliable price forecasts.

4.2 Electrolyser Optimisation Framework

This section establishes the theoretical foundation for the optimisation model developed in this thesis. The aim is to determine a cost-effective operational schedule for the electrolyser that aligns with hourly electricity price variations, while satisfying a fixed annual e-methanol production target. Although the electrolyser serves as the central decision, its operation directly affects the downstream methanol synthesis and distillation. Therefore, the optimisation must consider system constraints and interactions. The following subsections introduce the motivation, structure and methodology of the proposed optimisation framework, depicted in **Fig. 4.4**

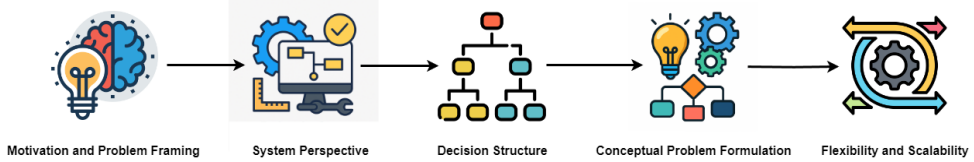

Figure 4.4
Conceptual representation of the optimization framework methodology.

4.2.1 Motivation and Problem Framing

E-methanol production relies heavily on both chemical processing and power system dynamics, making it particularly sensitive to fluctuations in electricity prices. The electrolyser, as the primary electricity consumer, serves as the main point of control for adapting production to economic conditions and grid constraints. In regions rich with renewable power generation, as Denmark, optimising its operation is essential for ensuring system performance and cost control.

The main challenge addressed in this thesis is to determine how the electrolyser should operate over a defined planning horizon. This includes deciding when to run, at what load, and when to remain idle or shut down, in order to minimise total operational costs while meeting a fixed methanol production target. This represents a constrained cost minimisation problem that must navigate electricity market fluctuations, process coupling constraints and mode transition dynamics.

While real time optimisation is often infeasible in practice due to computational or data latency constraints, many industrial energy systems rely on rolling horizon scheduling using short-term forecasts to preallocate resources over operational intervals such as 24 hours or one week [13]. In the case of PtX systems, electricity price forecasting becomes a key enabler for this strategy, allowing system operators to shift production toward lower price periods without leaning to risky long-term predictions [58].

However, the use of price forecasts in this thesis is not intended for market speculation. Instead, it serves as a supporting signal for ensuring that the hydrogen production aligns with period of favourable energy cost, within the constraints imposed by the physical plant. This distinguishes the modelling approach from profit driven strategies often applied in electricity trading applications.

Furthermore, the e-methanol system presents a highly coupled optimisation challenge where decisions made for electrolyser reflect upon the methanol synthesis reactor (MSR) and distillation column. Their dependency rules out natural approaches that treat components independently and requires a system level view when formulating the optimisation framework.

4.2.2 System Perspective

Although the optimisation model directly controls the operation of the electrolyser, its impact extends across the entire e-methanol production system. This system includes the electrolyser, the MSR and the distillation column. All hydrogen produced by the electrolyser is consumed by the MSR in real time, and methanol production dynamically scales with the hydrogen supply. Therefore, any change in electrolyser output, whether a shift in operating load or a transition to standby or shutdown, directly influences the downstream production rate and energy demands.

Unlike in traditional storage buffered systems, no significant hydrogen accumulation or shortage occurs under steady-state conditions. Instead, the MSR is designed to operate flexibly within a defined input range, adjusting its synthesis rate based on the electrolyser's hydrogen output. As long as the input remains above the minimum operational threshold(40% load), methanol production continues in proportion to available hydrogen. This coupling simplifies inventory management but imposes stricter requirements on synchronised scheduling between units.

To account for this behaviour without overcomplicating the optimisation process, the downstream MSR and distillation units are incorporated into the model using surrogate process constraints. These include minimum activation thresholds, fixed stoichiometric relationships, thermal inte-

gration logic and operation triggers for the distillation section. While the optimisation is not performed on the MSR and the distillation units directly, their responses to hydrogen availability are embedded into the model's logic.

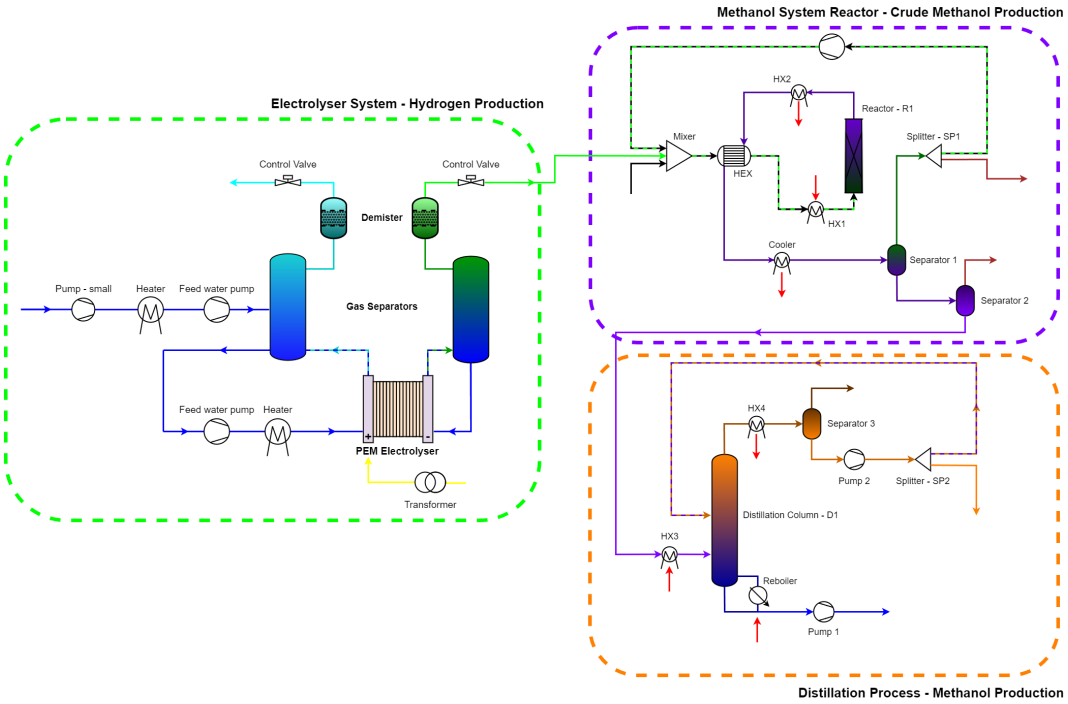

Figure 4.5
Process flow diagram of the integrated e-methanol production system.

By maintaining this system-wide perspective, as shown in **Fig. 4.5**, the optimisation model can capture the real trade off involved in shifting production across time. It ensures that scheduling decisions made for the electrolyser remain physically valid for the entire production chain, supporting cost minimisation without compromising operational feasibility.

4.2.3 Decision Structure

The optimisation problem formulated in this thesis is structured as a multi-period, discrete time decision problem, where the goal is to determine the operational state of the electrolyser for each hours across a one-year horizon. These decisions must collectively satisfy the annual methanol production target while minimising the total cost of electricity consumption and penalised transitions.

At every hour, the model must choose one of the available operational states for the electrolyser:

- **Shutdown** - No production and no load
- **Standby** - System is preheated, but no H_2 production
- **Running** -From 40% to 100% load, with step of 10%

Each state corresponds to a specific electricity usage and hydrogen output level, as detailed in **Sec. 2.5**. The decision making process must also account for transition dynamics, which are

mode changes that require time and energy, and these must be modelled explicitly to avoid unrealistic or inefficient switching. **Fig. 4.6** presents concept for how state changes will occur over optimised period of time.

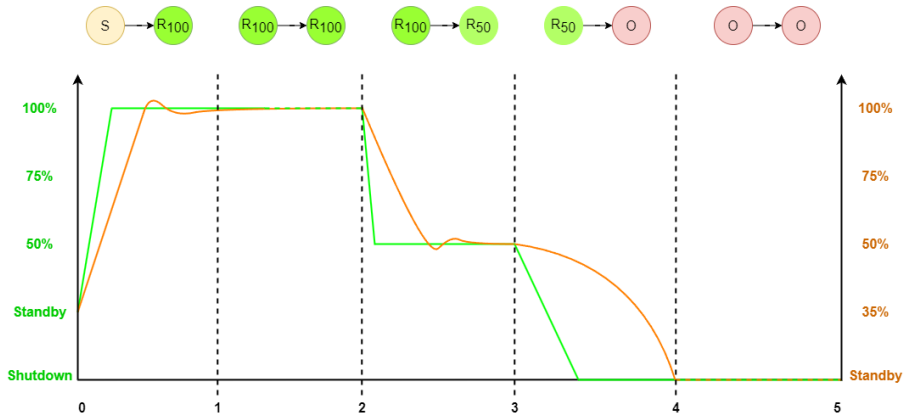

Figure 4.6
Conceptual illustration of electrolyser operational state changes over time, highlighting transitions between Shutdown, Standby, and Running modes.

The scope of the model is both operational and strategic. It focuses on day-ahead scheduling with imperfect foresight, using electricity price forecasts as guidance rather than certainties. At the same time, the full-year horizon ensures that the annual production target is enforced, introducing a long-term constraint into a short-term decision process. This dual perspective is crucial since operating purely on hourly cost minimisation may lead to insufficient production later, while ignoring electricity price variation may result in excessive cost.

To handle this balance, the optimisation is designed as a rolling-window model, where forecasts and decisions are updated daily, but the system tracks cumulative methanol production across the full year. This approach balances short-term responsiveness with long-term target satisfaction, making it suitable for realistic integration with forecast scheduling systems.

To summarise, these elements define the structural boundaries of the optimisation problem which is a dynamic and constraint driven scheduling task that aligns electrolyser operation with electricity price patterns while respecting technical, economic and production feasibility constraints.

4.2.4 Conceptual Problem Formulation

The key decision variable is the operational mode of the electrolyser at each hourly time step, which indirectly determines hydrogen production, methanol output and energy use.

The model's objective function is formulated from:

- **Electricity Costs** - Based on forecasted hourly prices.
- **Energy Consumption** - Each mode has its resulting energy use.
- **Transition Costs** - Expenses occurring during mode switches.
- **Other Costs** - CO_2 cost, Capital Expenditure (CAPEX)

The system is subject to several key constraints, derived from technical specifications and process dependencies:

- **Operational Mode Constraints** - At any time step, only one valid state is allowed
- **Transition Constraints** - Certain transitions require a predefined time and are associated with energy costs and ramp logic
- **Production Coupling** - Hydrogen output is mapped to methanol output through a fixed stoichiometric relationship. Methanol synthesis and distillation both respond to changes in electrolyser operation.
- **Minimum Operating Range** - The MSR requires $\geq$40% hydrogen input relative to nominal flow to remain active
- **Buffer Tank Constraints** - Transition from running to standby/shutdown use a buffer to supply MSR during decoupled hours, this tank must be refilled upon restart.
- **Annual Production Constraint** - The total methanol output at the end of the planning horizon must meet or exceed the predefined yearly target.

Together these constraints form a mixed-integer dynamic system, where the combination of binary decisions(mode selection), continuous parameters(energy consumption, price) and demand targets creates a complex but structured optimisation landscape.

The goal is not only to find cost optimal solution, but to ensure that the resulting operation plan is both realistically executable and system feasible. By modelling the relationships between electricity prices, electrolyser flexibility, process coupling and production needs, the optimisation framework reflects the key engineering balances present in PtMeOH systems.

4.2.5 Flexibility and Scalability

The optimisation framework developed in this thesis is intentionally designed to be modular and scalable, allowing it to adapt to future changes in the system layout, operational priorities or modelling assumptions. While the current formulation targets electricity cost minimisation under a fixed production constraint, the structure can readily change into alternative objectives.

Additionally, the framework can be scaled or restructured for different time resolutions. Although this thesis operates on an hourly basis over a full year, the model can be adapted to finer time steps, such as 15 minutes, or shorter horizons, such as weekly or monthly schedule, to suit different use cases.

Further potential flexibility is in the downstream system modelling. The surrogate constraints which are currently used to represent MSR and distillation behaviour could be replaced by real-time plant feedback in a digital twin setting.

This modularity ensures that the optimisation framework is not limited to the specific case studied within the scope of this thesis, but can serve as a foundation for future research or industrial implementation in the broader context of Power-to-X systems.

Electricity Price Forecasting 5

This chapter presents the development of the electricity price forecasting model that supports the operational optimisation of an electrolyser. As highlighted in **Chap. 4**, the forecasted electricity price is a critical input for scheduling, as it directly affects the cost efficiency of production. Therefore, the design of the forecasting model aims to balance predictive accuracy, adaptability to system dynamics and practical applicability.

To achieve set goals, the model is designed as a hybrid forecasting system, combining a sequence-based model for estimating future system conditions (LSTM) with a supervised machine learning model for price estimation (XGBoost). The resulting model structure enables both temporal pattern recognition and responsiveness to exogenous drivers of market prices.

The development process is divided into five stages, as it is shown in **Fig. 5.1**

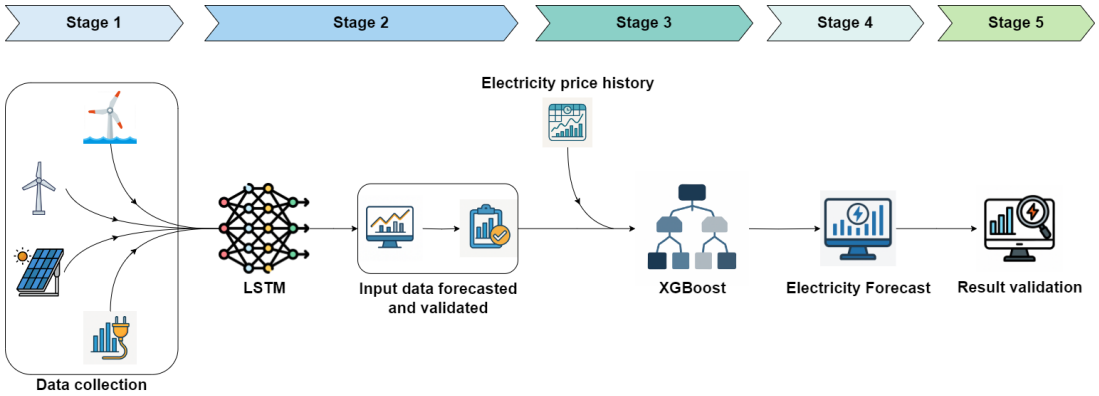

Figure 5.1
Graphical visualisation of hybrid model development stages

- **Stage 1: Data Collection and Preprocessing** - Prepares and transforms historical data to serve as input for both components of the forecasting model.
- **Stage 2: Forecasting Exogenous Drivers with LSTM** - Trains LSTM networks to generate forecast of electricity demand and renewable generation.
- **Stage 3: Feature Engineering for XGBoost** - Setting new predictive features using both LSTM outputs and historical trends to strengthen model performance.
- **Stage 4: XGBoost EPF** - Forecasting the final electricity price using the engineered features and historical price data.
- **Stage 5: Final Forecast and Results** - A full year produced forecast is validated and result interpretation is given.

Staged development of the model ensures that each part of the model is independently developed

and logically connected, leading to coherent and modular forecasting system ready for integration into the electrolyser optimisation framework.

5.1 Data Collection and Preprocessing

The first stage of the EPF model involves collecting and preparing the relevant data. Since the final model incorporates both historical price patterns and exogenous system conditions, this stage focuses on assembling a comprehensive dataset that captures the main drivers of electricity market dynamics.

5.1.1 Data Sourcing

All input data are collected for DK1 price zone, covering the period from 1^{st} of January 2021 to 31^{st} of March 2025, with an hourly resolution. All data is taken from European Network of Transmission System Operators for Electricity (ENTSO-e) [21].Variables that were selected are following:

- Solar generation (MW)
- Onshore wind generation (MW)
- Offshore wind generation (MW)
- Electricity demand (MW)
- Electricity price (DKK/MWh)

The scope of this thesis is to support the scheduling of electrolyser based on renewable electricity, particularly in context of PtX production. Therefore, one of the requirements, as mentioned in **Sec. 3.1**, is that the model is developed to forecast electricity prices based solely on renewable generation and electricity demand. Although electricity prices are influenced by a broader set of market factors, such as fossil fuels, cross-border exchanges and CO_2 emission costs, these are intentionally excluded from the forecasting model. This decision ensures that the model remains aligned with the objective of identifying low-price periods driven by renewable overproduction.

5.1.2 Timestamp Standardisation and Clean-up

Each input variable was initially downloaded as a separate Excel file covering a one-year period. These time series were then merged into a single dataset using a unified timestamp and sorted chronologically. Duplicate entries were removed, and missing values were addressed using linear interpolation when possible. A continuous hourly time index was ensured across the entire data range, which is essential for constructing sequential inputs for the LSTM model.

5.1.3 Additional Features

Additional variables are derived from the base dataset to support model learning. These include both time-based features and specific engineered variables:

- **Cyclical time features:** If model interprets hours as integers (e.g., hour = 0 to 23),

the model will not understand that 0 and 23 are actually next to each other. Therefore, hour-of-day and day-of-year values are transformed using sine and cosine functions to capture cyclical patterns in consumption and generation. These transformations help neural networks capture daily and seasonal effects that are not explicitly encoded in raw timestamps.

$$\begin{aligned} \text{sin\_hour} &= \sin\left(2\pi \cdot \frac{\text{hour}}{24}\right), \quad \text{cos\_hour} = \cos\left(2\pi \cdot \frac{\text{hour}}{24}\right) \\ \text{sin\_doy} &= \sin\left(2\pi \cdot \frac{\text{day of year}}{365}\right), \quad \text{cos\_doy} = \cos\left(2\pi \cdot \frac{\text{day of year}}{365}\right) \end{aligned} \tag{5.1}$$

- **Engineered variables:** Variables such as residual load, volatility and delta load are later derived to enhance the XGBoost model. These help capture periods of generation-demand imbalance and short-term variability.

5.1.4 Data Splitting

To support both the training and forecasting stages, the final dataset is divided into the following periods:

- **Training-validation period:** January 2021 to March 2025, used for model development and evaluation.
- **Forecast period:** April 2025 to April 2026, used for generating forward electricity price predictions.

This structure allows the forecast to be evaluated and validated for a period from 1^{st} to 14^{th} of April 2025, as this section is written during April 2025. Consequently, it is possible to compare the forecasted values with the actual data.

5.1.5 Overview of Dataset

The resulting dataset contains complete hourly records of electricity price, renewable generation and demand, along with time features and derived variables. These inputs form the foundation for all subsequent stages of model training and forecasting. An overview of electricity price trends during the historical period is presented in **Fig. 5.2**, while graphs of the input variables can be found in **Appendix A.1.1**.

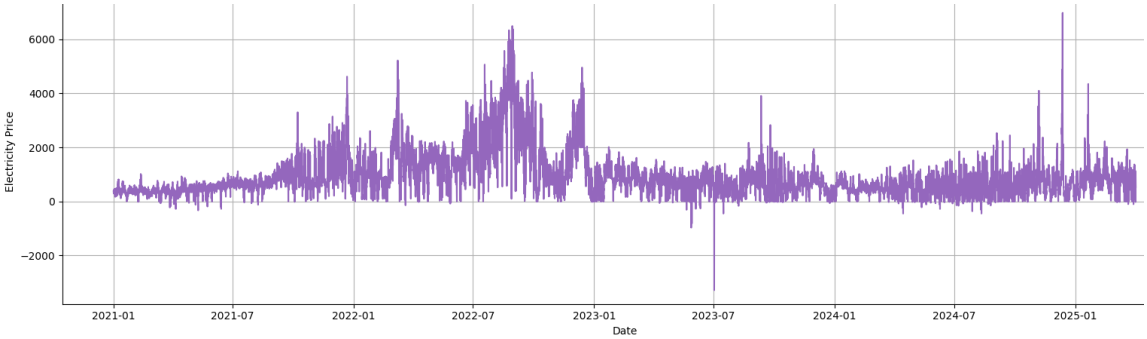

Figure 5.2
Hourly electricity prices in Denmark from January 2021 to March 2025, expressed in DKK/MWh.

As seen from graph in **Fig. 5.2**, electricity prices display significant variability, making it difficult to identify consistent patterns. A large spike occurs at the beginning of 2022, which could be explained by the Russo-Ukraine war, while prices appear more stable toward the end of the year. Furthermore, several extreme local spikes can be noticed, and these are removed during model training.

5.2 LSTM Exogenous Drivers Forecast

Stage 2 of the model development focuses on producing forward estimates for the key external variables that drive electricity price fluctuations. These include offshore wind generation, onshore wind generation, solar generation and electricity demand. Since these variables are not known for future periods, accurate forecasts are required to provide the necessary inputs for the electricity price forecasting model developed in Stage 4, see **Sec. 5.4**

The forecasting of these exogenous drivers is performed using LSTM models, a type of RNN specifically designed for handling time series data with temporal dependencies. A detailed explanation of the LSTM model structure, underlying equations and its role within the hybrid forecasting approach is provided in **Sec. 4.1.2**.

5.2.1 Forecasting Setup and Configuration

To generate realistic forecasts of renewable generation and electricity demand, a separate LSTM model is trained for each one of the four target variables. The model inputs are:

- The historical data values for four variables
- Time-based cyclical features, see **Eq. 5.1**

These inputs help the model learn both short-term dynamics and long-term seasonal cycles.

The input data for each model is structured using a rolling window approach, where a 168-hour sequence is used to predict the value for the next hour. This process creates overlapping sequences throughout the historical training period. For each training sample, the model receives an input matrix of shape [168,f], where f is the number of input features. The target is a single value representing the next time step's value for the respective variable.

All input features are normalized using Min-Max scaling, which rescales each variable to fall within the [0, 1] range. This is done using the transformation:

$$x_{\text{normalized}} = \frac{x - x_{\min}}{x_{\max} - x_{\min}} \tag{5.2}$$

This procedure ensures that all variables contribute proportionally during training and prevents features with larger numerical ranges from dominating the learning process. After forecasting, the inverse transformation is applied to convert normalised predictions back to their original values.

During training, the LSTM models are optimised using the Mean Squared Error (MSE) loss

function, which is calculated as:

$$\text{MSE} = \frac{1}{n}\sum_{i=1}^{n}(y_i - \hat{y}_i)^2 \tag{5.3}$$

Where y_i is the actual value and $\hat{y}_i$ is the predicted value. MSE measures the average squared difference between predictions and targets, while penalising larger errors more heavily. Its differentiability makes it suitable for gradient-based learning and ensures stable convergence during training. Training is performed using the optimiser, with early stopping applied to avoid overfitting. Model hyper parameters, such as the number of LSTM layers, neurons and batch size are selected through empirical tuning based on validation performance.

5.2.2 Recursive Forecasting Strategy

Once the LSTM models are trained, they are used to generate hourly forecasts for the entire prediction horizon, from 1^{st} of April 2025 to 31^{st} of April 2026. Since actual future values of the exogenous variables are unavailable during forecasting, a recursive prediction strategy is applied.

In this strategy, the model starts with the final 168-hour block from the historical dataset (ending 23:00:00 31/03/2025) as the initial input. It uses this input sequence to generate a prediction for the next time step, which is 00:00:00 01/04/2025. This predicted value is then appended to the sequence, while the oldest step is removed, maintaining the 168-hour input length. The process, depicted in **Fig. 5.3**, repeats itself for every hour in the forecast horizon. This method is commonly referred to as rolling window forecasting or autoregressive LSTM forecasting, where the model depends on its own past predictions to forecast future values.

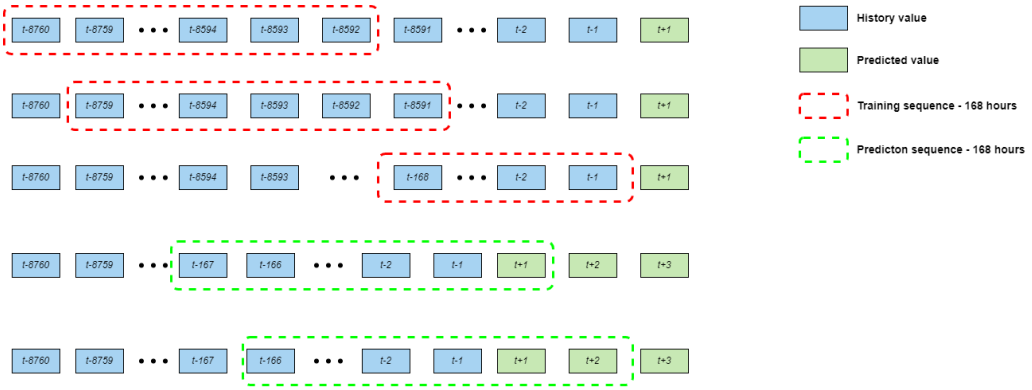

Figure 5.3

Overview of the recursive forecasting approach used to generate hourly electricity price predictions. Each step relies on previously forecasted values of exogenous variables, enabling sequential forward prediction over the desired horizon.

While this approach is practical and closely resembles real-world forecasting workflows, it introduces the potential for error accumulation. Because each predicted value is used as part of the next input, any initial inaccuracies may propagate over time. Despite this, recursive forecasting remains widely accepted method in long-horizon time series prediction due to its simplicity and flexibility, especially when no external forecasts are available [11].

5.2.3 Forecasted Values

Once trained, each LSTM model was used to generate hourly forecast for the period from 1^{st} of April 2025 to 1^{st} of April 2026. These predicted values serve as key input features for the electricity price model developed in Stage 4, see **Sec. 5.4**.

A combined overview of the generated forecast is presented in **Fig. 5.4**.

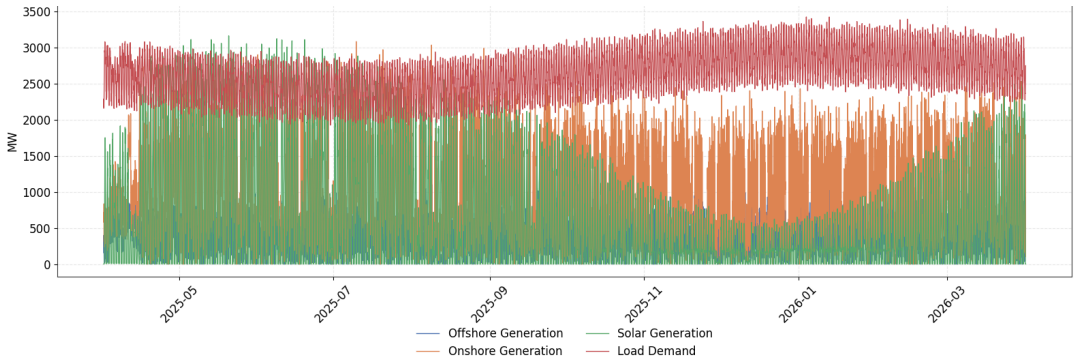

Figure 5.4
Hourly forecasted values of offshore wind, onshore wind, solar generation, and load demand for the period April 2025 to April 2026.

The figure highlights the distinct temporal characteristics of each variable:

- **Solar Generation** follows a strong diurnal cycle, peaking at midday and dropping to zero overnight, with significant seasonal differences across the year.
- **Wind Generation** (both offshore and onshore) shows high short-term variability with less predictable intra-day patterns.
- **Electricity Demand** shows consistent weekday-weekend variation and higher baseline levels during colder months.

For clearer inspection, individual line plots for each forecasted variable are provided in **Appendix A.1.2**. To provide a system perspective, **Fig. 5.5** presents a comparison between the total forecasted renewable electricity generation in comparison to the forecasted electricity demand.

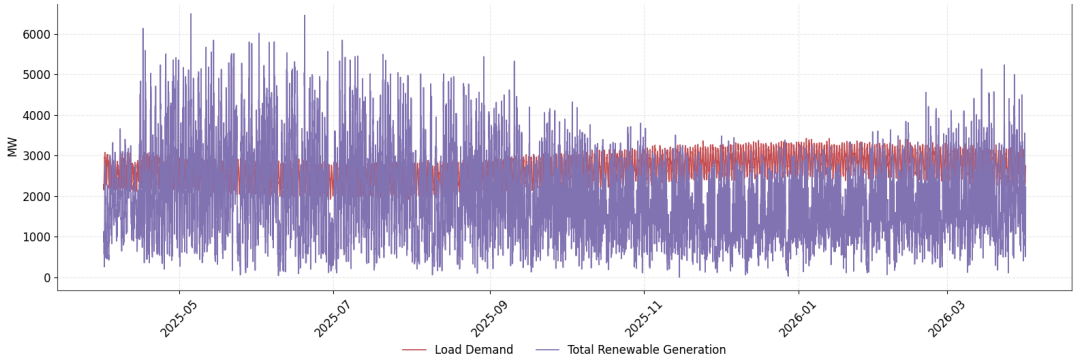

Figure 5.5
Comparison of forecasted electricity load demand and total renewable generation (sum of offshore wind, onshore wind, and solar) from April 2025 to April 2026.

As explained by the Merit Order Effect, see **Sec. 2.4.2**, periods where renewable generation surpasses load present opportunity for operating the electrolyser at low marginal cost. On the other hand, periods of renewable shortfall reflect moments when electricity will probably be supplied by conventional sources, such as gas or coal, potentially leading to higher prices and less favourable conditions for green hydrogen production.

5.2.4 Forecast Validation

To assess the short-term reliability of the LSTM models before deploying them for full-year forecasting, a two-week validation period is examined. The LSTM forecasts for the four exogenous variables are compared to actual recorded values from 1^{st} to 14^{th} of April 2025, a period for which real system data is available. This comparison provides insight into model's generalisation ability beyond the training horizon.

Fig. 5.6 presents the hourly electricity demand load between forecasts from the LSTM model against the actual data for observed period. As a point of comparison, the day-ahead ENTSO-e forecasts are included. Comparisons for renewable electricity generation could be observed in **APPENDIX. A.1.3**

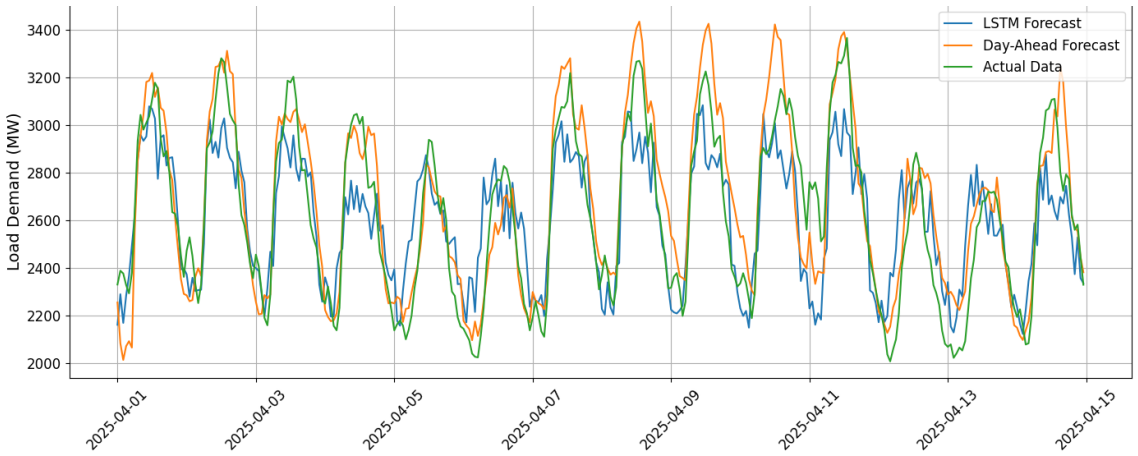

Figure 5.6
Comparison of hourly electricity load demand forecasts from the LSTM model and the ENTSO-E day-ahead forecast against the actual observed data.

As shown in graph both in **Fig. 5.6** and **Appendix A.1.3**, following observations are made:

- **Load Demand** - The load demand forecast follows clear daily cycles, and the LSTM model does a solid job of capturing these patterns. Both the LSTM and ENTSO-e have similar performance, with minor deviations during low-demand periods.
- **Offshore Wind Generation** - Offshore wind generation shows significant fluctuations, and LSTM forecasts capture this variability, although with different magnitude. The LSTM model tends to predict slightly higher generation levels compared to the actual data, particularly during periods of peak generation.
- **Onshore Wind Generation** - Onshore wind generation shows consistent, though less predictable, patterns than offshore wind. The LSTM model does a good job capturing

these fluctuations, particularly from 3^{rd} to 7^{th} of April. Both forecasting models face challenges in forecasting low-wind periods.

- **Solar Generation** - The LSTM model align well with the actual solar generation patterns, especially capturing the daily peaks and drops corresponding to sunrise and sunset.

The comparison between LSTM forecasts and actual data highlights the model's ability to track real-world system dynamics, especially in capturing daily cycles and fluctuations in renewable generation.

5.3 Feature Engineering for XGBoost

The third stage in the forecasting process focuses on developing a suitable input dataset for the electricity price prediction model. While the LSTM model in Stage 2, see **Sec. 5.2**, provide the necessary forecast of system variables, this stage transforms those outputs, along with additional engineered features, into a comprehensive and structured form usable by XGBoost.

Feature engineering plays a critical role in the performance of machine learning models, especially in structured tabular problems such as EPF. In this stage, both direct LSTM forecast and derived features are used to expand the model's input space, enabling it to capture short-term dynamics and non-linear relationships.

5.3.1 Integration of LSTM Forecast

The core inputs to the XGBoost model are the forecasted values generated by the LSTM models in Stage 2. These represent future estimates of key electricity system drivers and are structured as hourly time series over the full forecast horizon.

The following four variables are directly included in the feature set:

- Onshore wind generation (MW)
- Offshore wind generation (MW)
- Solar generation (MW)
- Electricity demand (MW)

Each of these variables were forecasted independently, as described in **Sec. 5.2**. Their inclusion enables the XGBoost model to make price predictions based on expected system conditions rather than purely on historical observations.

5.3.2 Time-Based Features

Electricity prices show strong temporal patterns due to the influence of consumption behaviour and generation cycles. To help the XGBoost model recognise these recurring structures, a set of calendar and cyclical time features, shown in **Tab. 5.1**, is included in the input dataset.

Table 5.1
Overview of Time-Based Features Used for Electricity Price Forecasting

Feature	Type	Description
Hour	Integer (0 - 23)	Captures daily variation in consumption and prices
DayofWeek	Integer (0 - 6)	Indicates the day of the week
Month	Integer (1 - 12)	Provides seasonal context
IsWeekend	Binary (0 / 1)	Differentiates weekday from weekend effects
sin_hour	Float	Cyclical encoding of hour; $\sin\left(2\pi \cdot \frac{\text{hour}}{24}\right)$
cos_hour	Float	Cyclical encoding of hour; $\cos\left(2\pi \cdot \frac{\text{hour}}{24}\right)$
sin_doy	Float	Cyclical encoding of day of year; $\sin\left(2\pi \cdot \frac{\text{day of year}}{365}\right)$
cos_doy	Float	Cyclical encoding of day of year; $\cos\left(2\pi \cdot \frac{\text{day of year}}{365}\right)$

5.3.3 Derived System Features

In addition to raw LSTM forecasts and time-based features, several engineered system features are included to improve the model's ability to capture the structural conditions that influence electricity price formation. These features reflect short-term stress, imbalance and variability within the system.

Residual Load

Residual load represents the portion of electricity demand that is not met by renewable sources and is a strong indicator of the need for conventional generation. It is computed as:

$$\text{Residual Load} = \text{Demand - (Onshore Wind + Offshore Wind + Solar Generation)} \quad (5.4)$$

Periods of high residual load are typically associated with higher marginal prices, as other sources, with higher operational costs, are used to met load demands.

Delta Load

This feature measures the hour-to-hour change in electricity demand, capturing load dynamics:

$$\Delta Load_t = Load_t - Load_{t-1} \quad (5.5)$$

Sudden changes in demand can trigger price spikes if the supply is not sufficiently flexible, especially in systems with high renewable penetration, as Denmark is.

Residual Load Volatility

To account for short-term fluctuations in net demand, a rolling 24-hour standard deviation of residual load is computed:

$$Residual\ Volatility_t = Std(Residual\ Load_{t-23\ to\ t}) \quad (5.6)$$

This feature helps the model recognise periods of instability or uncertainty, which often lead to market price volatility due to imbalance risk.

5.3.4 Noise Injection for Realism

While LSTM forecasts of demand and renewable generation provide a structured view of future system conditions, they remain model-generated estimates. While in reality such predictions are subject to uncertainty. To reflect this and improve the generalisation of the XGBoost price model, controlled Gaussian noise is injected into the forecasted input variables.

This technique simulates the typical variability found in operational forecasting tools and prevents the price model from overfitting to overly smooth or deterministic LSTM outputs. It also allows the model to learn how to handle moderate deviations in system condition forecasts, which is especially relevant for real world integration.

For each variable, zero-mean Gaussian noise is added with a specific standard deviation, calibrated based on historical volatility. The noise is applied as:

$$\tilde{x}_t = x_t + \mathcal{N}(0, \sigma^2) \tag{5.7}$$

Where:

- x_t is the LSTM forecast at time t
- σ is the noise standard deviation defined per variable
- $\mathcal{N}(0, \sigma^2)$ is the Gaussian noise term

A standard deviation of 10 MW is applied to solar generation to capture occasional variability due to weather conditions, while higher values of 20 MW and 25 MW are used for onshore and offshore wind, respectively, given their greater fluctuation patterns. A lower value of 5 MW is used for load demand, which is generally more stable. This approach provides a more robust training input set for the XGBoost model by capturing realistic variability without introducing extreme distortion. It also mirrors conditions in actual system operations, where forecast error is an inherent part of market dynamics.

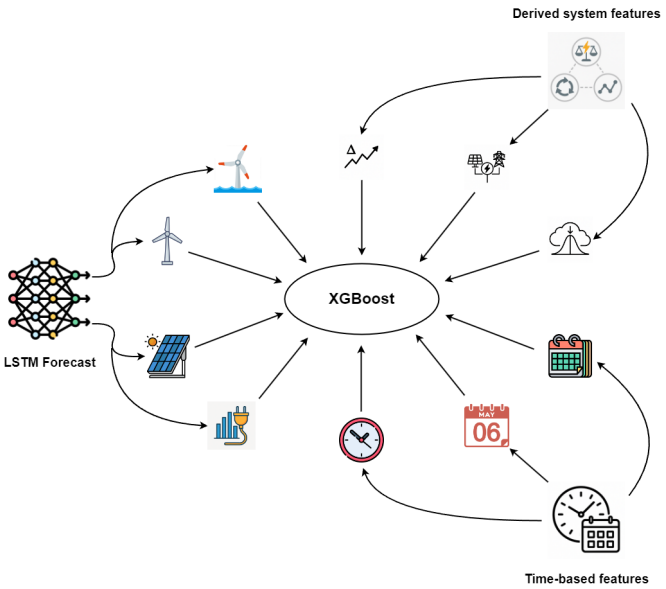

Figure 5.7
Overview of Input Parameters Used in the Electricity Price Forecasting (EPF) Model.

5.3.5 Final Dataset Assembly

After completing the integration of LSTM forecasts, application of controlled noise and generation of time-based and system features, the final dataset is assembled for input to the XGBoost EPF model, as depicted in **Fig. 5.7**

Depicted features are now ready to be used as input for model training and price forecasting in the next stage.

5.4 XGBoost Electricity Price Model

The XGBoost model plays a crucial role in forecasting electricity prices in the hybrid approach developed for this thesis. Building on the forecasts generated by LSTM models for renewable generation and electricity demand, explained in **Sec. 5.2**, the XGBoost model is used to predict the corresponding electricity prices.

5.4.1 Data Preparation and Feature Selection

For training the XGBoost model, the dataset is prepared by combining LSTM forecasts with engineered features as outlined in **Sec. 5.3**.

The data is processed as follows:

1. **Forecasted Variables** - The forecasted values are derived from the LSTM model, and used as primary predictors for the EPF.
2. **Engineered Features** - Additional features are created to capture system dynamics better.
3. **Noise injection** - Controlled Gaussian noise is added to the forecasted variables to reflect the uncertainty in real-world forecasts. The noise levels are defined for each feature as follows:
   - Onshore Generation: 20 MW - Onshore wind generation can show significant daily and seasonal variability.
   - Offshore Generation: 25 MW - Offshore wind is typically more variable than onshore generation.
   - Solar Generation: 10 MW - Solar generation is more predictable, but still can vary due to weather conditions (such as cloud cover).
   - Load Demand: 5 MW - Electricity demand is relatively predictable compared to other variables.

   The noise is essential for making the model robust to real-world variability and preventing overfitting to overly smooth LSTM predictions.
4. **Scaling** - All features are scaled using Min-Max normalization, as explained in **Eq. 5.2**, to ensure uniformity in scale. This ensures that no single feature dominates the model, allowing the XGBoost algorithm to learn from the full set of features.
5. **Data Splitting** - The dataset is split into training, validation and test sets. The training set spans from 1^{st} of January 2021 to 31^{st} of December 2024, the validation set covers 1^{st} of January 2025 to 31^{st} of March 2025 and the test set spans from 1^{st} of April 2025 to 1^{st} of April 2026.

By preparing the data with these steps, the XGBoost model is trained on a set of features that accurately represent the system conditions that influence electricity prices. The next section will

detail the configuration and hyperparameter settings used for the model.

5.4.2 XGBoost Model Configuration

The XGBoost model is configured using several hyperparameters to ensure efficient training. The configuration and tuning of the model are critical steps in ensuring that it performs well on the prepared data.

Hyperparameters

The following parameters were chosen for the model configuration:

- **n_estimators** = 800
  This represents the number of boosting rounds, or trees to be built. A larger number of estimators allows the model to learn more complex relationships. In this case, 800 estimators were chosen after experimentation to find a balance between performance and overfitting.
- **learning_rate** = 0.01
  The learning rate controls the contribution of each new tree to the model's prediction. A lower learning rate ensures gradual learning, helping the model avoid large jumps in weight updates that could lead to instability. With higher number of estimators, lower learning rate, that is close to 0.01, should be used.
- **max_depth** = 8
  The maximum depth of each tree limits the complexity of the model and controls how deep each individual tree can grow. A value of 8 is selected after tuning, as it prevents the model from becoming too complex while still capturing important interactions between features.
- **subsample** = 0.8
  This parameter controls the fraction of samples used for fitting each tree. Setting subsample to 0.8 means that each tree will be trained on 80% of the data.
- **colsample_bytree** = 0.8
  Similar to subsample, this parameter controls the fraction of features that are randomly selected to build each tree. Setting this value to 0.8 ensures that each tree is trained on a different subset of features.
- **objective** = 'reg:squarederror'
  This specifies the objective function for the regression task for predicting continuos values. Selected function minimises the mean squared error between the predicted and actual value.

Cross-Validation and Early Stopping

To optimise the model and prevent overfitting, Time Series Split cross-validation is used. This method splits the dataset into multiple training and testing sets, ensuring that each fold preserves the temporal order of the data. By using cross-validation, the model's performance is evaluated across different subsets of data.

Early stopping is applied during the training process to stop further training if the model's per-

formance on the validation set no longer improves. This prevents the model from overfitting to the training data.

5.4.3 Forecasting Results

Once the XGBoost model was configured, the next step is to run it on prepared dataset for EPF. Once the model is trained, the model's output is a time series of predicted electricity prices for each hour from 1^{st} of April 2025 to 1^{st} of April 2026, as shown in **Fig. 5.8**.

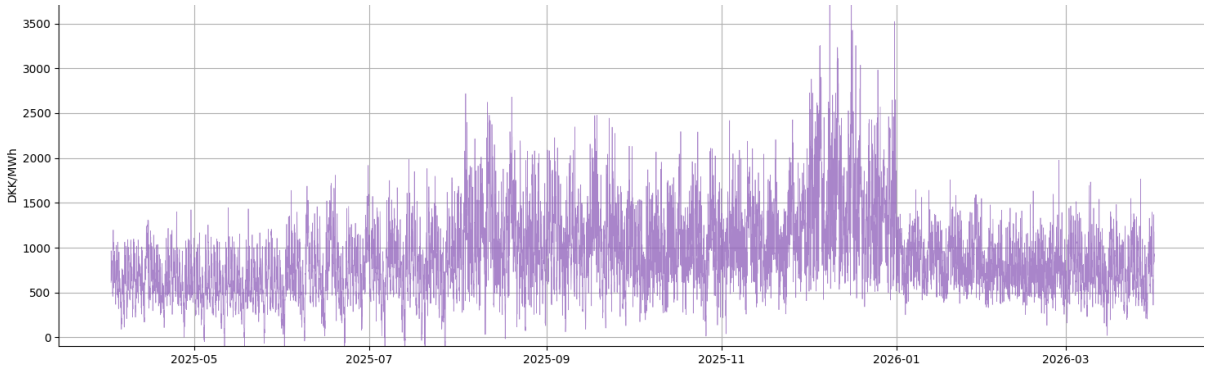

Figure 5.8
Forecasted Electricity Prices (DKK/MWh) from April 2025 to April 2026 Using XGBoost Model

Forecasted electricity clearly depicts the seasonal trends in price, with higher prices in winter and lower prices in summer months due to changes in renewable generation and load demand. Next section finalises EPF development by validating forecasted results.

5.5 Forecast Validation

This section provides a validation basis for the performance of the XGBoost model by comparing the forecasted electricity prices with actual market prices for the period from 1^{st} to 14^{th} of April 2025. The objective is to evaluate the model's ability to accurately predict price fluctuations using real-world data on renewable generation and electricity demand. Before presenting the validation results, the performance metrics used are introduced and defined.

5.5.1 Evaluation Metrics

To evaluate the performance of the XGBoost model, several key metrics are used to quantify the accuracy of the forecasted electricity prices compared to the actual market prices over the period of first two week in April 2025. Each metric provides different insight into the model's performance.

Mean Absolute Error - MAE

MAE measures the average magnitude of the errors between forecasted and actual values:

$$\text{MAE} = \frac{1}{N}\sum_{t=1}^{N}|\text{Actual}_t - \text{Forecast}_t| \tag{5.8}$$

It provides a direct and interpretable estimate of the typical absolute difference in DKK/MWh between predicted and actual prices. It is widely used in time series evaluation due to its simplicity and interpretability.[31]

Mean Absolute Percentage Error - MAPE

MAPE expresses the average absolute difference between forecasted and actual values as a percentage of the actual values:

$$\text{MAPE} = \frac{1}{N}\sum_{t=1}^{N}\left|\frac{\text{Actual}_t - \text{Forecast}_t}{\text{Actual}_t}\right| \times 100 \tag{5.9}$$

This metrics is scale independent and is often favoured in economics and energy forecasting because it allows for easy interpretation and comparison across scales.[9]

Root Mean Squared Error - RMSE

RMSE is the square root of the average of squared differences between forecasted and actual values:

$$\text{RMSE} = \sqrt{\frac{1}{N}\sum_{t=1}^{N}(\text{Actual}_t - \text{Forecast}_t)^2} \tag{5.10}$$

RMSE penalises larger errors more then MAE and is, therefore, particularly useful in applications like EPF, where extreme peaks and volatility are common.[58]

Error-to-Average Ration - EAR

To describe the magnitude of the forecast errors, the EAR metric compares the MAE during the validation period to the average forecasted electricity price over the full forecast horizon:

$$\text{EAR} = \frac{\text{Mean Absolute Error (Validation Period)}}{\text{Mean Forecasted Price (Full Year)}} \tag{5.11}$$

This ration provides insight into whether forecast errors are significant relative to expected price levels, a useful contextual tool in interpreting energy market model performance.[55]

These four metrics will be used in the following section to evaluate the model's performance over the two week validation window and interpret the results within the broader price period.

5.5.2 Results and Comparison

A graph comparing the hourly forecasted electricity prices to the actual prices during the validation period is shown in **Fig. 5.9**.

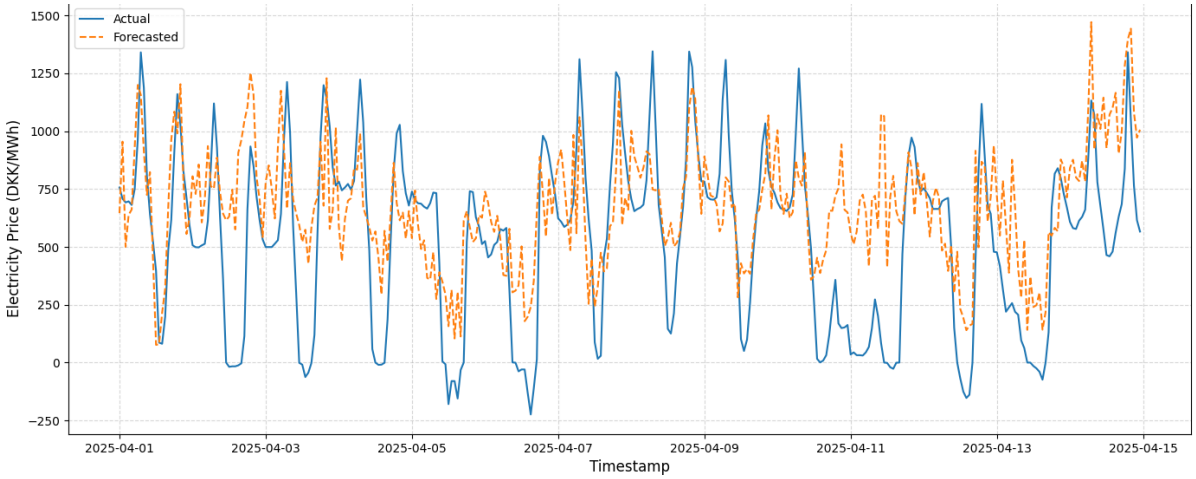

Figure 5.9
Comparison of Forecasted and Actual Electricity Prices (DKK/MWh) from April 1 to April 14, 2025

The forecasted curve follows in general the trend of the actual data, capturing the day-night fluctuations and periods of elevated market activity, such as afternoon peaks. Deviations between the curves are more visible in hours where actual prices are near zero or negative, often driven by renewable surplus and merit order effects. **Tab. 5.2** presents values for previously set evaluation metrics.

Table 5.2
Evaluation metrics for XGBoost model performance

Evaluation Metric	Value
Mean Absolute Error	268.5 DKK/MWh
Root Mean Square Error	334.8 DKK/MWh
Mean Absolute Percentage Error	549.5%
Average Forecasted Price	924.6 DKK/MWh
Error-to-Average Ratio	0.29

The MAE of 268.5 DKK/MWh represents approximately 30% of the full-year average electricity price (924.6 DKK/MWh), a result that aligns well with accepted benchmarks. In studies reviewed by Weron [58], typical MAE values often range between 5% to 20% of the average price, though that exclude broader market drivers (such as gas prices or interconnectors), as what developed model is, often fall towards the higher end of this spectrum.

The RMSE of 334.8 DKK/MWh also reflects reasonable forecasting accuracy, particularly when accounting for the model's use of only renewable generation and demand inputs, excluding many conventional market variables typically used to refine price predictions.

The extremely high MAE of 549.5% is mainly caused by the nature of the dataset and market conditions, and does not necessarily reflect poor model performance. As Hyndman & Koehler [31] emphasise, MAPE becomes unreliable when actual values approach zero or go negative,

and that condition is quite frequently encountered in the DK1 electricity market due to renewable surplus. In such cases, even modest forecast deviations can lead to disproportionately high percentage errors.

To contextualise forecast quality beyond raw error values, the EAR is applied. With an EAR of 0.29, the model's typical error is less then one third of the average electricity price over the forecast horizon, a level considered satisfactory in forecasting literature and competitions [37], [55].

Lastly, from **Fig. 5.9** it is evident that the forecasting model struggles to accurately capture periods of very low or negative electricity prices. A possible explanation is, although LSTM model captured renewable generation and demand sufficiently, that the XGBoost tended to expect higher market prices during this period. For the validation window, the weather conditions in the DK1 zone were unusually favourable, characterised with clear sky and intermittent strong winds. This led to lower electricity prices than expected, which the model did not fully predict, most likely because it had not seen similar patterns in the training data.

5.6 Summary

This chapter presented the development of the EPF model, which supports the scheduling of electrolyser operation in an e-methanol production system. A hybrid forecasting framework was adopted, combining LSTM models for predicting exogenous variables, renewable generation and load demand, with an XGBoost model to estimate hourly electricity prices. While the model does not aim to capture all market dynamics in full detail, such as non-renewable sources, it provides a sufficiently accurate and trend sensitive estimate of electricity prices based purely on renewable inputs and demand. Given that the primary goal of this thesis is not to develop a state-of-the-art forecasting system, but rather to investigate how price variability influences electrolyser operation, the model is considered fit for purpose. The next chapter builds on these forecasts to formulate an optimisation strategy that schedules electrolyser activity in response to electricity price signals.

Operational Optimisation 6

This chapter presents the development of the optimisation model for scheduling the electrolyser and methanol synthesis system operation based on electricity price forecasting. The objective of the optimisation is to minimise the total operational costs while ensuring that the annual methanol production target is satisfied.

The chapter is structured in five parts. First, the system parameters, objective function and basic constraints are defined. Afterwards, the model is developed through three phases, as shown in **Fig. 6.1**. Lastly, conceptual sensitivity analysis is performed.

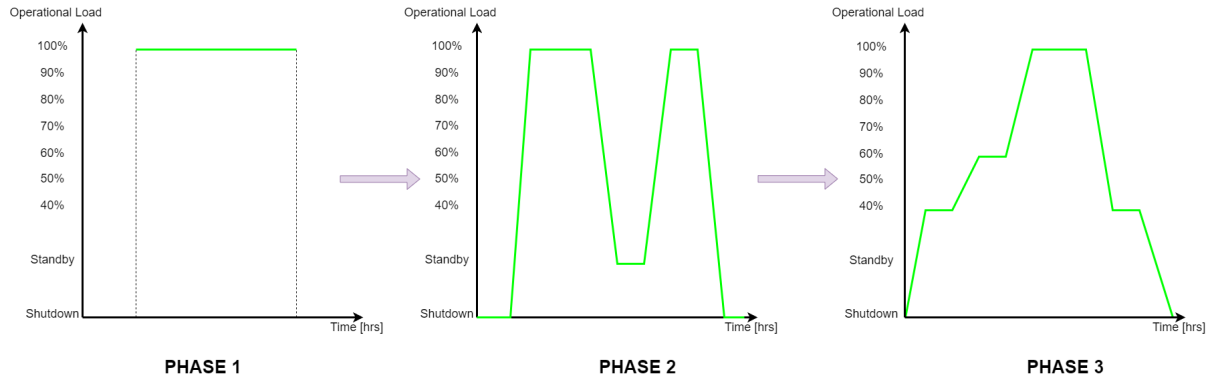

Figure 6.1
Evolution of optimisation model across three phases.

- **Phase 1**: Optimisation model when there is only Running state at full capacity.
- **Phase 2:** Introducing three operational states(Running, Standby and Shutdown), together with the logic behind their transition dynamics.
- **Phase 3:** Developing model that can determine load capacity from 40% to 100% based on forecasted electricity prices. This is considered full operating model.

Each phase expands the complexity of the optimisation framework to better reflect realistic operational flexibility.

6.1 System Setup

This section presents the key elements defining the optimisation problem. These include how the annual methanol production demand is distributed over the weeks, the treatment of capital expenditures (CAPEX) and their incorporation into operational cost calculations, the assumptions regarding CO_2 purchase and excess heat sales, the formulation of the objective function and the complete list of input parameters used in the model. This system setup is overlooking

generally, and it describes mostly just the first phase. Each subsequent phase will introduce new constraints and modify the objective function when needed.

6.1.1 Optimisation Setup

The optimisation model developed in this work is formulated as Mixed Integer Linear Programming (MILP) problem. Due to the need for discrete operating decisions, such as switching between different operational states, binary variables are introduced to represent system states at each hourly time step.

Due to the higher computational demands associated with solving large-scale integer programming problem over an entire year, the optimisation is performed on a rolling weekly basis. Each weekly window determines the operational schedule for the electrolyser and MSD per hour, using predicted electricity prices as input. The results of each week are then combined to meet the overall production target.

6.1.2 Methanol Demand

The e-methanol production system is designed to meet an annual production target of **25 000** tons. As rolling weekly window is used for simulation, the production target is distributed unevenly across weeks, based on average forecasted electricity price for each week.

The assumption here is that production should be shifted toward periods with lower electricity costs to result as improved economic performance of the system. To achieve this, the following steps were taken:

1. **Weekly Average Electricity Price -** Forecasted electricity over a year is split into weeks and the average electricity price for each week is calculated.
2. **Weighting Factor Calculation -** A weighting factor is assigned to each week based on the inverse of its average electricity price. Weeks with lower prices are assigned higher weights, implying greater production during these periods. The weekly weight w_i is determined by:

$$w_i = \frac{1/\text{AvgPrice}_i}{\sum_{j=1}^{52} \left(1/\text{AvgPrice}_j\right)} \tag{6.1}$$

   Where $AvgPrice_i$ is the average forecasted electricity price in week i.
3. **Weekly Methanol Demand -** The annual methanol production target M_{target} is multiplied by the weight of each week to determine the required methanol production for that week:

$$8M_i = w_i \cdot M_{\text{target}} \tag{6.2}$$

   Where M_i is the methanol production target for week i.

Following this steps, resulting weekly methanol demands are presented in **Fig. 6.2**

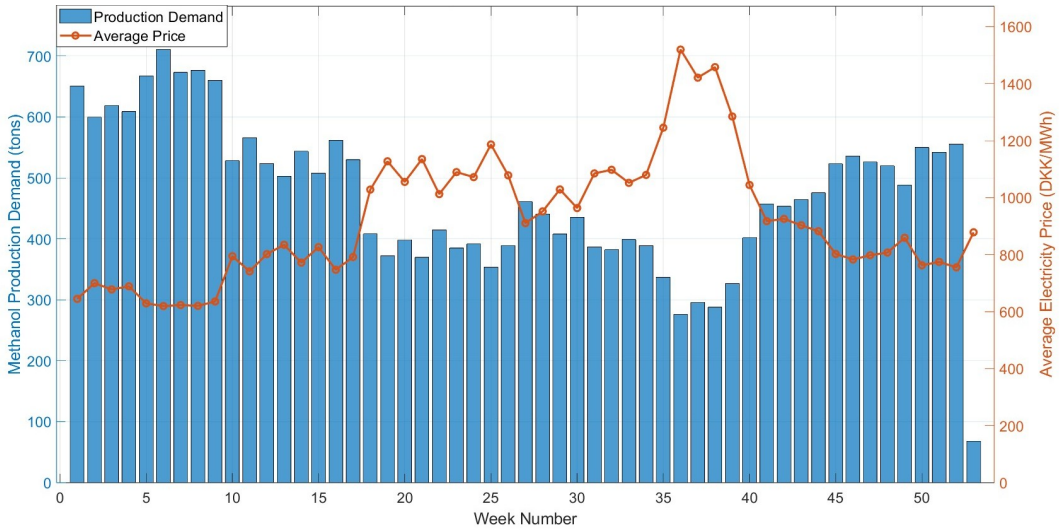

Figure 6.2
Final weekly methanol production demand and average electricity price.

This methodology allows the model to naturally prioritise production in cheaper weeks and avoid overproduction during high price periods, aligning economic and operational objectives.

6.1.3 Capital Expenditure

The CAPEX associate with the e-methanol production system is estimated by evaluating different technology configurations, as illustrated in **Appendix A.12**. Among the evaluated options, Case 5 is selected as the reference setup for the optimisation model, offering a good balance between performance, inlet quality and investment cost. The total CAPEX for Case 5 equals to 50,035,000 €.

Since the financial model assumes a project lifespan of 20 years, and the optimisation covers only a single year's operation, the capital costs are annualised by dividing the total CAPEX by 20:

$$\text{Annualised CAPEX} = \frac{50{,}035{,}000\ €}{20} = 2{,}501{,}000.75\ € \text{ per year} \tag{6.3}$$

In Danish kroner (DKK), assuming a conversion rate of 7.45 DKK/€ the CAPEX becomes 18,632,455.6 DKK per year. Therefore, this fixed value has to be added to the operational costs when evaluating the final cost structure for each optimisation phase.

6.1.4 CO_2 and Excess Heat

In addition to electricity costs and fixed capital costs, the economic model accounts for the costs and revenues associated with two other products, CO_2 consumption and excess heat generation.

CO_2 Costs

CO_2 is required as a feedstock for the methanol synthesis process. In the model, it is assumed that CO_2 is externally sourced at a fixed price of 0.375 DKK/kg [54]. No dynamics such as

market variability or supply limitations are incorporated. The total cost contribution of CO_2 indirectly reflected in the final total cost through the methanol production amount, with a correction factor that estimates the required CO_2 mass per kilogram of methanol. Equation describing cost of CO_2 can be described as:

$$CO_2 \text{ Cost} = \text{Total Methanol Production}_{kg} \cdot 1.416 \cdot 0.375 \tag{6.4}$$

Factor of 1.416 is used to estimate the CO_2 demand per unit of methanol produced.

Excess Heat

As a byproduct of the methanol production process, excess heat is recovered and monetised through district heating integration. There is a fixed revenue rate of 225 DKK per MWh of excess heat sold [54]. The amount of excess heat generated is proportional to the methanol produced, scaled by a coefficient of 0.0009 MWh/kg MeOH. This relationship can be then written as:

$$\text{Excess Heat Revenue} = \text{Total Methanol Production}_{kg} \cdot 0.0009 \cdot 225 \; DKK/MWh \tag{6.5}$$

These two terms are implemented at the end of optimisation model to adjust the total cost value after as:

$$\text{Operational Cost} = f_{el} + CO_2 \text{ Cost} + \text{Excess Heat Revenue} \tag{6.6}$$

Where f_{el} is the original value returned from the optimisation related to electricity consumption across modes and transitions.

6.1.5 Objective Function

As mentioned, the optimisation problem is formulated as a MILP, in which the operational mode of the electrolyser, therefore also for methanol production, is determined for each hour over a predefined time horizon T. The goal is to minimise the total cost for the system while meeting a methanol production requirement.

At each hour $t \in \{1, 2, \ldots, T\}$ the electrolyser may be in one of several discrete operational states, including running, standby or shutdown. In the base model, which is Phase 1, the system only considers either running or shutdown at fixed capacity, without distinguishing between varying load levels or incorporating thermal transition dynamics such as cold starts or hot starts, which are introduced in later phases.

The general objective function is then expressed as:

$$\min \sum_{t=1}^{T} \sum_{i=1}^{N} P_t \cdot E_{\text{EL},t}^{(i)} \cdot x_{t,(i)} \tag{6.7}$$

where:

- P_t - Electricity price at hour t [DKK/MWh],
- $E_{\text{el},t}^{(i)}$ - Electricity consumption of the system [MWh] at hour t when operating in state i,
- $x_{t,(i)} \in \{0,1\}$ - Binary decision variable indicating whether the system is in state i during hour t,
- N - Total number of distinct operational states included in the model for each hour.

In the initial phase, the operational states include:

- $i = 1$: Electrolyser in running mode (single fixed capacity level),
- $i = 2$: Electrolyser in standby mode (non-productive but consuming energy to stay warm and pressurised),
- $i = 3$: Electrolyser in complete shutdown mode (no production, minimal or zero consumption from the MSD system).

The total cost term $P_t \cdot E_{\text{el},t}^{(i)}$ captures the hourly operational expense for each mode, which includes both the electrolyser power consumption and power consumption by the methanol synthesis unit, as previously described in **Sec. 2.5**.

The energy consumption values $E_{\text{el},t}^{(i)}$ are considered fixed for each operational state, reflecting simplified static operation described as:

- For the running mode, $E_{\text{el},t}^{(1)} = E_{\text{electrolyser}} + E_{\text{MSD}}$,
- For standby mode, $E_{\text{el},t}^{(2)} = E_{\text{standby}} + E_{\text{MSD, standby}}$,
- For shutdown, $E_{\text{el},t}^{(3)} = E_{\text{MSD, standby}}$.

These constants are derived from the system design parameters, as described in **Sec. 2.5**. Later phases of the model will refine this structure by introducing multiple load levels, load dependent efficiencies and transition related energy costs.

Objective function is subject to binary activation constraints:

$$\sum_{i=1}^{N} x_t^{(i)} = 1 \quad \forall t \in \{1, \ldots, T\} \tag{6.8}$$

to ensure only one operational state is active at any given hour.

6.1.6 Input Parameters

The optimisation model relies on a set of technical and economic input parameters that define the behaviour of the electrolyser and MSD system. These inputs are consistent across all phases, although their interpretation and level of detail may evolve in later modelling stages. The key input parameters can be grouped into three primary categories as electricity price signals, system power consumption and methanol production target.

Electricity Price Signal

Electricity prices P_t are a time varying input to the model and represent the hourly forecasted cost of electricity, for the DK1 zone, as shown in **Chap. 5**. It can be expressed as:

$$P_t = \{P_1, P_2, \ldots, P_T\} \tag{6.9}$$

These values are expressed as DKK/MWh and they are main drive for cost minimisation logic and has strong influence for the optimal mode scheduling.

System Power Consumption

Each operational mode of the system is characterised by a specific electricity consumption level, based on the rated power demand of the electrolyser and the MSD unit, whose values are presented in **Tab. 2.7** in **Sec. 2.7**. The consumption values used as inputs are summarised in **Tab. 6.1**

Table 6.1

Electricity consumption per mode for the electrolyser and methanol synthesis (MSD) system

Mode	**Electrolyser Power [MWh/h]**	**MSD Power [MWh/h]**	**Total Power $\mathbf{E}_{\mathrm{el}}^{(\mathrm{i})}$ [MWh/h]**
Running	50.05	2.02	52.07
Standby	0.17	0.40	0.57
Shutdown	0.00	0.40	0.40

Methanol Production Demand

To ensure the production system satisfies its purpose, a total methanol target M_{target} $[kg]$ that equals 25 000 tons, imposes a constraint over the total simulation horizon T. This target translates to a hydrogen demand profile that must be met through the electrolyser's operation. Methanol production is assumed to be at 100% load:

$$\dot{M}_{\mathrm{MeOH}} = 4508\,\mathrm{kg/h} \tag{6.10}$$

The cumulative production is enforced by the constraint:

$$\sum_{t=1}^{T} \dot{M}_{\mathrm{MeOH}} \cdot x_t^{\mathrm{run}} \geq M_{\mathrm{target}} = 25000\ \mathrm{t} \tag{6.11}$$

where ${x_t}^{run} \in \{0,1\}$ indicates whether the system is running during hour t. The value of M_{target} can be reflected either yearly or weekly. In case of weekly production, M_{target} is distributed over weeks using weights for each week, as shown in **Sec. 6.1.2**.

6.2 Fixed Full Load Operation - Phase 1

This initial optimisation phase establishes the baseline cost and scheduling behaviour for the electrolyser operating strictly at 100% load, once started it must run continuously at 100% load until the specified methanol production demand is fulfilled. No intermediate shutdowns, standby periods or partial load operations are allowed. The optimisation is performed over a full year of hourly electricity price data. This simplified configuration assumes no thermal constraints, ramping or flexibility mechanisms and serves as the foundation upon which more advanced phases are developed

6.2.1 Objective Function

The objective of this phase is to identify the optimal starting time $t_{start} \in \{1, 2, \ldots, T - H + 1\}$, where:

- $T = 8760$ is the weekly time horizon in hours,
- H is the number of hours required to meet the methanol target M_{target} [kg],
- The electrolyser operates continuously at full capacity once started.

Let:

- P_t denote the electricity price at hour $t \in \{1, 2, \ldots, T\}$,
- E_{run} be the fixed electricity consumption at 100% load [MWh/h],
- $x_t \in \{0, 1\}$ indicate if the electrolyser is active during hour t.

The objective function minimises the total electricity cost:

$$\min_{t_{\text{start}}} \sum_{t=t_{\text{start}}}^{t_{\text{start}}+H-1} P_t \cdot E_{\text{run}} \tag{6.12}$$

Subject to:

$$H = \left\lceil \frac{M_{\text{target}}}{\dot{M}_{\text{MeOH}}} \right\rceil \tag{6.13}$$

where:

- $\dot{M}_{\text{MeOH}} = 4508$ kg/h is the constant methanol production rate,
- $E_{\text{run}} = 52.07$ MWh/h is the constant electricity consumption at 100% load.

This formulation effectively slides a window of size H across the electricity price vector and selects the window that has the lowest accumulated cost. Once this optimal interval is located, the electrolyser operates consequently throughout that period, producing methanol at the fixed nominal rate.

6.2.2 Model Constraints

The objective function is a subject to a set of constraints that ensure the methanol production target is satisfied while preserving operational feasibility within the yearly time window. To the constraints already mentioned in **Sec. 6.1**, constraints specific for this phase are added.

Let the binary decision variable $x_t \in \{0,1\}$ indicate whether the electrolyser is active at time $t \in \{1, 2, \ldots, T\}$, where $T = 8760$.

The electrolyser can only operate continuously over one activation window of H hours, where H is computed based on the methanol production requirement:

$$H = \left\lceil \frac{M_{\text{target}}}{\dot{M}_{\text{MeOH}}} \right\rceil \tag{6.14}$$

Only one such interval is allowed within the year. Therefore, we impose:

$$\sum_{t=1}^{T-H+1} y_t = 1 \tag{6.15}$$

where $y_t \in \{0, 1\}$ is an auxiliary binary variable indicating whether hour t is selected as the start of the full-load interval. Then, the operational state variable x_t can be defined as:

$$x_t = \sum_{\tau=\max(1,t-H+1)}^{\min(t,T-H+1)} y_\tau \cdot \mathbb{1}\left(t \in [\tau, \tau + H - 1]\right) \tag{6.16}$$

This relation ensures that only the time steps belonging to the selected start interval are set to 1 (active), and all others are 0.

The activation interval must not exceed the bounds of the yearly time horizon:

$$t_{start} + H + 1 \leq T \tag{6.17}$$

This constraint is satisfied by the upper bound of the summation index in **Eq. 6.15** and the domain of y_t.

During the operating period:

- The electrolyser power consumption is fixed: $E_t = E_{\text{run}} = 52.07$ MWh/h,
- Methanol production is fixed: $\dot{M}_{\text{MeOH}} = 4508$ kg/h,

and for inactive periods, both are zero. This can be expressed as:

$$E_t = E_{\text{run}} \cdot x_t \qquad \forall t \in \{1, \ldots, T\} \tag{6.18}$$

$$\dot{M}_{\text{MeOH},t} = \dot{M}_{\text{MeOH}} \cdot x_t \qquad \forall t \in \{1, \ldots, T\} \tag{6.19}$$

No ramping or transition dynamics are included in this phase.

6.2.3 Optimisation Results

The model is executed over a full year of hourly forecasted electricity price for DK1 zone. Given a fixed methanol production target M_{target} and $\dot{M}_{MeOH}$, required number of operating hours are:

$$H = \left\lceil \frac{M_{\text{target}}}{\dot{M}_{\text{MeOH}}} \right\rceil = \left\lceil \frac{25{,}000{,}000}{4508} \right\rceil = 5546 \text{ hours} \tag{6.20}$$

Therefore, the electrolyser must operate continuously for 5546 hours at full capacity to meet the annual production target

The model identifies the 5546 hour interval with the lowest cumulative electricity costs. As shown in **Fig. 6.3**, the selected window is from hour 3 to 5549, corresponding to the first half of the year.

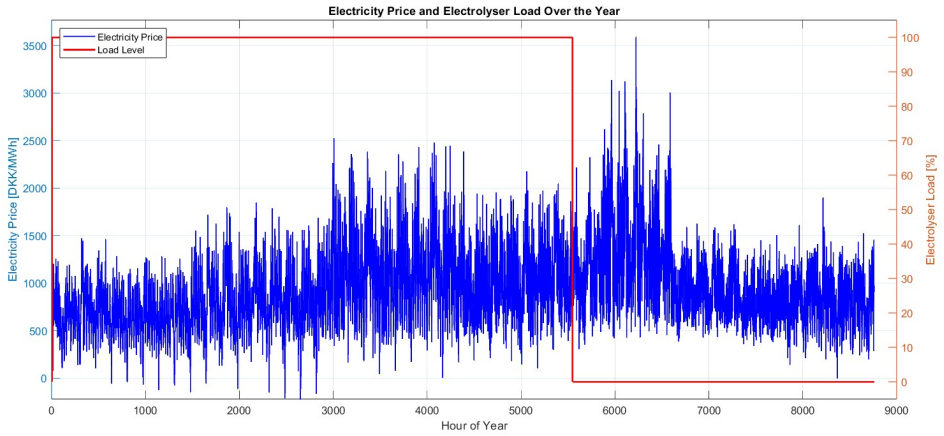

Figure 6.3
Electricity price and electrolyser load profile over a one-year horizon.

Key performance indicators and cost components associated with the optimal electrolyser operation are summarised in **Tab. 6.2**.

Table 6.2
Key performance and economic metrics for the optimal full-load operation of the electrolyser over one year to meet a 25,000-ton methanol production target.

Metric	Results
Produced Methanol	25 001 368 kg
Required Hours	5546 h
Optimal Start Hour	3
Operational Cost	254 140 507.17 DKK
Required CO_2	35 401 937 kg
CO_2 Cost	13 275 726.41 DKK
Excess Heat	22 501.23 MWh
Sold Excess Heat	5 062 777.02 DKK
Weekly CAPEX	18 632 455.63 DKK
Total Cost	280 985 912.16 DKK
MeOH cost	11 238.82 DKK/t

The outcome provides a baseline for evaluating the impact of more flexible operational strategies introduced in later phases. While this configuration ensures simplicity and uninterrupted operation, it does not uses temporal electricity price variability beyond selecting the cheapest continuous window. Subsequent optimisation phases will explore more dynamic approaches that could lead to significant cost reductions.

6.3 Three Operational States - Phase 2

Following the initial fixed full load optimisation model in Phase 1, Phase 2 introduces a more advanced and realistic representation of electrolyser operation by allowing multiple operational states and explicit transition constraints.

In this phase, the electrolyser can operate in one of three primary states, running, standby or shutdown. Running mode is further divided into load levels, only 40% and 100% loads are allowed to reduce complexity while still capturing system flexibility. Transitions between these states are modelled explicitly and require defined durations and energy costs. Additionally, both cold and hot startup procedures are included with their corresponding costs and temporal constraints. The methanol system is directly coupled with the electrolyser output, relying on the hydrogen supply to maintain reactor operation. A hydrogen buffer tank is included to allow for limited decoupling during mode transitions, ensuring reactor continuity even when the electrolyser is temporarily unavailable.

The simulation is executed over a full year (8760 hours), enabling a comprehensive assessment of system performance under seasonal variability in electricity prices. However, to ensure clarity and readability, graphical results are presented for three representative weeks corresponding to the minimum, median and maximum weekly methanol demand.

6.3.1 Objective Function

The objective function in Phase 2 aims to minimise the total operational cost of the system across the time horizon T. Compared to Phase 1, it now includes also:

- Power consumption at discrete load levels (40% and 100%, standby, shutdown)
- Cold and hot start costs and energy use
- Transition costs and durations (Running $\leftrightarrow$ Standby/Shutdown)
- Standby and shutdown power usage for methanol system

The objective function is expressed as:

$$min \text{ Total Cost} = C_{run} + C_{stabdby} + C_{shutdown} + C_{startup} + C_{transition} \tag{6.21}$$

Each component is detailed in subsequent sections.

Running Mode - C_{run}

For the allowed load levels $\lambda \in \{0.4, 1.0\}$, the cost of operating at each load level includes electricity use by both the electrolyser and methanol synthesis system:

$$C_{\text{run}} = \sum_{t=1}^{T} \sum_{l \in \lambda} x_{t,l} \cdot P_t \cdot (E_{\text{el},l} + E_{\text{msd},l}) \tag{6.22}$$

Where:

- $x_{t,l} \in \{0, 1\}$ is 1 if running at load l in hour t
- P_t is the electricity price [DKK/MWh]
- $E_{\text{el},l}$ and $E_{\text{msd},l}$ are electrolyser and MSD power at load l

Standby Mode - $C_{standby}$

In standby, the electrolyser and methanol system are consuming a small fixed power:

$$C_{\text{standby}} = \sum_{t=1}^{T} x_{t,\text{SB}} \cdot P_t \cdot (E_{\text{el,SB}} + E_{\text{msd,SB}}) \tag{6.23}$$

Where:

- $x_{t,\text{SB}} \in \{0, 1\}$ is 1 if standby is active at hour t
- $E_{\text{el,SB}}$ is the power consumption of the electrolyser in standby mode [MWh]
- $E_{\text{msd,SB}}$ is the power consumption of the MSD system in standby mode [MWh]

Shutdown Mode - $C_{shutdown}$

Shutdown involves zero electrolyser usage, but MSD power usage is same as for standby:

$$C_{\text{shutdown}} = \sum_{t=1}^{T} x_{t,\text{SD}} \cdot P_t \cdot E_{\text{msd,SB}} \tag{6.24}$$

Where:

- $x_{t,\text{SD}} \in \{0, 1\}$ is 1 if shutdown is active at hour t

Startup Modes - $C_{startup}$

Startups include both fixed and variable energy costs for cold and hot start procedures. These are applied when transitioning from shutdown/standby to 40% load:

$$C_{\text{startups}} = \sum_{t=1}^{T} (x_{t,\text{CS}} \cdot (C_{\text{cold}} + P_t \cdot E_{\text{CS}}) + x_{t,\text{HS}} \cdot (C_{\text{hot}} + P_t \cdot E_{\text{HS}})) \tag{6.25}$$

Where:

- $x_{t,\text{CS}}, x_{t,\text{HS}} \in \{0,1\}$ are binary indicators for cold and hot startup at time t

- C_{cold} is the fixed cold start cost for electrolyser; 1200 DKK
- C_{hot} is the fixed cold start cost for electrolyser; 82.50 DKK
- $E_{\text{CS}}, E_{\text{HS}}$ is the total electricity used during cold or hot startup

The total used electricity of startup modes accounts for multiple sub-phases during activation, including electrolyser warm-up, tank refill, MSD ramp-up and productive operation at 40% load. Phases for cold start are detailed in **Fig. 6.4**.

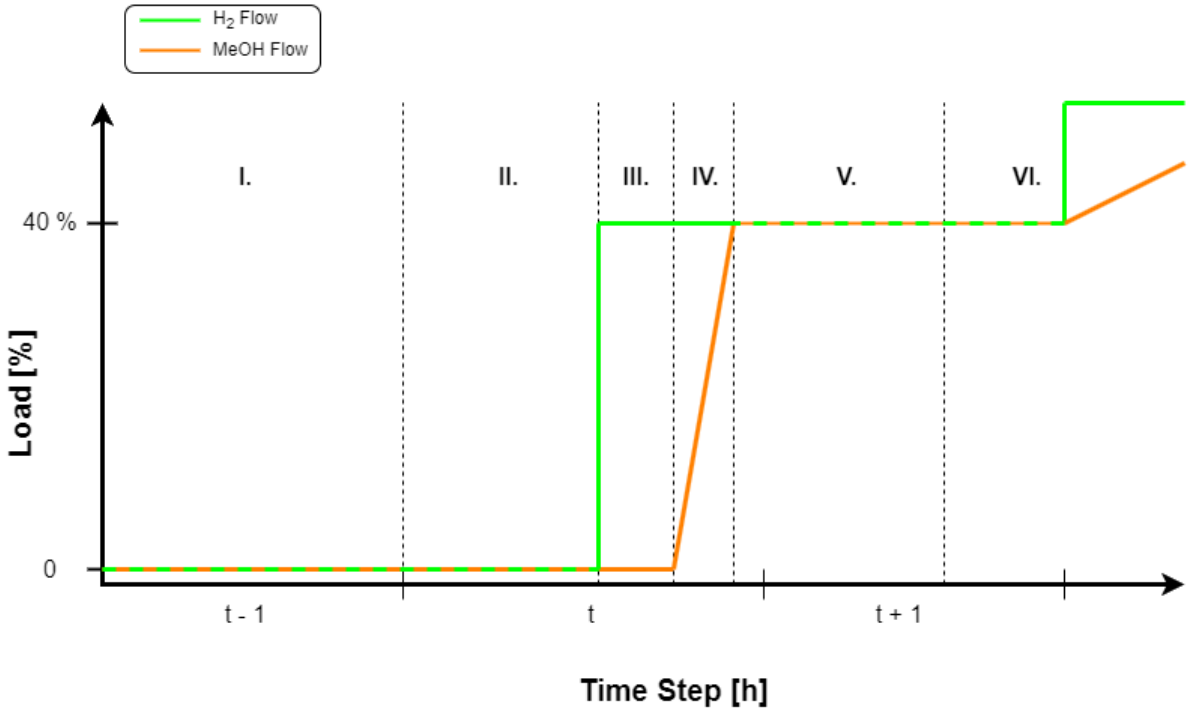

Figure 6.4
Illustration of methanol synthesis ramp-up dynamics following a cold start of the electrolyser.

The timeline in **Fig. 6.4** is divided into six segments, corresponding to the startup of the electrolyser and MSD unit:

- **I. Shutdown (t-1)**
  The electrolyser is in shutdown, with zero electricity consumption and no hydrogen output. The methanol synthesis unit is inactive.
- **II. Cold Start (t)**
  At the start of the hour t, a cold start is triggered. The electrolyser enters its warm-up pressurisation phase. This requires a transition period of $t_{cold} = 42$minutes and consumes 1200 DKK in electricity. No hydrogen is yet available to the methanol synthesis unit.
- **III. Tank Refill (t_{tank})**
  After cold start is completed, the electrolyser begins producing hydrogen. However, this first hydrogen output is allocated to refill the xx kmol H_2 buffer tank, which was used during the previous shutdown. The tank refill duration last 7 minutes. During this time, methanol production remains paused.
- **IV. MSD Start (t_{msd_up})**

Once the tank is fully refilled, the methanol unit begins its own 39 minutes long phase to enter operational phase. In phase **IV.** it spends first 6 minutes to come to 40% of H_2 load.

- **V. MSD Hold (t_{msd_up})**
  After initial 6 minutes of ramp-up, it takes 33 more minutes to stabilise the temperature and pressure inside the MSD system at load level of 40%.
- **VI. Future Hours** Once whole system is stabilised at 40%, electrolyser ramps up to 100% steeply, while MSD system follows it gradually.

These stages represent the complete startup sequence for cold starts. Hot start follows same logic, but changes are happening much faster as the system is already heated and pressurised to certain point.

Cold Start Energy - E_{CS}

$$E_{\text{CS}} = E_{\text{el,40}} \cdot (t_{\text{prod}} + t_{\text{tank}} + t_{\text{msd\_up}}) + E_{\text{msd,SB}} \cdot (t_{\text{cold}} + t_{\text{tank}}) + E_{\text{msd,up}} \cdot t_{\text{msd}} + E_{\text{msd\_up}} \cdot t_{\text{prod}} \quad (6.26)$$

Where:

- $t_{\text{prod}} = 1 - t_{\text{cold}} - t_{\text{tank}} - t_{\text{msd\_up}}$ - remaining time for full operation [h]

Hot Start Energy - E_{HS}

$$E_{\text{HS}} = E_{\text{el,40}} \cdot (t'_{\text{prod}} + t_{\text{tank}} + t_{\text{msd\_up}}) + E_{\text{msd,SB}} \cdot (t_{\text{hot}} + t_{\text{tank}}) + E_{\text{msd,up}} \cdot t_{\text{msd\_up}} + E_{\text{msd}} \cdot t'_{\text{prod}} \quad (6.27)$$

Where:

- $t_{\text{hot}} = \frac{2}{60}$ - hot start duration [h]
- $t'_{\text{prod}} = 1 - t_{\text{hot}} - t_{\text{tank}} - t_{\text{msd\_up}}$ - remaining time for full operation after hot start [h]
- $E_{\text{el,40}}$ - Electrolyser energy use at 40%
- E_{msd} - MSD energy use at 100%
- $E_{\text{msd,SB}}$ - MSD energy in standby
- $E_{\text{msd,up}}$ - MSD energy during ramp-up (40% of full)

Transition Modes - $C_{transition}$

Transitioning from running to either standby or shutdown incurs specific energy penalties due to ramp-down of MSD and switching dynamics:

$$C_{\text{transitions}} = \sum_{t=1}^{T} \left(x_{t,\text{SB\_TR}} \cdot P_t \cdot E_{\text{SB\_TR}} + x_{t,\text{SD\_TR}} \cdot P_t \cdot E_{\text{SD\_TR}} \right) \quad (6.28)$$

Where:

- $x_{t,\text{SB\_TR}}, x_{t,\text{SD\_TR}} \in \{0,1\}$ - transition indicators
- $E_{\text{SB\_TR}}$ - energy used during ramp-down from running $\rightarrow$ standby

- $E_{\mathrm{SD\_TR}}$ - energy used during ramp-down from running → shutdown

During electrolyser standbys or shutdowns, the system must manage both the decline in hydrogen supply and the stable ramp-down of the MSD. These transitions require careful coordination to avoid process instability. The phases in ramp-down are illustrated in **Fig. 6.5**.

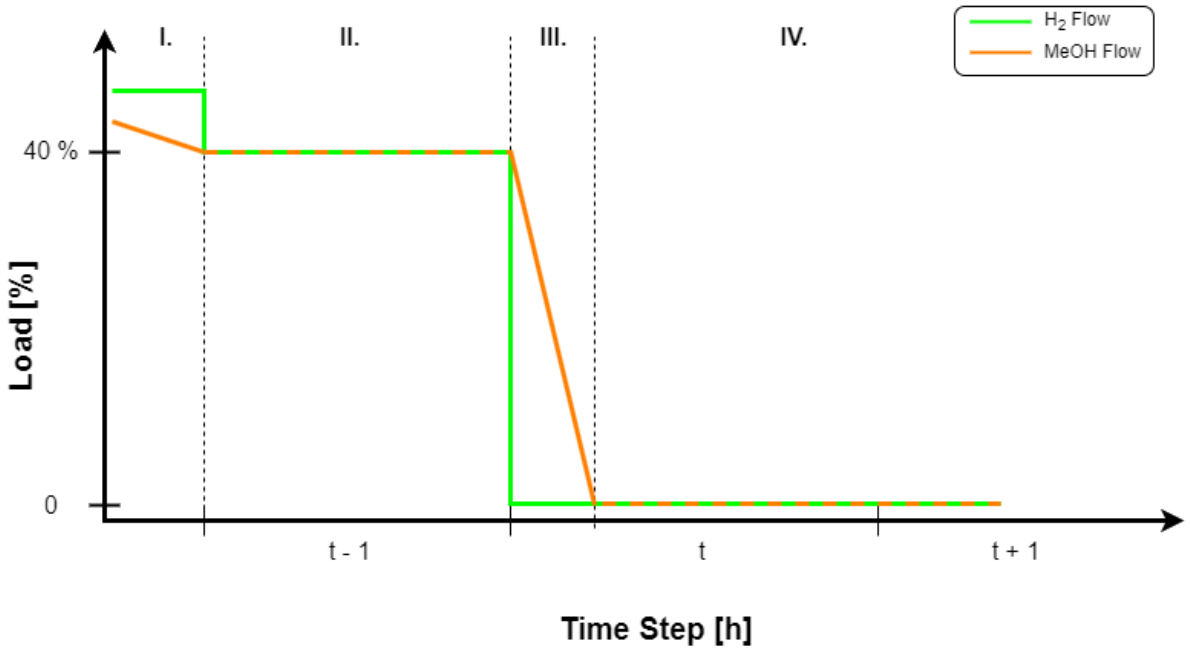

Figure 6.5
Representation of methanol synthesis ramp-down dynamics during electrolyser transition to standby or shutdown.

The timeline is divided into four segments, showing the sequence of events from full load operation to standby or shutdown:

- **I. Full Operation (t-2 to t-1)**
  The electrolyser was running at 100% load and it is reducing its load to 40%, as preparation for shutdown or standby transition.
- **II. Transition Initiation (t-1)**
  A transition decision is made at the end of this time step. Hydrogen flow drops immediately. The electrolyser enters a transition phase toward shutdown.
- **III. Transition Phase**
  The electrolyser fully stops hydrogen production at the beginning of hour t. To sustain methanol synthesis during this gradually reduction of load from 40% to 0%, that lasts 6 minutes, hydrogen from the tank is used.
- **IV. Shutdown/Standby State** (t_{msd_down})
  MSD has to be 90 minutes out of the function, to normalise pressure and temperature. Additionally, this ensures that every cold or hot start is performed within the same environment.

This ramp-down proposes constraints for minimal duration of shutdown or standby due to me-

chanical properties of MSD system.

Standby Transition Energy - E_{SB}

$$E_{\text{SB\_TR}} = E_{\text{el,SB}} \cdot (1 - t_{\text{SB}}) + E_{\text{msd,down}} \cdot t_{\text{SB}} + E_{\text{msd,SB}} \cdot (1 - t_{\text{msd\_down}}) \tag{6.29}$$

Where:

- $E_{\text{el,SB}}$ - electrolyser power in standby
- $E_{\text{msd,down}}$ - MSD ramp-down power (40% of full)
- $E_{\text{msd,SB}}$ - MSD energy use in standby

Shutdown Transition Energy - E_{SD}

$$E_{\text{SD\_TR}} = E_{\text{msd,down}} \cdot t_{\text{SB}} + E_{\text{msd,SB}} \cdot (1 - t_{\text{msd\_down}}) \tag{6.30}$$

Once objective function is defined, next step is to limit potential solutions with constraints.

6.3.2 Technical Constraints

To ensure operational feasibility to technical logic, the model includes a series of constraints. These include allowed and forbidden transitions coupled with minimum and maximum durations of operational states. All constraints are applied across the time horizon T.

Allowed transitions

Startup and shutdown modes must be followed by correct subsequent states:

- **Cold start → 40% load:**

$$x_{t,\text{CS}} = x_{t+1,0.4} \quad \forall t = 1, \ldots, T-1 \tag{6.31}$$

- **Hot start → 40% load:**

$$x_{t,\text{HS}} = x_{t+1,0.4} \quad \forall t = 1, \ldots, T-1 \tag{6.32}$$

- **Standby transition → Standby:**

$$x_{t,\text{SB\_TR}} = x_{t+1,\text{SB}} \quad \forall t = 1, \ldots, T-1 \tag{6.33}$$

- **Shutdown transition → Shutdown:**

$$x_{t,\text{SD\_TR}} = x_{t+1,\text{SD}} \quad \forall t = 1, \ldots, T-1 \tag{6.34}$$

Forbidden Transitions

Tab. 6.3 presents all constraints which are not allowed when changing states.

Table 6.3
Forbidden transitions between operational states across time steps.

From State	To State	Condition	Note
Running ($x_{t,l}$)	Cold Start ($x_{t+1,\text{CS}}$)	$\forall l$	Cold start is only allowed after Shutdown
	Hot Start ($x_{t+1,\text{HS}}$)	$\forall l$	Hot start is only allowed after Shutdown
	Shutdown ($x_{t+1,\text{SD}}$)	$\forall l$	Must pass through Shutdown Transition
	Standby ($x_{t+1,\text{SB}}$)	$\forall l$	Must pass through Standby Transition
Standby ($x_{t,\text{SB}}$)	Running ($x_{t+1,l}$)	$\forall l$	Standby cannot directly resume to load
	Shutdown ($x_{t+1,\text{SD}}$)	–	Must use Shutdown Transition
	SB Transition ($x_{t+1,\text{SB\_TR}}$)	–	Transitions can't follow a stable state directly
	SD Transition ($x_{t+1,\text{SD\_TR}}$)	–	Transitions can't follow a stable state directly
	Cold Start ($x_{t+1,\text{CS}}$)	–	Cold start only valid from Shutdown
Shutdown ($x_{t,\text{SD}}$)	Running ($x_{t+1,l}$)	$\forall l$	Must pass through a start phase
	Standby ($x_{t+1,\text{SB}}$)	–	Not allowed to jump to standby
	Hot Start ($x_{t+1,\text{HS}}$)	–	Only one startup type is allowed at a time
	SB Transition ($x_{t+1,\text{SB\_TR}}$)	–	Transitions not applicable from Shutdown
	SD Transition ($x_{t+1,\text{SD\_TR}}$)	–	Same as above

Minimum Running Period

To ensure thermal stability of the system, electrolyser after a startup has to run for at least 3 consecutive hours:

$$\sum_{i=t}^{t+2}(x_{i,0.4} + x_{i,1.0}) \geq 3 \cdot (x_{t-1,CS} + x_{t-1,HS}); \quad t = 2, \ldots, T-2 \tag{6.35}$$

This equation ensures that any hour following a startup triggers at least 3 hours of consecutive running mode.

Minimum Standby Duration

Because the MSD system takes longer to reach standby than the electrolyser, the electrolyser should stay in standby for at least 2 hours so both systems can be in the same state again:

$$\sum_{i=t+1}^{t+2} x_{i,SB} = 2 \cdot x_{t,SB\_TR}; \quad t = 1, \ldots, T-1 \tag{6.36}$$

Minimum Shutdown Duration

It takes nearly 12 hours for the MSD system to reduce its temperature and pressure to reach shutdown, while the electrolyser shuts down much faster. For the same reason as in the standby transition, when a cold start occurs, both the MSD and electrolyser should be aligned in their operational states:

$$\sum_{i=t+1}^{t+12} x_{i,SD} = 12 \cdot x_{t,SD\_TR}; \quad t = 1, \ldots, T-11 \tag{6.37}$$

6.3.3 Optimisation Constraints

Additionally to the technical constraints, optimisation constraints supports logic behind the transitions used for coding. These include initial conditions, load level restrictions and enforces certain logics. All constraints are applied across the time horizon T.

Mode Exclusivity

At each hour t, the system can be only in one mode:

$$\sum_{\lambda} x_{t,\lambda} + x_{t,\mathrm{SB}} + x_{t,\mathrm{SD}} + x_{t,\mathrm{CS}} + x_{t,\mathrm{HS}} + x_{t,\mathrm{SB\_TR}} + x_{t,\mathrm{SD\_TR}} = 1 \quad \forall t \in \{1, \ldots, T\} \tag{6.38}$$

Initial Condition

The electrolyser starts in running mode at 40% load at $t = 1$:

$$x_{1,0.4} = 1; \quad x_{1,j} = 0 \;\; \forall j \neq 0.4 \tag{6.39}$$

Load Level Restrictions

Only 40% and 100% load levels are allowed. All other levels are not implemented in this phase:

$$x_{t,l} = 0; \quad \forall l \in \{0.5, 0.6, 0.7, 0.8, 0.9\}, \; t = 1, \ldots, T \tag{6.40}$$

Load Logic Before/After Transitions

After any startup or before transitions, the electrolyser must operate at 40%:

- **After startup (at $t-1$):**

$$x_{t,0.4} \geq x_{t-1,\mathrm{CS}} + x_{t-1,\mathrm{HS}} \quad \forall t = 2, \ldots, T \tag{6.41}$$

- **Before standby/shutdown transitions (at $t+1$):**

$$x_{t,0.4} \geq x_{t+1,\mathrm{SB\_TR}} + x_{t+1,\mathrm{SD\_TR}} \quad \forall t = 1, \ldots, T-1 \tag{6.42}$$

100% Enforcement

In this development phase, 40% load is used due to technical constraints only during transitions, as system can not operate immediately at full 100% load. Therefore, system should operate minimally at 40% load level:

$$x_{t,0.4} \leq x_{t-1,SB} + x_{t-1,SD} + x_{t+1,SB\_TR} + x_{t+1,SD\_TR} \quad \forall = 2, \ldots, T-1 \tag{6.43}$$

This ensures 40% load is only used in hours when it comes from startup or it prepares for one of the transitions.

6.3.4 Methanol Production Constraint

The electrolyser is coupled with MSD system, meaning all hydrogen produced must be consumed by the reactor. To ensure stable downstream production and meet the annual methanol target, the optimisation model enforces methanol mass balance and production constraint over time.

Methanol Production at Running Mode

For each hour t, methanol production is a function of the load level at which the electrolyser is running. With only two allowed loads, methanol output per hour is:

$$M_t^{base} = x_{t,0.4} \cdot M_{0.4} + x_{t,1.0} \cdot M_{1.0} \tag{6.44}$$

Where:

- $M_{1.0} = 4508 kg/h$
- $M_{0.4} = 0.4 \cdot M_{1.0} = 4508 kg/h$

Methanol Production for Startups

As noted in **Fig. 6.4**, a cold start involves several sequential steps before methanol production can begin. First, the electrolyser takes 42 minutes to start up, followed by 7 minutes to refill the hydrogen tank. Only then can the methanol synthesis system ramp up, which takes 6 minutes to reach 40% load and another 33 minutes to achieve the required temperature and pressure for full operation. Because this entire sequence takes more than one hour, while the optimization model operates in hourly time steps, the first hour after a cold start cannot deliver the full expected production. Therefore, the methanol production at 40% load during hour $t+1$ must be adjusted to account for this loss. Therefore, the equation for produced methanol during cold start is:

$$M_t^{CS} = x_{t,CS} \cdot (M_{0.4} \cdot (6/2 + 33) + M_{0.4} \cdot t_{prod}^{CS} \tag{6.45}$$

Where:

- $t_{prod}^{CS} = 1 - t_{cold} - t_{tank} - t_{msd\_up}$

On the other hand, a hot start is significantly faster than a cold start. As a result, the transition from standby to running is completed within the same hour t. The equation used to calculate methanol production remains unchanged, with only the value of $t_{\text{prod}}^{\text{HS}}$ being adjusted accordingly:

$$M_t^{HS} = x_{t,CS} \cdot (M_{0.4} \cdot (6/2 + 33) + M_{0.4} \cdot t_{prod}^{HS} \tag{6.46}$$

Where:

- $t_{prod}^{HS} = 1 - t_{hot} - t_{tank} - t_{msd\_up}$

Methanol Production for Standby and Shutdown Transitions

When the MSD system transitions from a running state to either standby or shutdown, it does not stop operating instantly. Instead, it gradually ramps down, during which it continues to produce methanol at a decreasing rate. This linear ramp-down reflects the time required to safely lower the system's temperature and pressure. As a result, methanol is still produced during the transition period, and its amount is proportional to the duration of this ramp-down. The methanol produced during this phase can therefore be calculated using the following expression:

$$M_t^{SB\_TR} = x_{t,SB\_TR} \cdot M_{0.4}/2 \cdot t_{SB} \tag{6.47}$$

$$M_t^{SD\_TR} = x_{t,SD\_TR} \cdot M_{0.4}/2 \cdot t_{SD} \tag{6.48}$$

Weekly Methanol Production Constraint

The model operates on a rolling weekly horizon $T = 168$ and must satisfy a target methanol output over the horizon:

$$\sum_{t=1}^{T} M_t \geq M_{target,week} \tag{6.49}$$

Where:

- $M_t = M_t^{base} + M_t^{CS} + M_t^{HS} + M_t^{SB\_TR} + M_t^{SD\_TR}$

6.3.5 Optimisation Results

The optimisation model described from **Sec. 6.3.1** to **Sec. 6.3.4** is executed over 8760 hours using hourly electricity price input and a weekly rolling scheduling window. For each week, the optimiser selects the operational mode of the electrolyser to minimise total operational cost while ensuring weekly methanol demands.

Due to the large simulation scale, only three representative weeks are selected and presented graphically to highlight system behaviour under different demand scenarios which are summarised in **Tab. 6.4**.

Table 6.4
Selected representative weeks for graphical analysis based on methanol demand levels

Scenario	Figure	Week	Methanol Demand [kg]
Maximum demand	**Fig. 6.6a**	Week 6	710,640
Minimum demand	**Fig. 6.6b**	Week 43	464,690
Median demand	**Fig. 6.6c**	Week 36	276,186

The corresponding system behaviour for these three representative demand scenarios are presented in **Fig. 6.6**

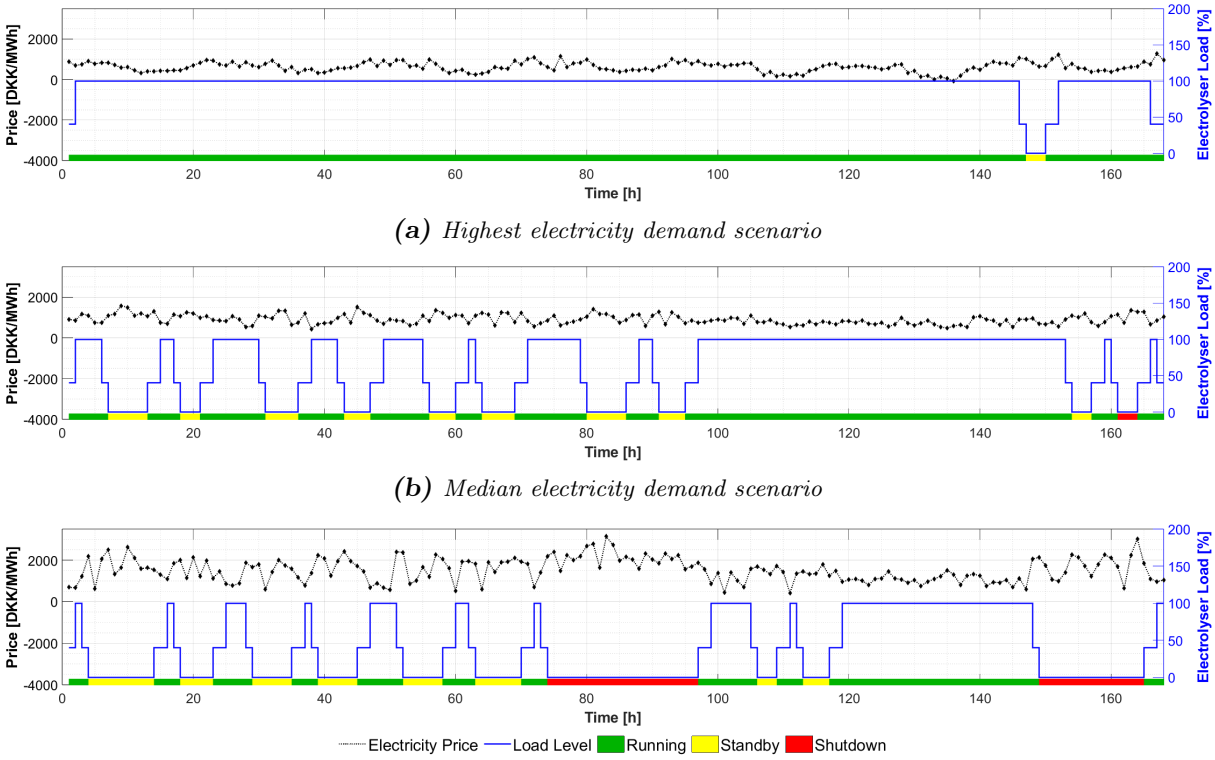

(a) *Highest electricity demand scenario*

(b) *Median electricity demand scenario*

(c) *Lowest electricity demand scenario*

Figure 6.6
Electrolyser operation under different electricity demand scenarios. Each subplot shows electricity price, load level and operational state (running, standby, shutdown).

These weeks provide insight into how the model balances cost and production under varying price and methanol demands.

The full-year simulation results are presented in **Tab. 6.5**.

A detailed breakdown of these cost components, expressed as percentages of the total final cost, is illustrated in **Fig. 6.7**.

The total amount of produced methanol is 25,230,293 kg, which is 0.92% higher than the target production. This slight surplus occurs because the model cannot produce the exact target amount, and the use of a rolling window approach leads to minor overproduction each week. The resulting cost per tonne of e-methanol is calculated to be **9,578.63 DKK/t**.

Table 6.5
Breakdown of total production cost for 25,230.29 tonnes of methanol

Cost Component	**Amount [DKK]**
Operational Cost – Electrolyser	205,220,304.86
Operational Cost – MSD System	9,530,846.14
CAPEX	18,632,455.60
CO_2 Cost	13,397,285.58
Excess Heat Revenue	-5,109,134.33
Total Production Cost	**241,671,757.85**

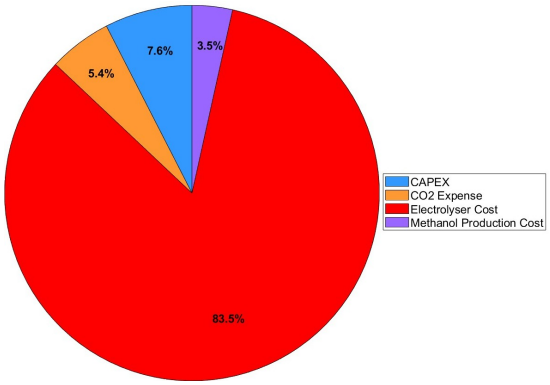

Figure 6.7
Percentage contribution of each cost component to the total methanol production cost.

The results of Phase 2 demonstrate the substantial economic and operational benefits of introducing load flexibility and strategically managing transitions between running, standby and shutdown states. Compared to full load operation, this more dynamic strategy reduces final cost per tonne of produced e-methanol for approximately 15%. However, methanol production is linearly approximated from discrete hydrogen flows without capturing potential nonlinear dynamics. To address these limitations and further improve optimisation model, the next phase introduces data driven surrogate modelling for methanol synthesis. These allow the model to accurately reflect system dynamics and evaluate partial load operation strategies across a continuous domain.

6.4 Full Operation - Phase 3

The third phase introduces two upgrades, the electrolyser is now allowed to operate at seven distinct load levels (ranging from 40% to 100% with 10% steps) and the methanol production is no longer linearly estimated. Instead, a data-driven methanol transition matrix is used to dynamically map the methanol output during each load shift. This enables the model to more precisely capture transition effects, energy penalties and realistically show behaviour of the methanol synthesis, as shown in **Sec. 2.5**.

6.4.1 Objective Function

Objective function stays same as defined in Phase 2, see **Eq. 6.21**, and includes contributions from electricity usage, transition energy penalties and startup costs. In Phase 3, the structure of the cost function is improved with additional load levels and it can be defined as:

$$\min \text{TotalCost} = \sum_{t=1}^{T} \left[\sum_{l \in \lambda} x_{t,l} \cdot P_t \cdot (E_{\text{el},l} + E_{\text{msd},l}) + \sum_{m \in \nu} x_{t,m} \cdot (C_m + P_t \cdot E_m) \right] \tag{6.50}$$

Where:

- $\lambda = \{0.4, 0.5, \ldots, 1.0\}$ is the set of allowed electrolyser load levels
- $x_{t,l} \in \{0, 1\}$ is the binary variable for operating at load level λ during hour t
- $E_{\text{el},l}$, $E_{\text{msd},l}$ are the electricity consumption rates of the electrolyser and MSD at load level λ
- $\mathcal{V} = \{\text{SB}, \text{SD}, \text{CS}, \text{HS}, \text{SB\_TR}, \text{SD\_TR}\}$ is the set of transition and idle states
- C_m is the fixed cost for each startup or transition (e.g., cold start cost C_{CS})
- E_m is the corresponding energy consumption for each mode or transition

6.4.2 Technical Constraints

Technical constraints defined in previous Phase 2, see **Sec. 6.3.2**, remains the same as those are defined by the system's capabilities and not by optimisation logic development.

Minimum Durations

Minimum time durations for standby(2h), shutdown(12h) and post startup running (3h) are enforced using the same constraints defined in Phase 2, see **Eq. 6.35, 6.36 and 6.37**.

6.4.3 Optimisation Constraints

The Phase 3 model retains the multi state operational logic and methanol production target introduced in Phase 2. However, new optimisation constraints are added or updated to support new load levels, ramping constraints between them and dynamic methanol production logic.

Mode Exclusivity

Eq. 6.38 is extended to include new load levels:

$$\sum_{l \in \lambda} x_{t,l} + \sum_{m \in \nu} x_{t,m} = 1 \quad \forall t \in \{1, \ldots, T\} \tag{6.51}$$

Where:

- $\lambda = \{0.4, 0.5, 0.6, 0.7, 0.8, 0.9, 1.0\}$
- $\nu = \{\text{SB, SD, CS, HS, SB\_TR, SD\_TR}\}$

Load Ramping Constraint

To avoid unrealistic jumps in electrolyser power levels between hours, a $\pm 40\%$ ramping limit is applied:

$$|\text{Load}_t - \text{Load}_{t-1}| \leq 0.4 \quad \forall t = 2, \ldots, T \tag{6.52}$$

This is implemented by binary matrix logic that compares load levels selected at t and $t-1$,

ensuring allowable transitions only.

Startup and Transition Logic

Enforced transitions from startup and standby/shutdown remain unchanged and are same as from Phase 2, see **Eq. 6.31** to **Eq. 6.34** for allowed transition and **Tab. 6.3** for forbidden transitions.

6.4.4 Methanol Production Constraint

In contrast to previous phase where methanol is linearly estimated from static hydrogen flows, see from **Eq. 6.44** to **Eq. 6.48**, Phase 3 introduces a transition methanol production matrix. This matrix realistically capture how the methanol synthesis reactor responds to changes between load levels.

Transition Matrix Concept

Methanol production M_t in any given hour is now determined by both the previous load level l_{t-1} and current load level l_t. The relationships are stored in $7x7$ matrix M_{trans}, as shown in **Fig. 6.8**

FROM \ TO	40%	50%	60%	70%	80%	90%	100%
40%	56.28	68.13	77.71	85.03	89.41	91.76	92.66
50%	58.29	70.35	82.72	91.79	99.49	104.69	109.47
60%	62.78	71.89	84.42	96.69	106.60	114.97	118.89
70%	69.74	76.75	86.04	98.49	110.80	120.72	128.84
80%	78.25	82.94	90.49	100	112.56	125.23	136.03
90%	89.24	92.13	95.90	103.64	113.68	126.63	139.56
100%	97.96	102.48	103.92	108.72	117.35	127.33	140.70

Figure 6.8
Methanol production matrix illustrating the estimated output (in kg/h) for transitions between operating load levels.

Where:

$$M_t = M_{trans}(l_{t-1}, l_t) \tag{6.53}$$

Each entry $M_{trans}(i,j)$ represents the methanol output $[kg/h]$ when transitioning from load level i to j, where $i,j \in \{0.4, 0.5, 0.6, 0.7, 0.8, 0.9, 1.0\}$. The diagonal terms represent steady-state operation, while off diagonal entries represent transient production states. These values are obtained from a trained surrogate model.

Surrogate Model

The values in the methanol transition matrix M_{trans} are not derived from physical equations, but from a data driven surrogate model trained on simulated process data. Specifically, a LSTM

model neural network is developed to capture the time dependent behaviour of the methanol synthesis reactor in response to varying hydrogen input levels.

The LSTM is trained using historical dynamic simulations of the coupled electrolyser and reactor system, in which the hydrogen feed is varied across all allowable transitions, as shown in **Appendix A.13**. For each transition, the resulting methanol output over time is recorded for every 1.5 minutes.

This surrogate model captures:

- Non-linearities in reactor response
- Ramp-up lag effects
- Losses due to suboptimal operating conditions
- Asymmetric transition behaviour

The surrogate's predictions are validated against process models, as shown in **Appendix A.14**, and then discretised into the $7x7$ matrix. This matrix is subsequently used in the MILP model for rapid evaluation of methanol output without re simulating system dynamics.

Transition Logic

To express this in the MILP framework, binary mapping is introduced:

$$z_{t,i,j} = \begin{cases} 1 & \text{if } x_{t-1,i} = 1 \text{ and } x_{t,j} = 1 \\ 0 & \text{otherwise} \end{cases} \tag{6.54}$$

Subject to:

$$\begin{aligned} & z_{t,i,j} \leq x_{t-1,i} \\ & z_{t,i,j} \leq x_{t,j} \\ & z_{t,i,j} \geq x_{t-1,i} + x_{t,j} - 1 \qquad \forall i, j \in \lambda \end{aligned} \tag{6.55}$$

Then methanol production per hour is defined as:

$$M_t = \sum_{i \in \lambda} \sum_{j \in \lambda} z_{t,i,j} \cdot \mathbf{M}_{\text{trans}}(i,j) \tag{6.56}$$

This ensures methanol output reflects not only the operating point but also load transition effects like ramp-up lag or efficiency dips.

The equations governing methanol production during startups and transitions to standby or shutdown remain unchanged from those presented in Phase 2. Moreover, the weekly methanol demand target is maintained at the same level.

6.4.5 Optimisation Results

The Phase 3 optimisation model is executed over the same full year simulation horizon as in previous phases, using a weekly rolling window. The key difference lies in the model's ability

to operate at seven discrete load levels and to capture transient methanol effects with LSTM surrogate matrix.

To provide insight into the model's performance across varying operating conditions, same representative weeks are selected as in Phase 2 for analysis in detail. These weeks are chosen to reflect different electricity pricing patterns and system responses under full operation. The aim is to showcase how the optimiser adapts the electrolyser load to minimise operational costs while satisfying production constraints. Three representative weeks are graphically presented in **Fig. 6.6**

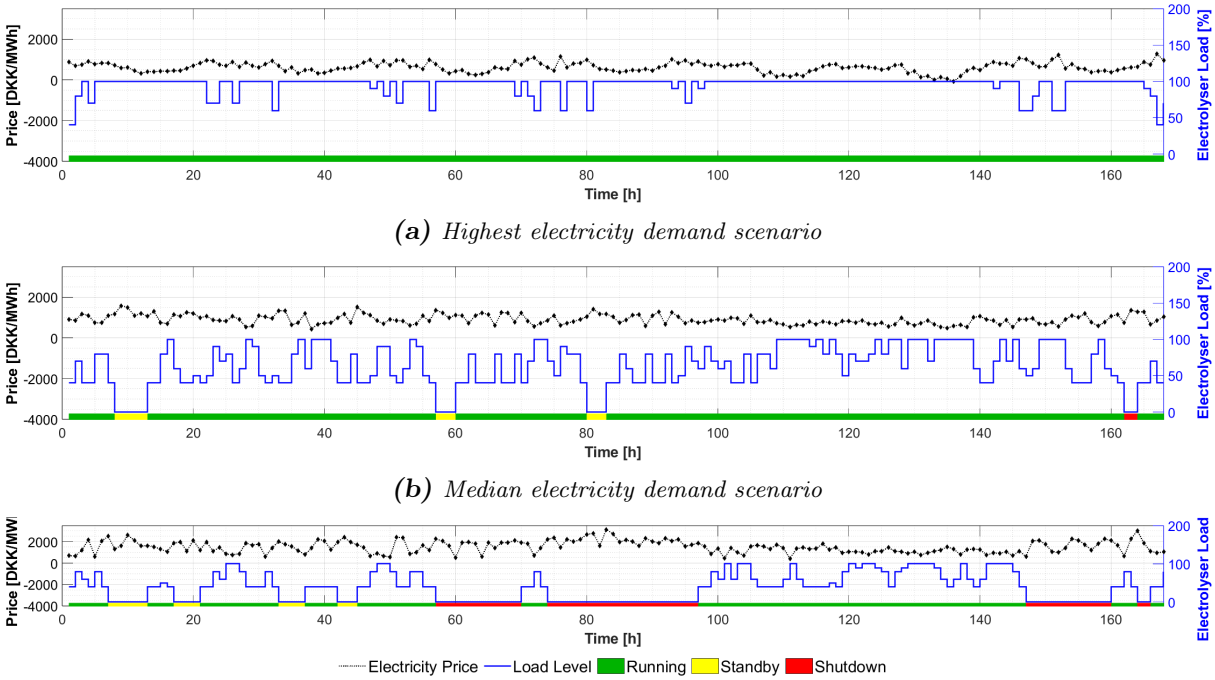

(a) *Highest electricity demand scenario*

(b) *Median electricity demand scenario*

(c) *Lowest electricity demand scenario*

Figure 6.9

Electrolyser operation under different electricity demand scenarios. Each subplot shows electricity price, load level and operational state (running, standby, shutdown).

Tab. 6.6 compares how many hours have electrolyser spent in three different modes for three representative weeks in Phase 2 and Phase 3.

Table 6.6

Weekly distribution of operating states (Running, Standby, Shutdown) during selected demand weeks for both phases.

Week Type	Phase	Running [h]	Standby [h]	Shutdown [h]
Maximum	2	162	6	0
	3	168	0	0
Median	2	124	40	4
	3	154	11	3
Minimum	2	82	47	39
	3	100	17	51
Total	2	368	93	43
	3	422	28	54

In Phase 3, the system operates in running mode more frequently across all weeks, with total running hours increasing from 368 to 422 hours. This reflects the optimiser's ability to better use flexible load levels under variable electricity prices. Standby hours significantly reduced, from 93 to 28, indicating less reliance on intermediate idle states. Instead, the model favours small, cost effective load adjustments within the running mode. Meanwhile, shutdown hours increased slightly, particularly in the minimum demand week, suggesting a more confident use of full shutdown when economically justified.

Fig. 6.10 presents the distribution of operational states over the entire year. The system operates in running mode for over 86% of the time, with the majority at 100% load. Standby accounts for 8.3%, and full shutdown only 5.4%.

This distribution reflects the model's ability to use intermediate load levels and avoid unnecessary transitions. The frequent use of full load operation, which is 33%, is complemented by significant time spent at other load levels, which demonstrates the optimiser's flexibility in responding to price variations while maintaining stable methanol output.

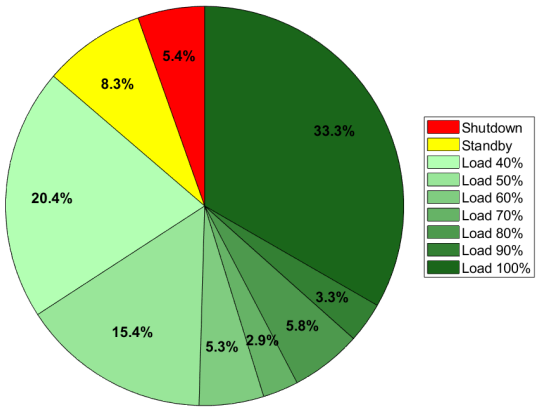

Figure 6.10
Distribution of electrolyser operational states throughout the full-year simulation in Phase 3.

The limited use of shutdown and standby improves energy efficiency but also supports long-term system durability, as frequent shutdowns and restarts can increase equipment wear, reduce electrolyser lifespan and increase maintenance needs. The results for a optimisation across full year are showcased in **Tab. 6.7**

Table 6.7
Breakdown of total production cost for 25,203.15 tonnes of methanol

Cost Component	**Amount [DKK]**
Operational Cost – Electrolyser	204,194,345.82
Operational Cost – MSD System	8,508,097.74
CAPEX	18,632,455.60
CO_2 Cost	13,382,874.66
Excess Heat Revenue	-5,103,638.64
Total Production Cost	**239,614,135.18**

The cost breakdown for the entire simulation period is shown in **Fig. 6.11**. The total operational cost for the full year is calculated as 239,614,135.18 DKK for production of 25,203.15 tonnes of e-methanol. Surplus of produced methanol in Phase 3 is lower then in Phase 2, meaning that model can now produce closer to methanol demand boundary. As shown in **Fig 6.11**, electrolyser's electricity consumption is the dominant cost driver with close to 84% of total expense, while all the other drivers are ranging from 3.5% to 7.6%. The average cost of methanol production for Phase 3 is calculated at **9507.31** DKK/t, showing a reduction of close to 1% compared to previous phase due to dynamic load control enabled by the surrogate model.

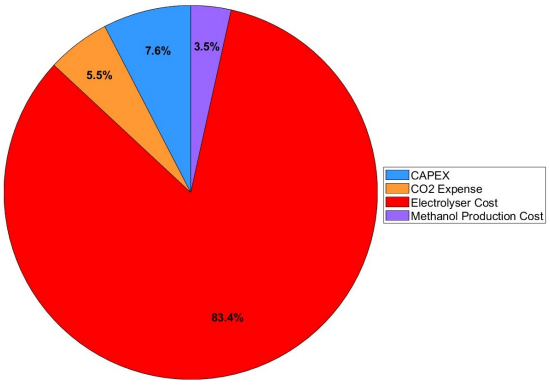

Figure 6.11
Percentage contribution of each cost component to the total methanol production cost.

To summarise, this final development phase demonstrates that introducing partial-load flexibility and a data-driven methanol production model enables more refined and cost effective scheduling of electrolyser operation. The system remains in productive states for the majority of the time, strategically navigating electricity price fluctuations while minimising inefficient transitions. These improvements not only reduce the total operational cost and methanol unit price compared to earlier phases, but also support more sustainable long-term operation by limiting unnecessary shutdowns and standbys.

While Phase 3 focused on optimising performance under fixed system parameters, it is important to explore how sensitive these results are to changes in key assumptions. Therefore, the next development phase moves towards a conceptual analysis, examining how varying CO_2 price, electrolyser efficiency and electricity pricing structure would impact the overall system behaviour and economic outcome.

6.5 Conceptual Scenarios - Phase 4

While previous optimisation phases focused on developing a realistic and operationally feasible operational framework for green methanol production, all simulations so far have assumed fixed system parameters and idealised electricity pricing. In reality, many of these parameters are uncertain or subject to future changes due to market dynamics, technological improvements or regulatory shifts.

Phase 4 introduces a series of conceptual sensitivity analyses aimed at evaluating how the system responds to changes in key external conditions, where changed parameters are:

- Electricity pricing
- CO_2 pricing
- Technical constraints

These variations do not represent physical changes to the system architecture, but rather serve as what if scenarios that help assess the robustness and adaptability of the model under different boundary conditions.

6.5.1 Historical Electricity Pricing

To assess how the electrolyser operational scheduling model performs under actual market dynamics, this scenario introduces real historical electricity price from the DK1 region from 1^{st} of April 2024 to 31^{st} of March 2025. Although the electricity mix in this dataset is not fully green, this test does not aim to assess carbon performance, but rather focuses on the operational

and economic impact of real-time market exposure. The results offer insight into how the optimiser would behave if the electrolyser were operating on spot market terms without a dedicated renewable Power Purchase Agreement(PPA).

Fig. 6.12 shows a comparison between the actual and forecasted data used in the same period, from April to April but in different years. While both profiles share a similar average price level, the actual price data is more volatile, experiencing more frequent and extreme downward spikes as well as occasional high peaks not present in the smoother forecasted profile.

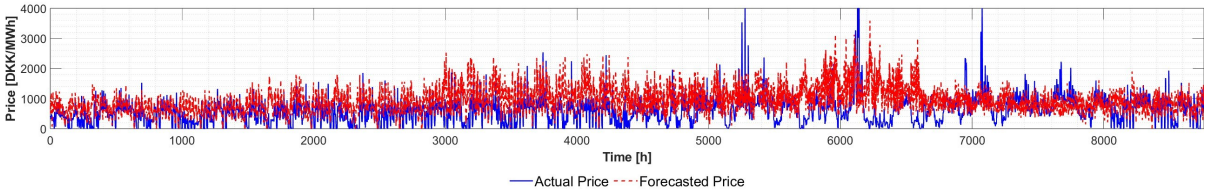

Figure 6.12
Comparison of Actual and Forecasted Hourly Electricity Prices

These price dynamics reflect the true nature of modern electricity markets with high renewable penetration, where sudden changes in wind or solar generation can drive large and rapid price fluctuations. Average electricity price for forecasted data is 668.09 DKK while average price for history data is 435.37 DKK.

As a direct consequence of the new price signal, since the optimisation is performed in weekly windows, the weekly methanol demand production has to be updated. **Fig. 6.13** illustrates the updated demand profile.

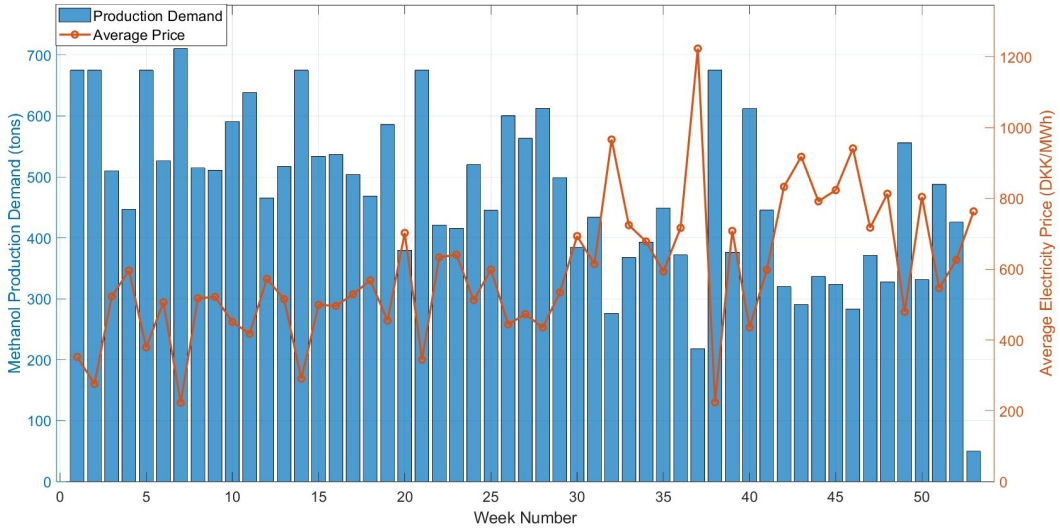

Figure 6.13
Weekly methanol production demand and average electricity price for history data from April 2024 to March 2025.

With presented demands for weeks, optimisation is performed by weekly rolling window for given time period. Results of optimisation are presented in **Tab. 6.8**

Table 6.8

Comparison of cost components between the 2024 model and forecasted model, showing percentage deviation. Results are presented for production of 25,256.05 ton of methanol for 2024 and 25,203.15 for forecasted model.

Cost Component	2024 Model [DKK]	Forecasted Model [DKK]	Difference
Operational Cost - Electrolyser	110,330,413.36	204,194,345.82	-45.97 %
Operational Cost - MSD System	4,597,100.56	8,508,097.74	-45.97 %
CAPEX	18,632,455.60		-
CO_2 Cost	13,410,960.35	13,382,875.66	+0.21 %
Excess Heat Revenue	-5,114,349.29	-5,103,638.64	-0.21 %
Total Production Cost	141,856,580.58	239,614,135.18	-40.79 %
Methanol Cost	5,616.74 per ton	9,507.31 per ton	-40.92 %

The results in **Tab. 6.8** provide a clear comparison of cost structures between the 2024 historical model and the forecasted based on just renewable electricity. Even though that history data is averagely lower by 34.83% from forecasted data, both the electrolyser and MSD system operational costs are lower by approximately 46%. CAPEX remains unchanged, while CO_2 costs and excess heat differs by negligible amount of 0.21%, which equals to difference between produced methanol. In total, the overall production costs declined by 40.79%, from approximately 239.6 million DKK to 141.9 million DKK. Difference percentage for produced methanol per ton is slightly higher, as more methanol is produced with 2024 model than with forecasted model.

6.5.2 Carbon Pricing

Carbon pricing is a key economic factor in e-methanol production, as CO_2 must be continuously supplied to the synthesis process. In previous phases, a fixed CO_2 price of 375 DKK/ton was assumed. However, in reality, this value is subject to change due to market conditions, availability of source and evolving emissions regulations under European Union.

In this scenario, a parametric sensitivity analysis is carried out using seven discrete CO_2 price levels, ranging from 25% to 250% of the nominal reference price. This range reflects following:

- Lowered prices (25% - 75%) represent scenarios where CO_2 is purchased from industrial or biogenic sources.
- Nominal case (100%) reflects the average market price which is used in optimisation
- Higher prices (150% - 250%) represents scenarios where CO_2 is obtained through on-site carbon capture systems, which involve higher operational and capital costs due to required processes

Exploring a broad range of carbon pricing scenarios is essential as it directly affects the cost-efficiency and operational feasibility of e-methanol production. Understanding influence of CO_2 on final cost is necessary for future investments and approaches. Final results using these seven scenarios are presented in **Tab. 6.9**.

Table 6.9
Impact of CO_2 price variation on total cost and methanol unit cost.

CO_2 Price [DKK/kg]	CO_2 Price [% of Base]	CO_2 Expense [DKK]	Total Expense [DKK]	Methanol Price [DKK/t]	Change vs Base
0.09375	25%	3,345,719	229,576,979	9,109	−4.19%
0.1875	50%	6,691,437	232,922,698	9,242	−2.79%
0.28125	75%	10,037,156	236,268,417	9,374	−1.40%
0.375	100%	13,382,874	239,614,135	9,507	0.00% (baseline)
0.5625	150%	20,074,312	246,305,572	9,773	+2.79%
0.75	200%	26,765,749	252,997,009	10,038	+5.59%
0.9375	250%	33,457,186	259,688,447	10,304	+8.38%

As expected, increasing or decreasing the CO_2 price leads to linear change in both total operational cost and cost per ton of methanol. The nominal case of 375 DKK/t results in a methanol cost of 9,507 DKK/t, while the lowest tested price drops it to 9,109 DKK/t and the highest increases it to 10,304 DKK/t.

Despite the great increase in CO_2 price, the resulting change in methanol production cost is relatively modest with only 8% increase from baseline.

6.5.3 Technical Improvements

As mentioned in **Eq. 6.37**, the system is required to remain in shutdown mode for a minimum of 12 hours once this state is entered. This constraint is based on the technical feasibility of the system, ensuring that internal pressures and temperatures reach stable conditions. It also guarantees that the system always initiates a cold start from consistent physical conditions. This section explores potential improvements in performance when the minimum shutdown duration is reduced, as some of those 12 hours may coincide with periods of favourable electricity prices.

The analysis is conducted over a week time horizon, for week 36, which represents the period with the lowest methanol demand. Low demand implies a higher number of potential shutdown hours, making it an ideal case for evaluating the effect of reducing the minimum shutdown duration. During this 168-hour period, the system is required to produce 276.186 tons of methanol. Cases that were investigated are when minimum duration is 4, 8 or 12 hours. Resulting number of hours spent in operational states are presented in **Tab. 6.10**

Table 6.10
Number of hours spent in each operational state for different minimum shutdown durations.

Scenario	Shutdown	Standby	40%	50%	60%	70%	80%	90%	100%
Min. 12h	44	23	46	5	6	5	18	5	16
Min. 8h	46	16	50	9	10	6	11	4	16
Min. 4h	62	3	47	5	11	4	14	4	18

Operational schedules for scenarios are presented in **Fig. 6.14**.

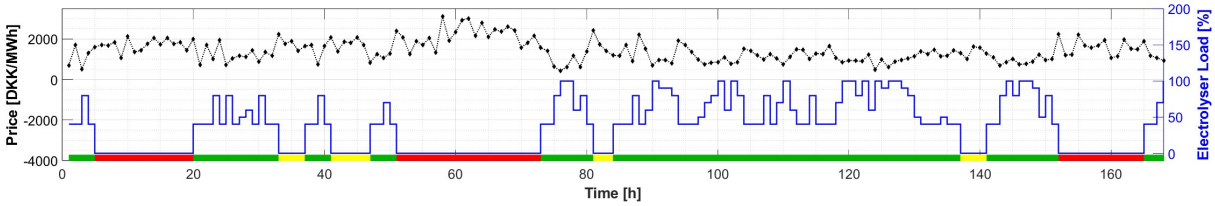

(a) *Electrolyser has to be at least 12 hours in shutdown.*

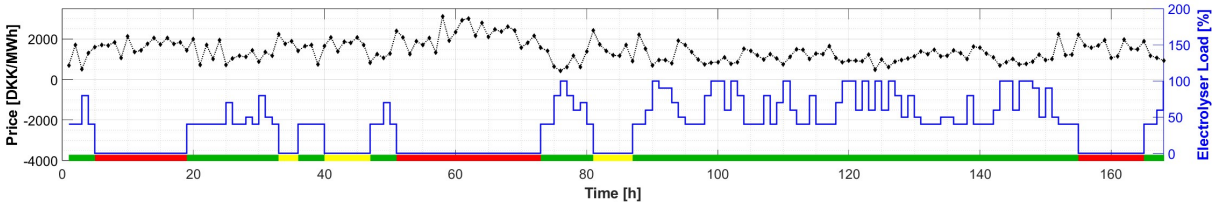

(b) *Electrolyser has to be at least 8 hours in shutdown.*

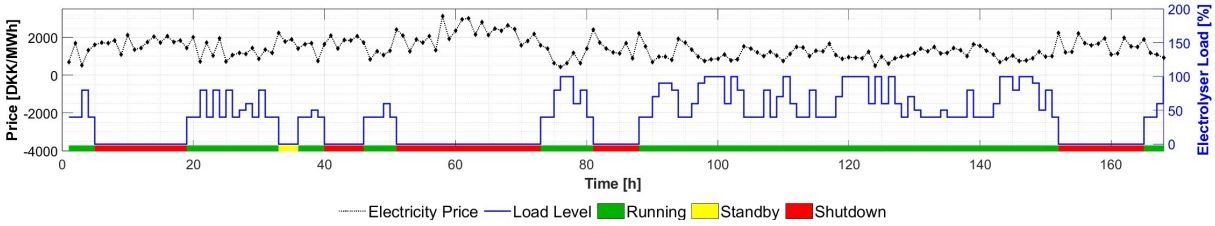

(c) *Electrolyser has to be at least 4 hours in shutdown.*

Figure 6.14

Electrolyser operation under different minimum durations for shutdown of electrolyser. Each subplot shows electricity price, load level and operational state (running, standby, shutdown).

All costs, together with final cost and cost per ton of methanol are presented in **Tab. 6.11**.

Table 6.11

Techno-economic summary for different minimum shutdown durations for a production of 276.186 tons of methanol.

Scenario	**Min. 12h**	**Min. 8h**	**Min. 4h**
Produced Methanol (kg)	277,526.60	277,258.79	278,557.65
Electricity Cost (DKK)	3,137,365.44	3,112,090.36	3,069,069.75
MSD Cost (DKK)	130,723.56	129,670.43	127,877.91
CAPEX (DKK)	358,316.45	358,316.45	358,316.45
CO_2 Emissions (kg)	147,366.63	147,224.42	147,914.11
Excess Heat (kWh)	-56,199.14	-56,144.91	-56,407.92
Total Operational Cost (DKK)	**3,717,572.94**	**3,691,156.75**	**3,646,770.30**
Cost per kg (DKK)	**13.40**	**13.31**	**13.09**

Reducing the minimum shutdown duration from 12 hours to 4 hours results in a 2.30% decrease in the weekly cost of methanol production. This suggests that more efficient equipment, which allows shorter shutdown periods, could lead to lower overall production costs. As previously discussed, the 12-hour shutdown duration was initially set to ensure that all cold starts have a uniform reference point. However, it is technically feasible to initiate a cold start earlier, provided that additional monitoring equipment is in place to accurately track the system's status. This highlights the potential for further reductions in methanol production costs through targeted R&D in electrolyser and MSD systems.

Project Results 7

This chapter summarises the outcomes of the developed forecasting and optimisation framework and evaluates how well the project objectives and requirements were fulfilled. Furthermore, a critical reflection on the obtained outcomes will be provided, including their implications. These results will also be used to challenge the developed models, serving as a basis for identifying limitations and guiding potential directions for future work.

7.1 Project Requirements

To ensure the system addressed both economic and operational challenges in methanol production, six specific requirements were outlined in **Sec. 3.1**. These covered both the forecasting and optimisation aspects of the project. This section evaluates how each is fulfilled in the final implementation.

The first requirement was to develop a forecasting model capable of estimating hourly electricity prices over a full year using historical data. This is achieved through a hybrid approach combining XGBoost and LSTM, trained on real DK1 market data, including historical load and renewable generation forecasts. The model successfully generated hourly predictions for 8760 hours, enabling a reliable input signal for operational decisions.

The second requirement specified that the forecast model must rely solely on renewable inputs such as solar generation, offshore and onshore winds. This constraint is fully respected throughout the forecasting setup to ensure the model aligned with the green energy focus of PtX systems. No fossil based indicators were included.

Once forecasting was developed, the third requirement was to integrate the forecasted electricity prices into the optimisation model. This is successfully implemented, with all scheduling logic driven by forecast inputs.

From optimisation point of view, the fourth requirement indicates for the implementation of at least three distinct states. In Phase 2, see **Sec. 6.3**, these states are introduced with clearly defined energy consumption, transition costs and state switching logic. Their behaviour is developed even further in Phase 3, see **Sec. 6.4**, with the introduction of different distinct load levels and dynamics between them.

To ensure time consistent planning, the fifth requirement specified that all operational decisions

should be made on an hourly basis, matching the intention of the electricity pricing input. This is consistently defined throughout the modelling, with the optimiser producing a full year hourly operation schedule using a rolling window formulation.

Finally, the sixth and most important requirement was to minimise operational costs while still fulfilling a fixed methanol production target. This condition is satisfied in all phases. The model ensured the full production of 25,000 ton of methanol annually while strategically adjusting operating patterns to use low-price windows and avoid costly transitions.

To summarise, all six requirements are fulfilled. The developed models demonstrated its ability to make economically driven decisions while maintaining technical feasibility.

7.2 Result Assessment

This section evaluates the electricity price forecasting model and the optimisation model. The aim is to critically assess performance outcomes, but also to identify practical limitations and areas for improvement.

While the project succeeded in meeting its technical requirements, it is essential to reflect on the accuracy, robustness and applicability of each subsystem, particularly given the reliance on forecasted inputs and operational constraints in a highly dynamic energy environment.

7.2.1 Evaluation of Forecasting Results

The forecasting model is built with a clear focus on renewable inputs, with focus on solar and wind generated electricity. This is a intentional modelling constraint, aligning with the assumption that e-methanol system are operating primarily on green electricity. As such, no market price signals, fuel cost indicators or fossil generation shares were included in the prediction logic.

Consequently, it was expected that a forecast based only on renewable sources might result in slightly higher prices during periods when renewable output is insufficient to meet demand, as is case in DK1, where fossil generation is still used to balance generation and demand. This hypothesis is confirmed later during Phase 4, see **Sec. 6.5.1**, where historical data from 2024-25 are compared to the model's forecasted prices. The analysis shows that the e-methanol production cost based on historical electricity prices was approximately **40%** lower than the cost using forecasted prices.

However, the forecast model served its intended purpose effectively, which is to provide a green price signal for evaluating how a flexible methanol production would respond in an idealised PtX future scenario. It supported full year scheduling without critical deviations and enabled realistic testing of the optimiser's behaviour.

It is important to note that this forecasting component was not the primary focus of the project.

Therefore, it was not investigated or fine-tuned beyond its functional requirements. The model is not benchmarked against other forecasting tools or subjected to hyperparameter optimisation. This is a conscious decision, as the primary objective of the thesis is to explore operational optimisation rather than prediction accuracy. Nonetheless, the model remains a valid foundation for further development.

7.2.2 Evaluation of Optimisation Results

The optimisation framework is developed incrementally across three phases, each introducing higher operational realism and increased modelling flexibility.

In Phase 1, the optimiser served as a baseline, scheduling the electrolyser at full capacity based only on electricity price signals. While this phase delivered results for methanol price per ton by just 17% higher then next phase, it lacked technical feasibility by ignoring essential constraint such as startup energies and transitions between states.

Phase 2 introduced discrete operational states with defined transitions and minimum duration constraints. This significantly improved realism, allowing the model to choose how a electrolyser would respond to fluctuating electricity prices. It also demonstrated how idle states could be strategically used to avoid high-cost hours while still fulfilling production targets.

Lastly, Phase 3 has the most significant advancement by incorporating partial-load flexibility, a methanol transition matrix and finer ramping constraints. These changes enabled the optimiser to operate across seven load levels (40% - 100%) and capture the real dynamic response of the methanol synthesis unit. Results improved by approximately 1% compared to Phase 2. However, results now respect all equipment and process limitations, which was not the case in previous phase where some parts were idealised. Furthermore, Phase 3 showcased that flexible load scheduling can maintain demanded productivity without relying heavily on full shutdowns or standby, which are costly both economically and from a system durability standpoint.

While the first three phases focused on improving operational logic and feasibility, Phase 4 served a different role. It is introduced as a sensitivity phase, aimed at testing the system's robustness under changing external conditions. By varying price structures, CO_2 pricing and technical constraints, Phase 4 explored:

- Which external factor have the greatest influence on cost
- How system performance might evolve under future market conditions
- Where future R&D and investment should be directed

The impact of changes in the electricity pricing structure had the most significant influence on the cost outcome. By replacing the forecasted prices with historical 2024/25 prices, a new cost structure emerged. Although the average annual price difference is slightly above 30%, the variation in operational costs reaches nearly 50%. This imbalance is coming from the fact that the electrolyser operates only around 85% of the time, meaning that the price differences during ac-

tive production hours are likely higher, while prices during standby or shutdown periods have less influence. Another contributing factor is the nature of the electricity source. Electricity derived exclusively from renewable sources tends to be more expensive than electricity from the Danish grid, which is a mix of renewables and fossil-based generation. Fossil-based sources contribute to price stability and offer more low-cost hours, which helps to suppress price spikes. This finding suggests that while renewable-based pricing is valuable for evaluating the long-term feasibility of Power-to-X systems, short and mid-term economic planning should consider the current energy mix to avoid overestimating operational costs. A potential solution can be seen in the Kassø facility, where electricity supply is sourced from both the grid and an adjacent solar park [24].

Furthermore, sensitivity analysis explored the impact of changing CO_2 pricing. Prices were assumed to be lower, for cheaper biogenic CO_2 from plants, or higher, for more expensive CO_2 captured on-site using carbon capture systems. Results showed that even a 250% increase in CO_2 price resulted in only about an 8% increase in the final methanol cost. It supports findings from PtX studies [54], which shows that electricity is the dominant expense and suggests that variations in CO_2 price do not critically influence system performance. Moreover, this highlights a strategic consideration for future investments where improving electricity efficiency or securing cheaper renewable power has a far greater impact on economic feasibility.

An additional analysis introduced in Phase 4 focused on relaxing the minimum shutdown duration from 12 hours to 4 hours. This change led to a measurable reduction in the weekly methanol production cost by 2.30%, highlighting the economic potential of reducing downtime in the electrolyser system. The results suggest that enabling earlier cold start initiation, possibly through advanced monitoring and control systems, could further decrease production costs. This finding emphasises the importance of technological improvements in system responsiveness and supports that case for further R&D efforts to minimise forced idle periods without compromising system integrity.

To summarise, Phase 4 provided valuable insights into the system's robustness. It revealed that changes in electricity price structure significantly influence operation and costs, while variations in CO_2 price have a marginal effect. These insight are not only relevant for technical optimisation but also for guiding future R&D, infrastructure planning and resource prioritisation, helping stakeholders decide where investment will have the greatest impact.

7.3 Result Comparison

To benchmark the developed optimisation framework and assess its realism, a comparison is made between the results obtained in Phase 3 of this thesis and selected recent studies from the Nordic region. Particular attention is given to the Kassø project, analysed by Taslimi et al. [54], which also served as a reference for several input parameters during the model development. Additional studies are included for comparison purposes for methanol price per ton.

7.3.1 Operational Mode Distribution

In Phase 3, the optimiser operated the electrolyser using a flexible scheduling approach across seven load levels. The total time spent in each state over the full simulation year is:

- **Running Mode:** 86.3%
- **Standby Mode:** 8.3%
- **Shutdown Mode:** 5.4%

This distribution shows a strong preference for continuous operation, with short and not frequent transitions to idle states. In comparison, Taslimi et al. [54] reported that electrolyser in the Kassø facility had availability from 66% to 72% for different cases. The higher running percentage in this thesis indicates that model preferred to shift between load levels rather than using a combination of higher load levels with standby or shutdown periods.

7.3.2 Cost Distribution

The breakdown of total operational cost in Phase 3 is as follows:

- **Electrolyser electricity consumption:** 83.4%
- **Methanol synthesis unit:** 3.5%
- **CO_2 cost:** 5.5%
- **CAPEX:** 7.6%

The distribution is in line with Taslimi et al., which consistently identify electricity consumptions by the electrolyser as the dominant cost factor. It reports that Kassø facility account for 87.2% of production cost, while CO_2 is 7.5%.

7.3.3 Methanol Cost

The final methanol cost in Phase 3 is calculated at 9.51 DKK/kg, equivalent to approximately 1.28 €/kg. This value falls within common range of $1.0 - 1.5$ €/kg found in following literature:

- **Andersson[6]:** $0.95 - 1.87$ €/kg across Nordic countries
- **Taslimi et al. [54]:** ~ 1.12 €/kg for DK1
- **Schneider and Lagoni [48]** ~ 1.09 €/kg
- **Andrae et al. [7]** $1.06 - 1.51$ €/kg

The results obtained in this thesis is within the expected range. The slight difference can be due to plant scale, assumed electricity prices and transition modelling in this project.

7.4 Limitations

While the project successfully delivered a functioning and adaptable optimisation model with integrated forecasting, several limitations were identified during development that may influence both the accuracy and applicability of the results. These limitations are outlined below to ensure transparency and guide future improvements.

7.4.1 Forecast Model Simplicity

The electricity price forecasting model is developed with a limited feature set focused only on renewable generation and demand. While this design aligns with a green transition perspective, it exclude influential factors such as cross-border exchange, fuel prices or reserve market signals. As a result, while sufficient for conceptual scheduling, the model may not capture extreme price events or market shifts.

7.4.2 Load Levels and Discrete Operation

The optimiser handles operation at predefined discrete load levels (in 10% steps), which simplifies the MILP formulation but does not represent the continuous control capability of modern electrolyser systems. Similarly, transitions are modelled in discrete state changes rather than as continuous ramping, which may over or underestimate the impact of mode switching. These simplifications were necessary for computational manageability but could be addressed in future work using nonlinear or dynamic optimisation frameworks.

7.4.3 CO_2 Source and Quality

While CO_2 is priced at different levels in Phase 4 to reflect sourcing differences, the model assumes 100% pure and available CO_2 at all times. It does not consider the variability in CO_2 availability, purity or compression cost, all of which could influence both the scheduling and the overall economics. In real systems, CO_2 access may be constrained by upstream process reliability or transportation infrastructure.

7.4.4 Economic Model Boundary

Lastly, the cost model primarily focuses on electricity, CO_2, CAPEX and methanol production costs, excluding broader financial factors such as maintenance, workers, taxation or market participation mechanisms. Therefore, the results represent operational feasibility but do not reflect a full techno-economic analysis. A future expansion could include full lifecycle modelling.

While these limitations do not invalidate the findings, they highlight areas where the model could be further expanded or refined to support real-world deployment and improve predictive accuracy. The current framework lays a strong foundation, but like any optimisation tool, its effectiveness improves as input assumptions and system resolution evolve.

Conclusion 8

This thesis develops an operational strategy to optimise the operational behaviour of an electrolyser in an eMeOH production system. The strategy responds dynamically to fluctuating electricity prices with the aim of minimising operational costs while ensuring a stable and sufficient hydrogen flow for demanded methanol synthesis. The focus lies in aligning the electrolyser's operation with electricity price volatility while respecting technical constraints such as transition durations, system limitations and methanol production requirements.

To achieve this, the thesis is structured around two core components, electricity price forecasting and operational optimisation. A hybrid forecasting model combines LSTM to predict renewable generation and demand, with XGBoost used to forecast electricity prices on a day-ahead basis. This combination provides accurate and timely price signals, which serve as direct input to the scheduling optimisation.

The optimisation model is formulated using a mixed integer linear programming approach. It determines the optimal sequence of operational states(running, standby, shutdown) and transition paths over a yearly time horizon. Across development phases, the model integrates constraints such as minimum durations for states, cold and hot start limitations, transition energy penalties and production target tracking. A data-driven LSTM surrogate model is integrated to estimate methanol output based on hydrogen input and recent operating history, ensuring that system behaviour is captured realistically.

Through simulation and scenario testing, the model shows its ability to reduce operating costs caused by electricity, while adapting to price fluctuations. It ensures hydrogen availability for methanol synthesis, meeting predefined production targets. The sensitivity of the model to electricity price variability confirms its robustness and flexibility under real-world conditions.

In conclusion, the developed solution demonstrates that operational scheduling of electrolyser can be effectively optimised using a combination of predictive modelling and mathematical programming. It enables cost-effective and stable operation in dynamic energy market. This thesis establishes a strong foundation for further development, including real-time integration, coupling with broader Power-to-X infrastructure or extension toward market participation strategies.

Future Work 9

This chapter outlines key directions for future research. These include increasing the complexity and realism of the forecasting model, expanding the optimisation framework to better reflect operational constraints and flexibility and identifying promising areas for further R&D efforts that could support system integration and technological maturity.

9.1 Enhancing Forecast Model

While the current electricity price forecasting model achieves solid performance within a yearly window, extending prediction over longer horizons, as a year is, proves to be increasingly infeasible. The electricity market, particularly in regions with high renewable penetration like Denmark, is influenced by numerous volatile local factors such as wind forecasts, unexpected demand spikes, network constraints and market participant behaviour. These effects accumulate over time, making long-term predictions unreliable.

Therefore, a key direction for future work lies in developing a more dynamic, real-time forecasting approach that is deeply integrated with the production system. Instead of relying on static forecasts generated for longer periods, the system should continuously update predictions with the most recent input data. This would enable rolling day-ahead or intra-day forecasting that better reflect market volatility.

Ultimately, future forecasting should not be viewed as a single component but as a tightly coupled module within the broader production system. This level of integration would enable production decisions to be made on an hour by hour basis, improving responsiveness to changing conditions and improving the economic viability of e-methanol production systems.

9.2 Adding Complexity to Optimisation Model

The optimisation model developed in this thesis has proven effective in demonstrating the potential for cost savings through optimal scheduling of electrolyser operation. However, the simplifications made to maintaining model tractability also introduces limitations that reduce its applicability to actual systems. Several key areas have been identified where the model can be expanded to capture a higher degree of operational realism and flexibility.

9.2.1 Load Resolution

Currently, the electrolyser operates in discrete load levels, from 40% to 100%, which simplifies the optimisation but restricts the solution space. In practice, modern PEM electrolysers, such as the Siemens Silyzer 300, are capable of continuous operation across a wide dynamic range. A more advanced optimisation model should treat load as a continuous variable, allowing the system to freely adjust power consumption within operational limits. This would better reflect actual system capabilities and could decide on more cost-efficient operating strategies, especially during volatile electricity pricing periods.

9.2.2 Flexible Timing

Another simplification in the current model is the assumption that operational changes occur only at the start of an hour. In reality, system controllers can respond to price signals and production demands in real time. Future models should implement flexible transition timing, allowing mode changes to occur at arbitrary points in time. This requires moving from hourly time steps and adopting higher resolution time discretisation, which would significantly improve alignment with electricity market operation and intra-day variations.

9.2.3 CO_2 Sourcing and Variable Pricing

The current model assumes a constant CO_2 supply with a fixed price. However, CO_2 can be sourced from multiple streams, such as:

- Industrial flue gas - from cement or steel plants
- Biogenic sources - biomass facilities
- Direct Air Capture

Each of these sources has a different cost, carbon intensity and availability profile. Incorporating this into the model would require creating a CO_2 procurement module capable of selecting from various sources at different times based on pricing, availability and sustainability targets. This added dimension would improve the economic and environmental realism of the optimisation and could enable multi-objective optimisation, balancing cost minimisation with carbon reduction

9.3 Strategic R&D Focus Areas

The techno-economic modelling in this thesis clearly illustrates which components of the system have the greatest potential in reducing total operational costs. This insight provides a strong foundation for prioritising future R&D efforts that can deliver the most impactful improvements in both performance and cost-effectiveness.

9.3.1 Electrolyser System

the electrolyser emerged as the most influential cost driver in the overall system. Its electricity consumption directly correlates with operational cost and even small improvements in efficiency can yield substantial long-term savings. Therefore, R&D should be directed toward increasing electrolyser efficiency and how to improve dynamic performance, giving an opportunity for faster and smoother transitions between states. Next generation of PEM or newly SOEC electrolysers should be a central component of future R&D programs.

9.3.2 Electricity Pricing

While electricity price forecasting and integration strategies can support better scheduling, they do not address the real problem that is the high and volatile cost of electricity. To improve economic feasibility at the system level, efforts must be made to structurally reduce electricity price available for PtX such as:

- Dedicated renewable generation - Direct coupling of electrolysers to wind or solar farms can bypass markets and avoid transmission fees.
- Grid fee exemption for PtX - Policy and laws could enable reduced tariffs or exemptions for PtX installations, as they decarbonise the environment.
- Increasing renewable capacity - Investments in renewable electricity would grant potential for PtX facilities.

To reduce the levelised cost of e-methanol, technology engineers, system designers and policy-makers must converge their efforts on the two most sensitive parameters which are electrolyser performance and electricity price structure.

Literature

[1] Thomas Ackermann. "Wind Power in Power Systems, Second Edition." In: *Wind Power in Power Systems, Second Edition* (Apr. 2012). DOI: 10.1002/9781119941842. URL: https://onlinelibrary.wiley.com/doi/book/10.1002/9781119941842.

[2] Muflih A. Adnan and Md Golam Kibria. "Comparative techno-economic and life-cycle assessment of power-to-methanol synthesis pathways." In: *Applied Energy* 278 (Nov. 2020). ISSN: 03062619. DOI: 10.1016/j.apenergy.2020.115614.

[3] A. Ajanovic et al. "The economics and the environmental benignity of different colors of hydrogen." In: *International Journal of Hydrogen Energy* 47.57 (July 2022), pp. 24136–24154. ISSN: 0360-3199. DOI: 10.1016/J.IJHYDENE.2022.02.094.

[4] Saleh Albahli et al. "Electricity Price Forecasting for Cloud Computing Using an Enhanced Machine Learning Model." In: *IEEE Access* 8 (2020), pp. 200971–200981. ISSN: 21693536. DOI: 10.1109/ACCESS.2020.3035328.

[5] AleaSoft. *The drop in the LCOE of renewable energies over the past decade drives the energy transition - AleaSoft Energy Forecasting*. Sept. 2023. URL: https://aleasoft.com/drop-lcoe-renewable-energies-past-decade-drives-energy-transition.

[6] Hanna Andersson. *Potential of Implementing Power-to-Methanol Projects Based on Biogenic Carbon in the Nordics*. Tech. rep.

[7] Elisabeth Andreae et al. "Cost minimization of a hybrid PV-to-methanol plant through participation in reserve markets: A Danish case study." In: *International Journal of Hydrogen Energy* 68 (May 2024), pp. 190–201. ISSN: 03603199. DOI: 10.1016/j.ijhydene.2024.04.158.

[8] Simon Araya et al. *Aalborg Universitet Power-to-X Technology overview, possibilities and challenges*. Tech. rep. 2022.

[9] Chris Beaumont et al. "Forecasting: Methods and Applications." In: *The Journal of the Operational Research Society* 35.1 (Jan. 1984), p. 79. ISSN: 01605682. DOI: 10.2307/2581936.

[10] Bjorn Bofinger. *What are Power-to-X solutions?* 2022. URL: https://as-schneider.blog/2022/03/02/what-are-power-to-x-solutions/.

[11] Gianluca Bontempi et al. "Machine learning strategies for time series forecasting." In: *Lecture Notes in Business Information Processing* 138 LNBIP (2013), pp. 62–77. ISSN: 18651348. DOI: 10.1007/978-3-642-36318-4{_}3.

[12] Mai Bui et al. "Carbon capture and storage (CCS): the way forward." In: *Energy & Environmental Science* 11.5 (May 2018), pp. 1062–1176. ISSN: 1754-5706. DOI: 10.1039/C7EE02342A. URL: https://pubs.rsc.org/en/content/articlehtml/2018/ee/c7ee02342a%20https://pubs.rsc.org/en/content/articlelanding/2018/ee/c7ee02342a.

[13] Antonio J. Conejo et al. "Decision Making Under Uncertainty in Electricity Markets." In: International Series in Operations Research & Management Science 153 (2010). DOI: 10.1007/978-1-4419-7421-1. URL: https://link.springer.com/10.1007/978-1-4419-7421-1.

[14] Francesco Dalena et al. "Methanol Production and Applications: An Overview." In: *Methanol: Science and Engineering* (2018), pp. 3–28. DOI: 10.1016/B978-0-444-63903-5.00001-7.

[15] DNV. *Energy transition outlook 2022*. Tech. rep. 2022.

[16] DNV. "Pathway to zero emissions." In: (2023).

[17] R Dones et al. *GREENHOUSE GAS EMISSIONS FROM ENERGY SYSTEMS: COMPARISON AND OVERVIEW*. Tech. rep.

[18] Øyvind Sekkesaeter Eirik et al. *Project team MARITIME Biofuels in shipping Content*. Tech. rep.

[19] *Energinet EN*. URL: https://en.energinet.dk/.

[20] International Energy Agency. *Renewables 2024*. Tech. rep. 2024. URL: www.iea.org.

[21] *ENTSOE*. URL: https://www.entsoe.eu/.

[22] Dogan Erdemir and Ibrahim Dincer. "A perspective on the use of ammonia as a clean fuel: Challenges and solutions." In: *International Journal of Energy Research* 45.4 (Mar. 2021), pp. 4827–4834. ISSN: 1099114X. DOI: 10.1002/ER.6232.

[23] European Associaton for Storage of Energy. *Power to Ammonia - Gasoline synthesis from H2 and N2 by using water electrolysis and Air Separation*. Tech. rep. 2018. URL: www.ease-storage.eu.

[24] European Energy. *Development of e-methanol production and offtake Kassø Integrated PV and e-methanol facility Denmark*. Tech. rep. 2025.

[25] Karim Ghaib and Fatima Zahrae Ben-Fares. "Power-to-Methane: A state-of-the-art review." In: *Renewable and Sustainable Energy Reviews* 81 (Jan. 2018), pp. 433–446. ISSN: 1364-0321. DOI: 10.1016/J.RSER.2017.08.004.

[26] Christian M. Grams et al. "Balancing Europe's wind-power output through spatial deployment informed by weather regimes." In: *Nature Climate Change 2017 7:8* 7.8 (July 2017), pp. 557–562. ISSN: 1758-6798. DOI: 10.1038/nclimate3338. URL: https://www.nature.com/articles/nclimate3338.

[27] GWEC. *Global Wind Report - 2024*. Tech. rep. 2024. URL: www.gwec.net.

[28] Ramzi Hage et al. *dawn*. Tech. rep. 2020. URL: https://www.iea.org/reports/the-future-of-hydrogen.

[29] Dominik Heide et al. "Seasonal optimal mix of wind and solar power in a future, highly renewable Europe." In: *Renewable Energy* 35.11 (Nov. 2010), pp. 2483–2489. ISSN: 09601481. DOI: 10.1016/J.RENENE.2010.03.012.

[30] Sepp Hochreiter and Jürgen Schmidhuber. "Long Short-Term Memory." In: *Neural Computation* 9.8 (Nov. 1997), pp. 1735–1780. ISSN: 08997667. DOI: 10.1162/NECO.1997.9.8.1735.

[31] Rob J. Hyndman and Anne B. Koehler. "Another look at measures of forecast accuracy." In: *International Journal of Forecasting* 22.4 (Oct. 2006), pp. 679–688. ISSN: 0169-2070. DOI: 10.1016/J.IJFORECAST.2006.03.001.

[32] Jaakko Hyypia et al. "Optimizing E-Methanol Production: Effect of Electricity Price and Renewable Energy Volatility on Optimum Dimensioning and Operation." In: 2024, pp. 99–110. DOI: 10.2991/978-94-6463-455-6{_}11.

[33] Institute for Sustainable Process Technology. *Power to Ammonia*. Tech. rep. 2017.

[34] International Energy Agency. *Ammonia Technology Roadmap – Analysis - IEA*. 2021. URL: https://www.iea.org/reports/ammonia-technology-roadmap.

[35] Banafsheh Jabarivelisdeh et al. *Ammonia Production Processes from Energy and Emissions Perspectives: A Technical Brief*. Tech. rep. 2022.

[36] Janina C. Ketterer. "The impact of wind power generation on the electricity price in Germany." In: *Energy Economics* 44 (July 2014), pp. 270–280. ISSN: 0140-9883. DOI: 10.1016/J.ENECO.2014.04.003.

[37] Jesus Lago et al. "Forecasting spot electricity prices: Deep learning approaches and empirical comparison of traditional algorithms." In: *Applied Energy* 221 (July 2018), pp. 386–405. ISSN: 0306-2619. DOI: 10.1016/J.APENERGY.2018.02.069.

[38] J. F. Manwell et al. "Wind Energy Explained: Theory, Design and Application." In: *Wind Energy Explained: Theory, Design and Application* (Dec. 2010). DOI: 10.1002/9781119994367. URL: https://onlinelibrary.wiley.com/doi/book/10.1002/9781119994367.

[39] Hamza Mubarak et al. "Day-Ahead electricity price forecasting using a CNN-BiLSTM model in conjunction with autoregressive modeling and hyperparameter optimization." In: *International Journal of Electrical Power & Energy Systems* 161 (Oct. 2024), p. 110206. ISSN: 0142-0615. DOI: 10.1016/J.IJEPES.2024.110206.

[40] S. Nady et al. "Power to X Systems: STATE-OF-THE-ART (PTX)." In: *IFAC-PapersOnLine*. Vol. 55. 12. Elsevier B.V., 2022, pp. 300–305. DOI: 10.1016/j.ifacol.2022.07.328.

[41] Jakub Nowotarski and Rafał Weron. "Recent advances in electricity price forecasting: A review of probabilistic forecasting." In: *Renewable and Sustainable Energy Reviews* 81 (Jan. 2018), pp. 1548–1568. ISSN: 1364-0321. DOI: 10.1016/J.RSER.2017.05.234.

[42] George A. Olah. "Towards Oil Independence Through Renewable Methanol Chemistry." In: *Angewandte Chemie International Edition* 52.1 (Jan. 2013), pp. 104–107. ISSN: 1521-3773. DOI: 10.1002/ANIE.201204995. URL: https://onlinelibrary.wiley.com/doi/full/10.1002/anie.201204995%20https://onlinelibrary.wiley.com/doi/abs/10.1002/anie.201204995%20https://onlinelibrary.wiley.com/doi/10.1002/anie.201204995.

[43] Mar Pérez-Fortes et al. "Methanol synthesis using captured CO2 as raw material: Techno-economic and environmental assessment." In: *Applied Energy* 161 (Jan. 2016), pp. 718–732. ISSN: 0306-2619. DOI: 10.1016/J.APENERGY.2015.07.067.

[44] M.H. Ranjbar et al. *(PDF) Reaching the Betz Limit Experimentally and Numerically*. 2019. URL: https://www.researchgate.net/publication/335991097_Reaching_the_Betz_Limit_Experimentally_and_Numerically.

[45] Konstantin Räuchle et al. "Methanol for Renewable Energy Storage and Utilization." In: *Energy Technology* 4.1 (Jan. 2016), pp. 193–200. ISSN: 2194-4296. DOI: 10.1002/ENTE.201500322. URL: https://onlinelibrary.wiley.com/doi/full/10.1002/ente.201500322%20https://onlinelibrary.wiley.com/doi/abs/10.1002/ente.201500322%20https://onlinelibrary.wiley.com/doi/10.1002/ente.201500322.

[46] International Renewable Energy Agency. *RENEWABLE ENERGY STATISTICS 2024 STATISTIQUES D'ÉNERGIE RENOUVELABLE 2024 ESTADÍSTICAS DE ENERGÍA RENOVABLE 2024*. 2024. ISBN: 9789292606145. URL: www.irena.org.

[47] Edward S. Rubin et al. "The cost of CO2 capture and storage." In: *International Journal of Greenhouse Gas Control* 40 (Sept. 2015), pp. 378–400. ISSN: 1750-5836. DOI: 10.1016/J.IJGGC.2015.05.018.

[48] Nils Thomas Schneider and Zenia Lagoni. *An investigation of the flexibility provided through electricity consumption in different scenarios for 2030*. Tech. rep.

[49] Frank Sensfuß et al. "The merit-order effect: A detailed analysis of the price effect of renewable electricity generation on spot market prices in Germany." In: *Energy Policy* 36.8 (Aug. 2008), pp. 3086–3094. ISSN: 0301-4215. DOI: 10.1016/J.ENPOL.2008.03.035.

[50] Siemens Energy. *Overview of the PEM Silyzer Family*. Tech. rep.

[51] Stefano Sollai et al. "Renewable methanol production from green hydrogen and captured CO2: A techno-economic assessment." In: *Journal of CO2 Utilization* 68 (Feb. 2023). ISSN: 22129820. DOI: 10.1016/j.jcou.2022.102345.

[52] Iain Staffell and Stefan Pfenninger. "The increasing impact of weather on electricity supply and demand." In: *Energy* 145 (Feb. 2018), pp. 65–78. ISSN: 0360-5442. DOI: 10.1016/J.ENERGY.2017.12.051.

[53] Szabolcs Szima and Calin Cristian Cormos. "Improving methanol synthesis from carbon-free H2 and captured CO2: A techno-economic and environmental evaluation." In: *Journal of CO2 Utilization* 24 (Mar. 2018), pp. 555–563. ISSN: 2212-9820. DOI: 10.1016/J.JCOU.2018.02.007.

[54] Melika Sadat Taslimi et al. "Optimization and analysis of methanol production from CO2 and solar-driven hydrogen production: A Danish case study." In: *International Journal of Hydrogen Energy* 69 (June 2024), pp. 466–476. ISSN: 03603199. DOI: 10.1016/j.ijhydene.2024.05.033.

[55] James W. Taylor. "Triple seasonal methods for short-term electricity demand forecasting." In: *European Journal of Operational Research* 204.1 (July 2010), pp. 139–152. ISSN: 0377-2217. DOI: 10.1016/J.EJOR.2009.10.003.

[56] Wei Tong. "Wind Power Generation and Wind Turbine Design(Google ebook)." In: (2010), p. 725. URL: http://books.google.com/books?id=wU9bgvrl4rQC&pgis=1.

[57] Abhishiktha Tummala et al. "A review on small scale wind turbines." In: *Renewable and Sustainable Energy Reviews* 56 (Apr. 2016), pp. 1351–1371. ISSN: 1364-0321. DOI: 10.1016/J.RSER.2015.12.027.

[58] Rafał Weron. "Electricity price forecasting: A review of the state-of-the-art with a look into the future." In: *International Journal of Forecasting* 30.4 (Oct. 2014), pp. 1030–1081. ISSN: 0169-2070. DOI: 10.1016/J.IJFORECAST.2014.08.008.

[59] *XGBoost Documentation — xgboost 3.0.0 documentation.* URL: https://xgboost.readthedocs.io/en/release_3.0.0/.

[60] Guangling Zhao et al. "Life cycle assessment of H2O electrolysis technologies." In: *International Journal of Hydrogen Energy* 45.43 (Sept. 2020), pp. 23765–23781. ISSN: 0360-3199. DOI: 10.1016/J.IJHYDENE.2020.05.282.

[61] Yi Zheng et al. "Data-driven robust optimization for optimal scheduling of power to methanol." In: *Energy Conversion and Management* 256 (Mar. 2022). ISSN: 01968904. DOI: 10.1016/j.enconman.2022.115338.

[62] Florian Ziel and Rick Steinert. "Probabilistic mid- and long-term electricity price forecasting." In: *Renewable and Sustainable Energy Reviews* 94 (Oct. 2018), pp. 251–266. ISSN: 18790690. DOI: 10.1016/J.RSER.2018.05.038. URL: http://arxiv.org/abs/1703.10806%20http://dx.doi.org/10.1016/j.rser.2018.05.038.

Appendix A

A.1 EPF Development

All graphs used in EPF development are presented under this section.

A.1.1 Historical data for input variables

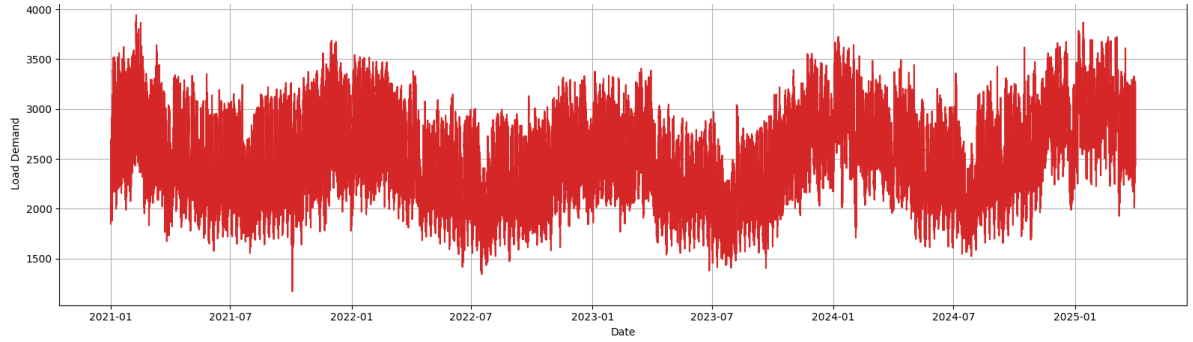

Figure A.1

Hourly electricity demand in Denmark from 2021 to 2025, displaying clear seasonal patterns and daily fluctuations.

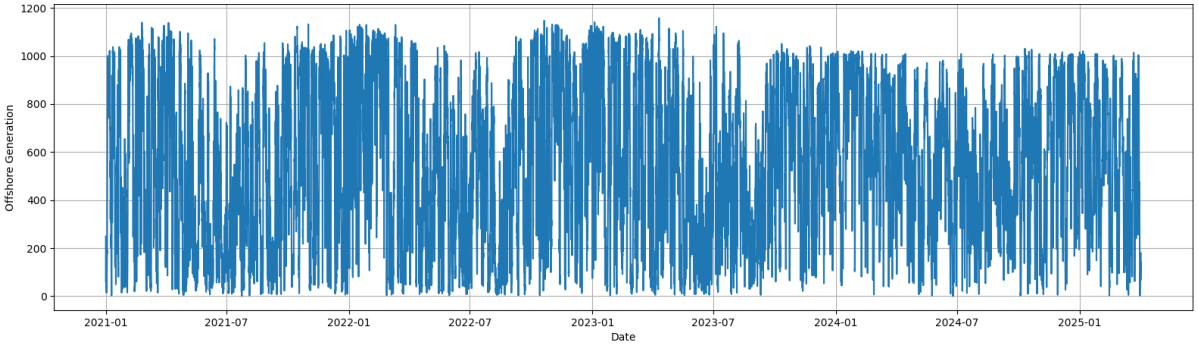

Figure A.2

Hourly offshore wind power generation from 2021 to 2025, characterized by high variability and strong wind activity throughout the period.

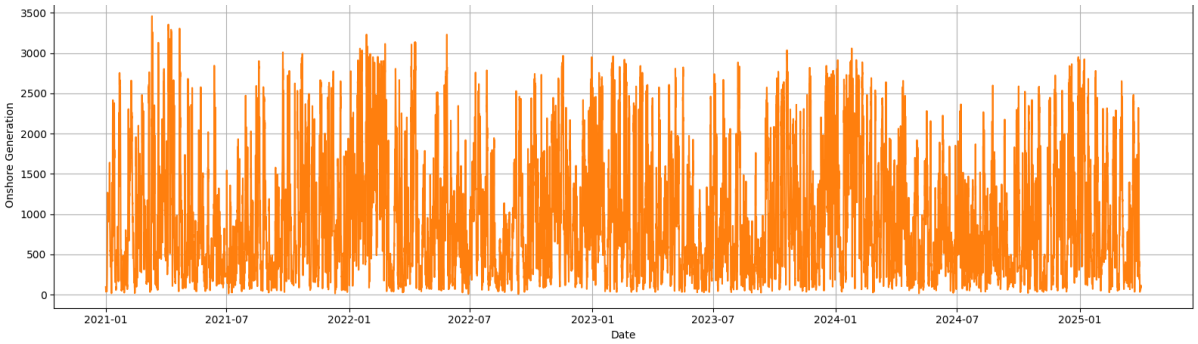

Figure A.3

Hourly onshore wind generation from 2021 to 2025, showing frequent fluctuations driven by variable wind conditions.

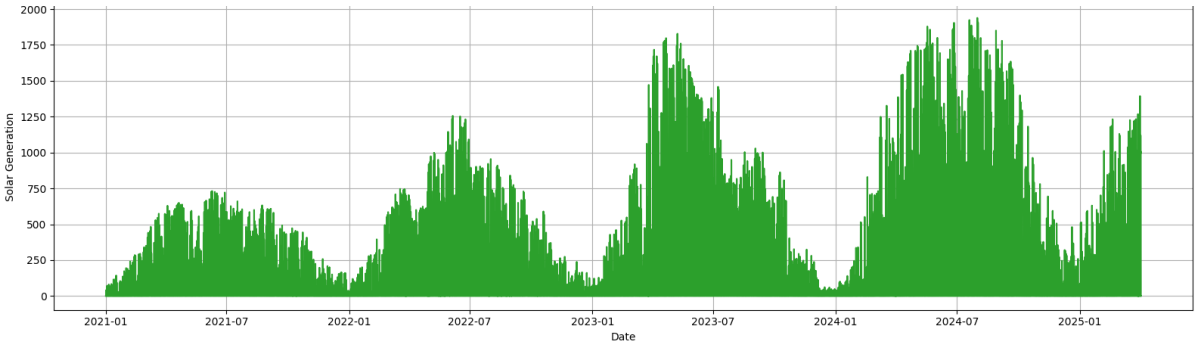

Figure A.4

Hourly solar power generation from 2021 to 2025, showing strong seasonal variation with peaks during summer months.

A.1.2 Forecasted values with LSTM model

Figure A.5

Forecasted electricity load demand from April 2025 to April 2026 produced by the LSTM model.

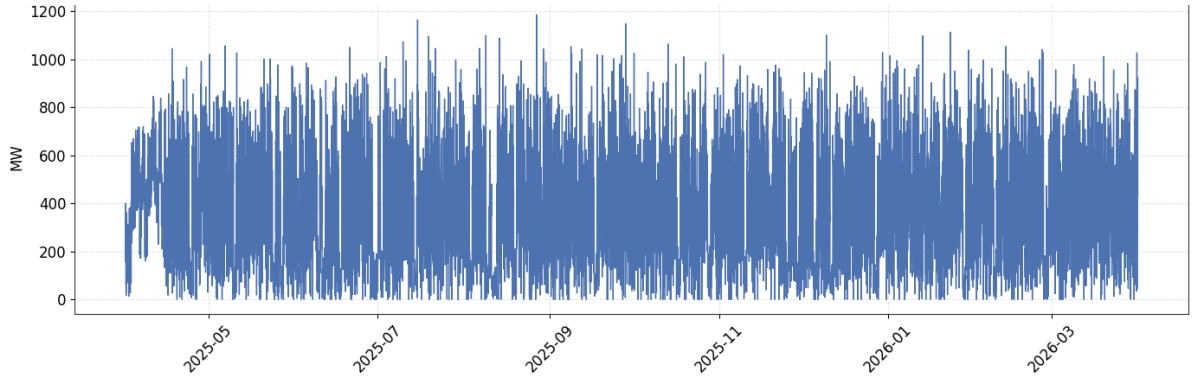

Figure A.6
Forecasted offshore wind power generation from April 2025 to April 2026 using the LSTM model.

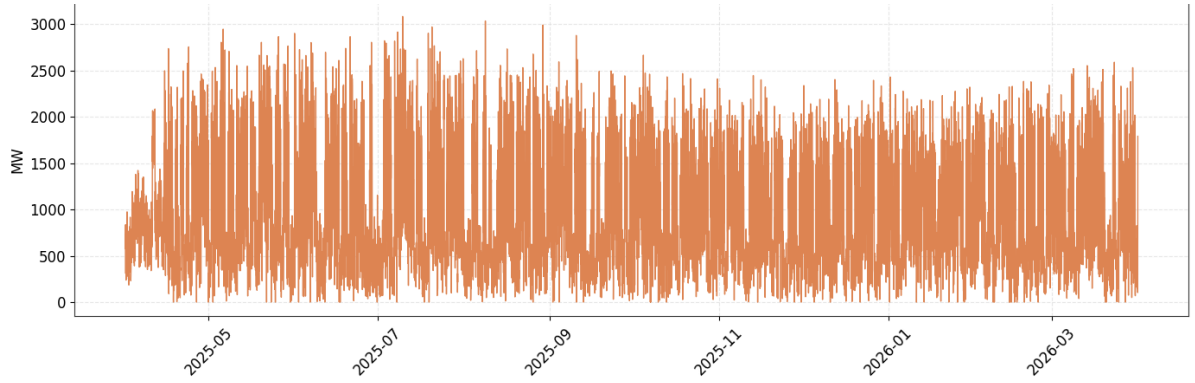

Figure A.7
Forecasted onshore wind power generation from April 2025 to April 2026 using the LSTM model.

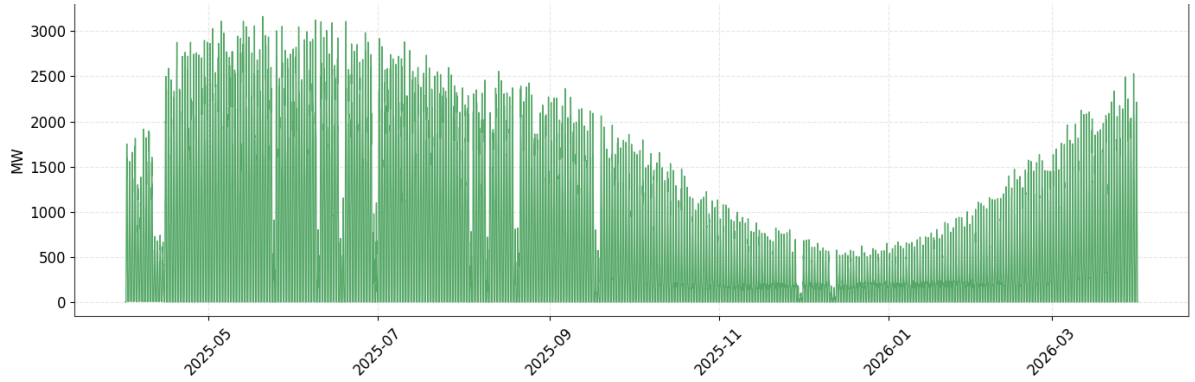

Figure A.8
Forecasted solar power generation for the period April 2025 to April 2026 based on LSTM predictions.

A.1.3 Validation Plots for Renewable Electricity Generation

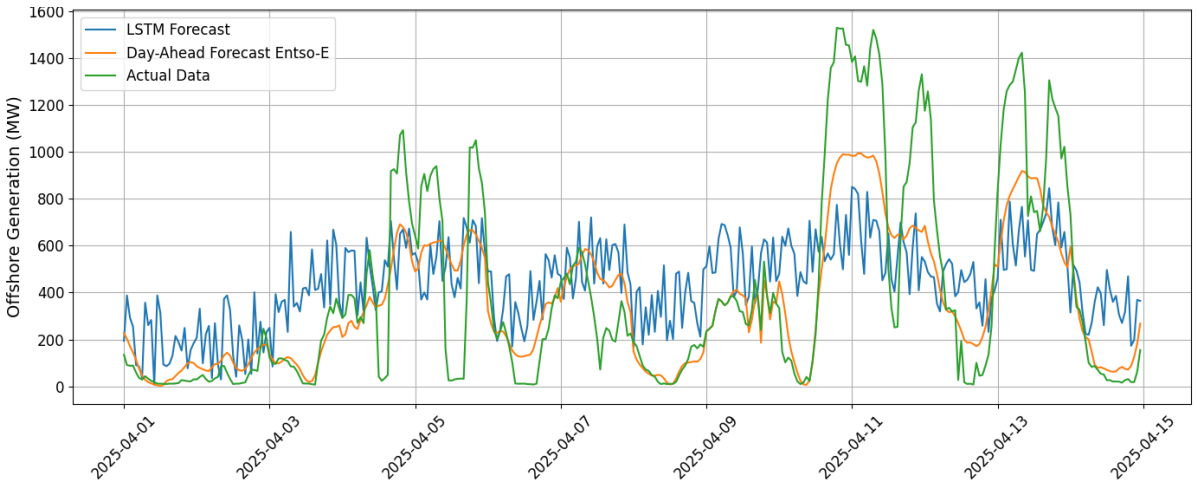

Figure A.9

Forecasted offshore wind generation from the LSTM model and ENTSO-E day-ahead values are evaluated against actual offshore output.

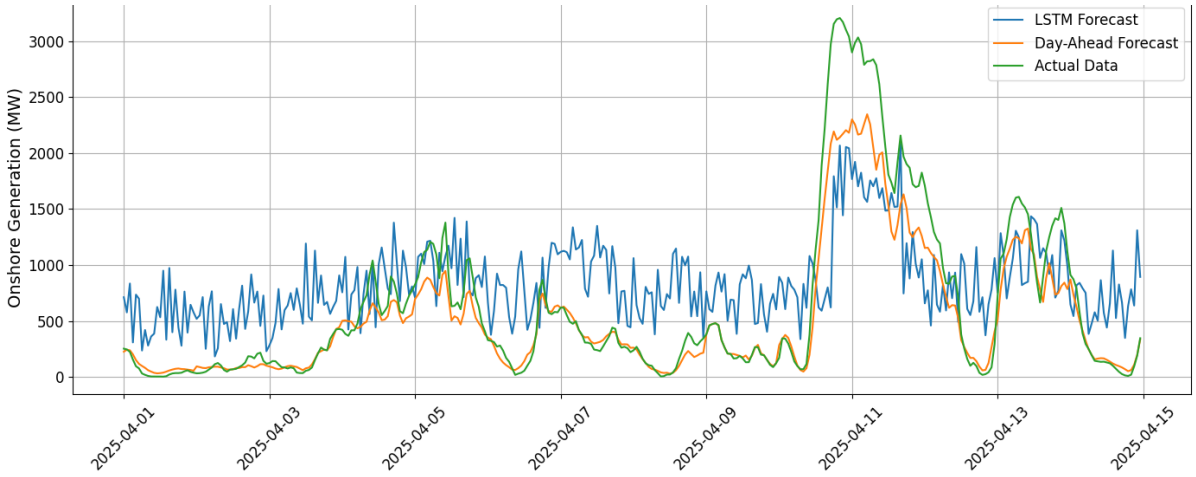

Figure A.10

Hourly onshore wind generation forecasts from the LSTM model and ENTSO-E day-ahead data are compared to actual values.

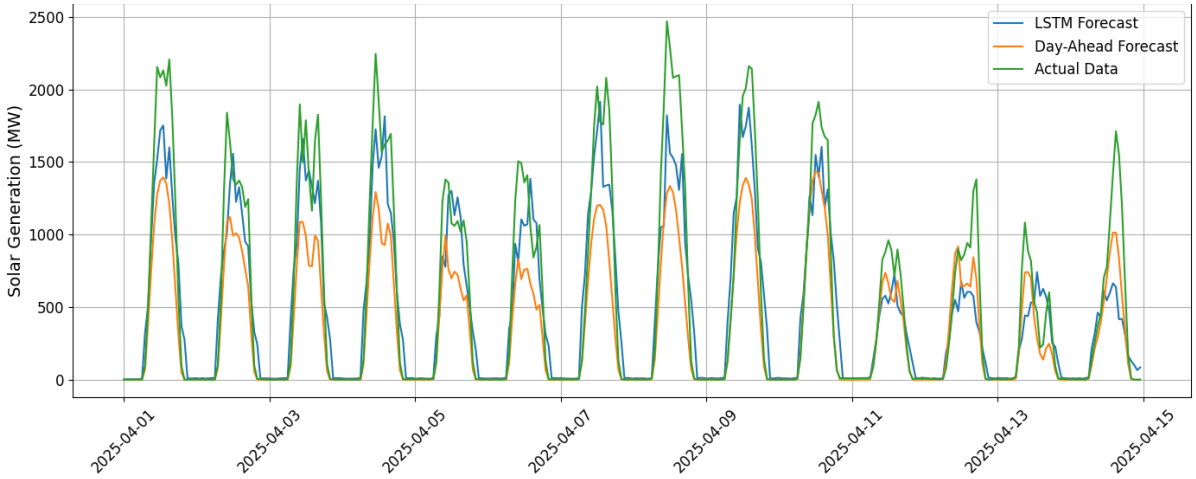

Figure A.11

Hourly solar generation forecasts from the LSTM model and ENTSO-E day-ahead data are compared with actual measurements.

A.2 Optimisation Development

CAPEX Calculations

Electrolyser	CASE 1	CASE 2	CASE 3	CASE 4	CASE 5
Type of electrolyser	AEL		PEM		
Cost (€/kW)	482.5676	482.5676	462.2448	462.2448	462.2448
Total cost of electrolyser (k€)	48257	48257	46224	46224	46224
H2O pump					
Power duty (kW)	12	12	12	12	25
Material	SS (high grade)	SS (high grade)	SS (high grade)	SS (high grade)	SS (high grade)
Cost (k€)	75	75	75	75	140
H20 pump - big					
Power duty (kW)	47	47	47	47	47
Material	SS (high grade)	SS (high grade)	SS (high grade)	SS (high grade)	SS (high grade)
Cost (k€)	158	158	158	158	196
H2 compressor					
Power duty (kW)	0	364	0	364	0
Material		SS (high grade)		SS (high grade)	
Cost (k€)	0	447	0	447	0
Reactor					
L/D ratio	4	5	4	5	5
Length (m)	8.15	8.35	8.15	8.35	8.35
Thickness (m)	0.013	0.022	0.013	0.022	0.022
Material	SS (high grade)	SS (high grade)	SS (high grade)	SS (high grade)	SS (high grade)
Pressure (bar)	35	70	35	70	70
Cost (k€)	2881	2502	2881	2502	2502
Recycle compressor					
Power duty (kW)	1268	334	1268	334	334
Material	SS (high grade)	SS (high grade)	SS (high grade)	SS (high grade)	SS (high grade)
Cost (k€)	616	423	616	423	423
Distillation Column					
Cost (k€)	549	597	597	597	549
Total Cost (k€)	52536	52458	50551	50426	50035
	INLET GAS VELOCITY	GOOD INLET GAS	GOOD INLET	GOOD INLET	GOOD INLET

Figure A.12

Summary of equipment specifications and costs for different system configurations (Case 1–5).

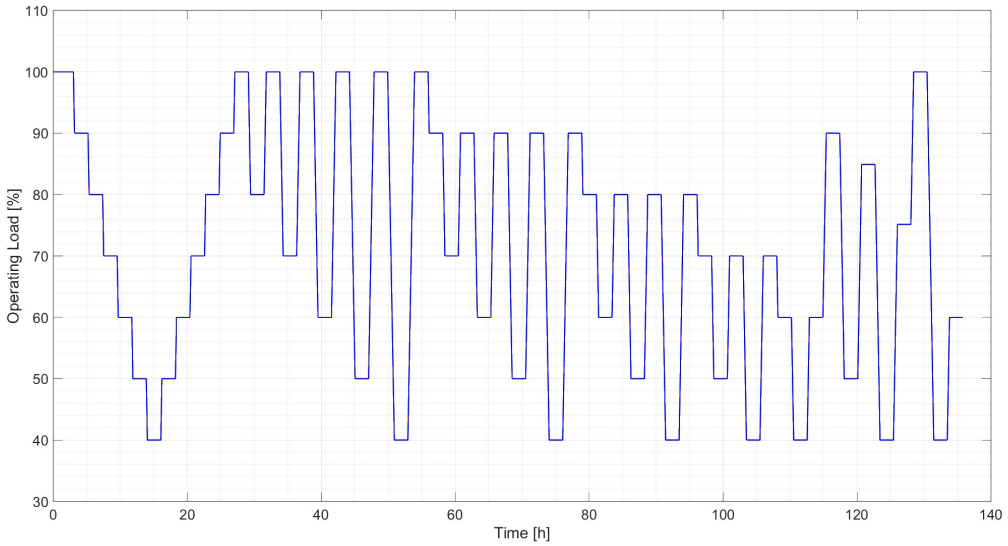

Figure A.13

Hydrogen input in MSD system, where output methanol is tracked in software program. Hydrogen input and methanol output are used to train surrogate model with LSTM model.

Surrogate Model

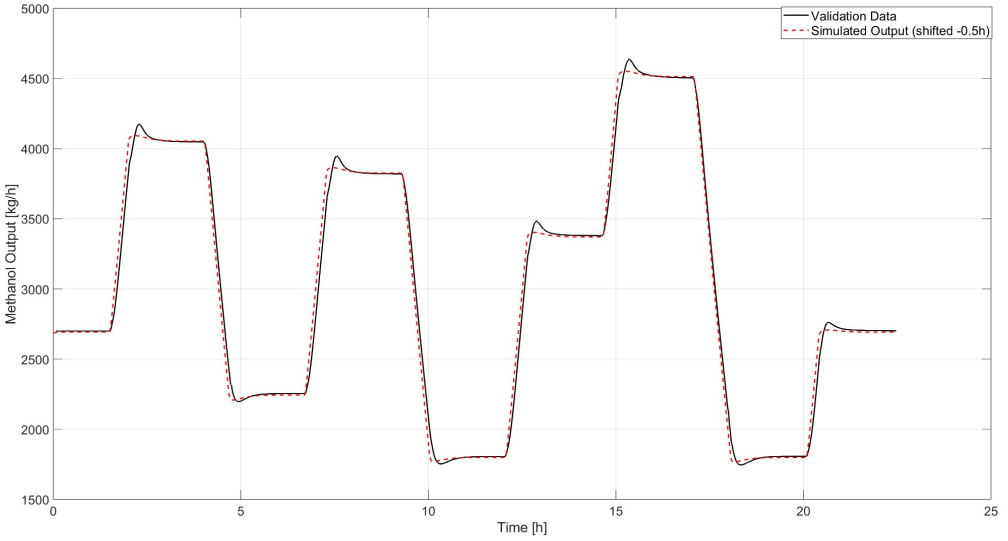

Figure A.14

Comparison between simulated and validation methanol output over a 24-hour window. Resulting differences are following; Mean Validation Output = 3015.74 kg/h, Mean Simulated Output = 3015.76 kg/h, RMSE = 0.02 kg/h, MAE = 0,02 kg/h, R^2 = 1.0000